

1-1-2001

Effects of exposure to continuous low doses of ionizing radiation

Kathleen Anne Meehan
Cape Technikon

Recommended Citation

Meehan, Kathleen Anne, "Effects of exposure to continuous low doses of ionizing radiation" (2001). *Cape Technikon Theses & Dissertations*. Paper 156.
http://dk.cput.ac.za/td_ctech/156

This Text is brought to you for free and open access by the Theses & Dissertations at Digital Knowledge. It has been accepted for inclusion in Cape Technikon Theses & Dissertations by an authorized administrator of Digital Knowledge. For more information, please contact barendsc@cput.ac.za.

**EFFECTS OF EXPOSURE TO CONTINUOUS LOW DOSES
OF IONISING RADIATION**

KATHLEEN ANNE MEEHAN

Thesis submitted in compliance with the requirements for the degree of

Doctor Technologiae (Biomedical Technology)

to the Faculty of Applied Sciences, Cape Technikon

Department of Biomedical Technology

Faculty of Applied Sciences

Cape Technikon

Cape Town, 2001

External Supervisor : Professor MI Parker

Internal Supervisor : Professor EJ Truter

I declare that this thesis is my own work.

It is being submitted for the degree of
Doctor Technologiae (Biomedical Technology)
to the Cape Technikon, Cape Town,

It has not been submitted before for any degree or examination
at any other Technikon or tertiary institution.

The work was undertaken at the Faculty of Applied Sciences, Cape Technikon
and the Department of Medical Biochemistry,
University of Cape Town.

The opinions and conclusions drawn are not necessarily
those of the Cape Technikon.



Kathleen Anne Meehan



Date

I dedicate this thesis to my husband, Alan,
my two daughters, Michelle and Jessica
and my parents, Dick and Sylvia.

CONTENTS

Abstract

Acknowledgements

Glossary of abbreviations

Chapter 1. Introduction and literature review

1.0	Genotoxic effects of carcinogens	1
1.1	Biomarkers of genotoxicity	2
1.1.1	Protein adducts	2
1.1.2	DNA adducts	3
1.1.3	Single cell gel electrophoresis (comet) assay	4
1.1.4	HPRT mutations in lymphocytes	5
1.1.5	Chromosome aberrations in lymphocytes	6
1.1.6	Apoptosis studies	8
1.2	<i>Ionising radiation and thorium exposure</i>	9
1.3	Histology of radiation exposed tissues	14
1.4	The role of p53 in radiation exposure	16
1.5	Radiation effects on the haematopoietic system	19
1.6	Assays to evaluate radiation induced DNA damage	25
1.6.1	The micronucleus assay in peripheral lymphocytes	25
1.6.2	The micronucleus assay in peripheral reticulocytes	26
1.6.3	The single cell gel electrophoresis (comet) assay	26

1.7 Radiation-induced chromosomal aberrations	27
1.8 Steenkampskraal monazite mine	29

Chapter 2. Materials and Methods

2.1 Sample collection	33
2.2 Histological methodology	34
2.2.1 Tissue preparation	34
2.2.2 Staining techniques	34
2.3 Immunohistochemistry using monoclonal p53 antibody	35
2.4 Haematological methodology	36
2.4.1 Peripheral blood analysis	36
2.4.2 Trephine biopsies	39
2.4.3 Bone mineralisation using image analysis	39
2.5 DNA damage evaluation	40
2.5.1 Micronucleus assay in peripheral lymphocytes	41
2.5.2 Micronucleus assay in peripheral reticulocytes	41
2.5.3 Single cell gel electrophoresis (comet) assay	42
2.6 Cytogenetic techniques	43

Chapter 3. Results

3.1 Histology	45
3.2 p53 Immunohistochemistry	48

3.3 Haematology	54
3.3.1 Peripheral blood analysis	54
3.3.2 Trephine biopsies	73
3.3.3 Bone mineralisation using image analysis	78
3.4 DNA damage evaluation	80
3.4.1 Micronucleus assay in peripheral lymphocytes	80
3.4.2 Micronucleus assay in peripheral reticulocytes	83
3.4.3 Single cell gel electrophoresis (comet) assay	86
3.5 Cytogenetic investigation	90
Chapter 4. Discussion	92
Chapter 5. Conclusions and directions for future studies	98
References	101
Appendix	116

LIST OF FIGURES

	Page
Figure 1: Photograph of monazite	10
Figure 2: Structural features of the p53 gene	17
Figure 3: Radiation induced chromosome aberrations	28
Figure 4: Locality map of Steenkampskraal	30
Figure 5: <i>Rhinolophus capensis</i>	32
Figure 6: Leukocytes in bat peripheral blood	38
Figure 7: Comet showing DNA damage	43
Figure 8: (a) Liver section stained with Haematoxylin and Eosin	45
(b) Liver section stained with Alcian Blue PAS	46
(c) Liver section stained with Verhoeff van Gieson	46
Figure 9: (a) Lung section stained with Haematoxylin and Eosin	47
(b) Lung section stained with Verhoeff van Gieson	47
Figure 10: p53 immunohistochemistry positive control	48
Figure 11: (a) p53 immunohistochemistry of bronchiolar lining and alveolar cells	49
(b) lung section of a control bat	49
(c) positive p53 staining of bronchiolar lining cells	49
(d) positive p53 staining of alveolar cells	49
Figure 12: (a) liver section of a control bat	50
(b) positive p53 staining of liver section	50
Figure 13: Graphical representation of p53 immunohistochemical staining	51
Figure 14: Graphical representation of full blood counts	58

Figure 15:	DAB myeloperoxidase staining of neutrophils	61
Figure 16:	Graphical representation of differential counts	67
Figure 17:	Graphical representation of absolute counts	72
Figure 18:	(a) Trephine biopsy of a control bat	74
	(b) Trephine biopsy of a radiation exposed bat	74
Figure 19:	(a) Osteocyte distribution in bone marrow of a control bat	75
	(b) Osteocyte distribution in bone marrow of a radiation exposed bat	75
Figure 20:	Osteoblastic islands in bone marrow of a radiation exposed bat	75
Figure 21:	Graphical representation of G:L:E ratios	77
Figure 22:	(a) Bone mineralisation in a control bat	78
	(b) Bone mineralisation in a radiation exposed bat	78
Figure 23:	Micronuclei in bat peripheral lymphocytes	80
Figure 24:	Graphical representation of micronuclei in bat peripheral lymphocytes	83
Figure 25:	Micronuclei in bat peripheral reticulocytes	84
Figure 26:	Graphical representation of micronuclei in bat peripheral reticulocytes	86
Figure 27:	Comets showing DNA damage in bat lymphocytes	87
Figure 28:	Graphical representation of comet assay	89
Figure 29:	(a) Metaphase spread of a control bat	91
	(b) Dicentric chromosome in a radiation exposed bat	91
	(c) Ring chromosome in a radiation exposed bat	91

LIST OF TABLES

	Page
Table I: Results of p53 immunohistochemistry	52
Table II: (a) Full blood counts of control bats	55
(b) Full blood counts of 20 $\mu\text{Sv/h}$ exposed bats	56
(c) Full blood counts of 100 $\mu\text{Sv/h}$ exposed bats	57
Table III: p-values of full blood counts	59
Table IV: (a) Differential counts of control bats	62
(b) Differential counts of 20 $\mu\text{Sv/h}$ exposed bats	63
(c) Differential counts of 100 $\mu\text{Sv/h}$ exposed bats	65
Table V: p-values of differential counts	68
Table VI: (a) Absolute counts of control bats	69
(b) Absolute counts of 20 $\mu\text{Sv/h}$ exposed bats	70
(c) Absolute counts of 100 $\mu\text{Sv/h}$ exposed bats	71
Table VII: p-values of absolute counts	73
Table VIII: Bone marrow morphology	76
Table IX: p-values of bone marrow morphology	77
Table X: Bone mineralisation and p-values	79
Table XI: Micronuclei in bat peripheral lymphocytes	82
Table XII: Micronuclei in bat peripheral reticulocytes	85
Table XIII: Single-cell gel electrophoresis (comet) assay	88

ABSTRACT

Ionising radiation has the ability to induce, *inter alia*, DNA damage and is well established as a causative agent of carcinogenesis and mutagenesis. The effects of high doses of short duration have been well documented, whereas the effects of continuous exposure to low doses of ionising radiation have not, nor are they as clearly understood and current risk estimates are largely extrapolated from high-dose data of atomic bomb survivors. This study evaluated the clastogenic effects of low dose ionising radiation on a population of bats (*Chiroptera*) residing in an abandoned monazite mine. Bats were sampled from two areas in the mine, with external radiation levels measuring around 20 $\mu\text{Sv/h}$ (low dose) and 100 $\mu\text{Sv/h}$ (high dose). A control group of bats was collected from a cave with no detectable radiation above normal background levels.

The most frequently encountered genetic event in human malignancy is the alteration of the p53 gene. Mutant p53 proteins have a longer half-life than the wild-type variant and accumulate to high levels in the nucleus of tumour cells. The study showed that not only was there a significant increase in p53 positive cells of radiation exposed bats, but also in the degree of positivity, especially in the cells lining the bronchioles of the lungs.

Although experimental studies have shown that exposure to radiation may lead to the onset of fibrosis and an inflammatory response in the lung and other tissues, the magnitude of the dose exposure was not comparable to this study and histological examination of bat lung and liver tissues showed no morphological changes in radiation exposed bats when compared to the control group.

It has been documented that chronic radiation exposures may give rise to a number of specific haematological defects which are collectively termed "preleukemia" or myelodysplastic syndrome. Full blood counts on bat samples showed a significant decrease in the MCV indicating microcytic erythrocytes from the radiation exposed bats. Differential counts performed on the peripheral blood of the bats showed a marked neutropenia. Neutrophils also showed marked dysplasia including pseudo-Pelger Huet cells in radiation-exposed bats. Cytochemical analysis using DAB myeloperoxidase showed that control bats had hypogranular neutrophils and radiation-exposed bats had largely agranular neutrophils. Bone marrow biopsies were taken from both control and radiation-exposed bats and evaluated for cellularity, granulocyte: lymphocyte: erythrocyte (GLE) ratio and megakaryocyte morphology. A hypocellular bone marrow, a decreased granulocytic haematopoiesis and dysplastic megakaryocyte morphology were observed in radiation-exposed bats. Mineralisation of bone osteoid was determined using image analysis and showed a highly significant decrease in the bone matrix from radiation-exposed bats. All haematological features observed are congruent with current literature describing secondary (radiation-induced) myelodysplastic syndrome. As there is considerable debate as to what dose radiation exposure is harmful, the results of these findings may prove significant in establishing haematopoietic effects of continuous low dose exposure to ionising radiation.

The micronucleus assay was used to evaluate residual radiation damage in binucleated lymphocytes and showed that the micronucleus frequency was higher in the test group than the control group. This study showed that bats exposed to radiation also presented with an increased number of micronuclei in reticulocytes compared to the control group. The Single Cell Gel (Comet) assay further showed increased DNA damage as indicated by the length of the comet

tails. The results of the micronucleus and the comet assays showed not only a statistically significant difference between test and control groups, but indicated a dose dependent increase in DNA damage. These findings were supported by the presence of chromosomal aberrations in metaphases of radiation exposed bats. These assays may thus be useful in evaluating the potential clastogenicity of exposure to continuous low doses of ionising radiation.

Although one has to be cautious about extrapolating data from bats to humans, the results of this study clearly indicate the potential risk of continuous exposure to low doses of ionising radiation.

As a monazite mine at Steenkampskraal, South Africa, is likely to reopen in the near future, it will be essential to make use of a biodosimetry service to monitor radiation exposed individuals on a regular basis for early signs of DNA damage thereby ensuring the right of all employees to a safe working environment. The biodosimetry service can be extended to incorporate exposure to any potential mutagen such as in the paint, pesticide and plastics industries.

ACKNOWLEDGEMENTS

I would like to thank the management of the Cape Technikon for affording me the opportunity to undertake this study and for their financial support throughout the project. I am grateful to the Dean, Professor Lionel Slammert and the assistant Dean, Mr Frans du Toit, of the Faculty of Applied Sciences for their encouragement and for allowing me the time to complete the study.

I thank Professor Ernie Truter for sharing his valuable expertise with me and for his guidance. I also thank Professor Iqbal Parker for accepting to supervise this thesis. It has been an honour to be guided by him.

I am indebted to Mr Robbie Louw from Rare Earth Extraction Company for his insight in identifying this interesting project. I have learned so much from him. I would like to sincerely thank Western Cape Nature Conservation Board, for granting the permits as well as their assistance in collecting the samples for this study especially Mr Jaco van Deventer and Mr Ben Swanepoel.

I am indebted to Mr Rolf Proske, subject librarian at the Cape Technikon, for his unfailing support throughout the project and for the many hours he spent assisting me in the literature search.

I would like to thank Dr Kobus Slabbert from the Radiation Biophysics Division at the National Accelerator Centre for training me in the field of radiobiology and for so willingly sharing his knowledge with me and to Mr Schalk Schmidt for his technical assistance.

To the South African Institute for Medical Research (SAIMR), I thank you for your assistance in the histological preparation and examinations. I also thank Dr Betsy Lombard from the Department of Anatomical Pathology, University of Cape Town for her advice in the haematological examinations. I appreciate the assistance from Ms Rochelle Barnard and Dr Rob Bowen also from the Department of Anatomical Pathology in standardising the p53 immunohistochemistry for bats.

I thank Mr Ronnie Smart from the Department of Human Genetics, University of Cape Town for sharing my frustration in the analysis of bat chromosomes.

I would like to thank the people that I have met at international congresses over the last few years for their encouragement and their interest as well as their advice in the study, especially Dr Raymond Tice, Dr David De Marini, Dr Peggy Olive, Dr Karl Johanson, Drs Elizabeth and James Parry, Dr Makato Hayashi and Prof Broerse.

I would like to thank Mr Henry Neethling and Ms Aldina Santos from the Faculty of Applied Sciences, Cape Technikon for all their technical assistance and to my Biomedical Technology student assistants, Pauline Sebastian, Quentin Botha and Alicia Elliott, thank you for all the hours you gave and for your enthusiasm and dedication.

I am indebted to all my colleagues and friends for their continued support and encouragement throughout the project which nurtured my enthusiasm to continue.

Lastly, to my family, who sacrificed so much that I may reach my dream - thank you.

Glossary of abbreviations

$\mu\text{Sv/h}$	microsievert per hour
Sr	strontium
Tl	thallium
Pb	lead
Rn	radon
Ac	actinium
Th	thorium
Co	Cobalt
μl	microlitre
μm	micrometre
PAS	Periodic Acid Schiff
EDTA	ethylenediaminetetra-acetic acid
μg	microgram
M	molar
mM	millimolar
HMAR	heat mediated antigen retrieval
HRP	horseradish peroxidase
DNA	deoxyribonucleic acid
kD	kilodalton
V	volt
mA	milliampere
nm	nanometre

g	gravitation
TE	Tris EDTA
dl	decilitre
fl	femtolitre
α	alpha
γ	gamma
β	beta
Ci	Curie
pCi	picoCurie
Bq	Bequerel
rem	röntgen-equivalent-man
kD	kiloDalton
kb	kilobase
dsb	double strand break
PHA	Phytohaemagglutinin
LET	linear energy transfer

CHAPTER 1

Introduction and Literature Review

1.0 Genotoxic effects of carcinogens

Carcinogenesis and mutagenesis has been well established with three main causative agents, viz. chemical carcinogens which cause changes in the DNA sequence, viruses which introduce foreign DNA into a cell and ionising radiation which results in chromosome breaks and induces DNA translocations (Malkin, 1994). Although most carcinogens in the environment are genotoxic, not all genotoxic agents have been shown to be carcinogenic. The focus on end-point biomonitoring is largely associated with carcinogenicity, however, there is interest in monitoring genotoxicity as an end-point. End-point assays used most commonly in assessment of genotoxicity are reviewed by Albertini *et al* (2000) and include chromosome aberrations using cytogenetic techniques (Bender *et al*, 1974), fluorescent *in situ* hybridisation (FISH) analysis using chromosome painting (Smith *et al*, 1998), micronuclei frequency, (Fenech and Morley, 1985) DNA damage using biochemical or electrophoretic assays (Östling and Johanson, 1984), formation of protein adducts (Törnqvist and Ehrenberg, 1994) or DNA adducts (Hemminki *et al*, 1994) and identification of induced mutations e.g. hypoxanthine-guanine phosphoribosyltransferase (HPRT) (Albertini *et al*, 1988). Mutations in the p53 gene are also well documented (Harris and Hollstein, 1993). Although other germ cell and gene mutations as well as markers for oxidative stress are reported, the data is limited. Biomarkers may be used to determine either the measure of exposure or the effect i.e. an indicator of cancer risk.

Inter-individual variability plays an important role in biomarkers. The mechanisms differ for each biomarker and some have not been determined as yet. Using biomarkers cannot always elucidate the causative agent e.g. DNA and protein adducts are identified as arising from a specific chemical whereas chromosome aberrations or gene mutations are not and the causative agent has to be established. Association between exposure and the biomarker has however been demonstrated using chromosome aberrations and ionising radiation and ethylene oxide and haemoglobin adducts (Albertini *et al*, 2000). As interest in the field of genetic toxicology grows, data from studies show that biomarkers may be important predictors of cancer risk.

1.1 Biomarkers of genotoxicity

1.1.1 Protein adducts

A protein adduct is a chemical bound covalently to a protein (Törnqvist and Ehrenberg, 1994). As many carcinogens form protein adducts, they are used as biomarkers, usually of exposure. Many electrophilic chemicals or their metabolites react with amino acid side chains in haemoglobin and albumin. As the lifespan of human erythrocytes is approximately 120 days, haemoglobin adducts may be used to determine exposures that occurred weeks before sampling of blood (Törnqvist *et al*, 1986), whereas albumin remains in the blood for approximately 28 days. The most common reaction sites are at cysteine, histidine and N-terminal valine. Haemoglobin adducts are characterised by precipitation of globin from lysed erythrocytes and analysis using gas-chromatography-mass spectrophotometry for S-alkylcysteines, N-alkyl histidines and N-alkylvalines (Osterman-Golkar and Bond, 1996). Albumin is extracted from serum and adducts are detected either by immunochemistry of aflatoxin B₁ (Groopman and

Kensler, 1999) or hydrolysis of the adduct and analysis of the released 4-aminobiphenyl or S-phenylcysteine (Tannenbaum *et al*, 1993).

1.1.2 DNA adducts

A DNA adduct is defined as a chemical which is covalently linked to DNA (Hemminki *et al*, 1994). Most carcinogens form DNA adducts and are detected as modified bases, deoxynucleosides or oligonucleotides and are identified either by chemical-specific techniques or non-specific techniques. Modified bases may be excreted in urine as a result of DNA repair and may be used as a biomarker. DNA has to be purified from the sample and adducts are usually identified using ^{32}P -postlabelling. Labelled nucleosides are separated using high performance liquid chromatography (HPLC) and are visualised by autoradiography. Adduct spots are quantified using scintillation counting (Prahalad *et al*, 1997). Mass spectrophotometry may be used where DNA is digested and adducts separated by chromatography. Adducts are identified by an increase in molecular weight compared to normal bases (Farmer and Sweetman, 1995). The radioimmunoassay method may also be used and involves the addition of a radioactive tracer adduct bound to a specific antibody which is displaced by adducts in the unknown sample (Müller and Rajewsky, 1981). A number of ELISA techniques have also been reported where a known amount of adduct-bound DNA is added to a microtitre well coated with specific antibody as well as samples of unknown amounts of DNA adduct. The quantity of unknown DNA adduct is inversely proportional to the fraction remaining after the addition of the second antibody (Adamkiewicz *et al*, 1985). The immunoslotblot assay may also be used for the qualitative and quantitative identification of DNA adducts. DNA is sonicated to generate

fragments of around 100 base pairs and slotblotted onto filters which are subsequently treated with antibodies specific for the adduct of interest. After the second antibody-enzyme conjugate is added, filters are soaked in a chemiluminescence reagent and emitted light is detected. Intensities of bands may be measured to quantify concentrations of the adducts (Nehls *et al*, 1984).

1.1.3 Single-cell gel electrophoresis (comet) assay

As most carcinogens are genotoxic and various types of DNA damage have been characterised for many of them, the comet assay is increasingly being used to detect DNA damage in cells treated with many of these agents. The DNA damage detected by this assay identifies exposure and not risk, i.e. it is characterised as an effect biomarker. The data accumulated from the use of this assay has not as yet been used to predict a predisposition to cancer. Any cell population may be used to evaluate DNA damage and in this assay, first described by Östling and Johanson (1984), cells suspended in molten agar are lysed under high salt conditions and DNA is subsequently electrophoresed under varying pH conditions (Singh *et al*, 1988). Cells with increased DNA damage display increased migration and the resulting “comets” are viewed under fluorescence microscopy using appropriate staining. The tail length or tail moment (tail length multiplied by the fraction of DNA in the tail) may be used to report the amount of DNA damage (Fairbairn *et al*, 1995). The use of this assay in the field of radiation biodosimetry is described in detail in 1.6.3 (pg. 26).

1.1.4 Hypoxanthine-guanine Phosphoribosyl Pyrophosphate (HPRT) mutations in lymphocytes

The HPRT gene reflects a variety of genetic alterations e.g. DNA base pair substitutions, deletions, inversions and chromosome recombinations in response to exposure of genotoxic agents (Albertini and Hayes, 1997). The HPRT gene controls the enzyme hypoxanthine-guanine phosphoribosyltransferase which catalyses the reaction of hypoxanthine and guanine with phosphoribosylpyrophosphate in the salvage of purines. HPRT also catalyses the conversion of purine analogues e.g. 6-thioguanine, rendering them cytotoxic to normal cells. Therefore, following HPRT mutation, cells deficient in the enzyme survive treatment with 6-thioguanine (Albertini and Hayes, 1997). Two methods are used in quantifying purine analogue resistant lymphocytes in peripheral blood. A short term method described by Albertini *et al* (1988) used to measure HPRT variants is termed the autoradiographic assay and a longer term method involving culture of cells is termed the cloning assay and is used to identify mutants. In the autoradiographic assay, lymphocytes are stimulated into cellular division with PHA and the addition of 6-thioguanine. Tritiated thymidine is added and incubated until culture termination at 42 hours to label DNA-synthesising cells and 6-thioguanine containing cultures are enumerated. In the cloning assay described by O'Neill *et al* (1987), cells are plated on microtitre wells and positive clones are cultured for 12 to 17 days and may then be isolated and further propagated for molecular analysis of the mutant HPRT genes.

Although direct comparisons of HPRT mutations to other endpoints for known chemicals have shown to be the least sensitive (Tates *et al*, 1991), population exposures are often to unspecified

chemicals. Thomas *et al* (1999), reported HPRT mutations at low dose, subacute occupational radiation exposures in patients 6 to 10 years after from the Chernobyl nuclear power plant accident.

1.1.5 Chromosome aberrations in lymphocytes

Structural chromosomal aberrations may result from direct DNA breakage, replication on a damaged DNA template or inhibition of DNA synthesis (Bender *et al*, 1974). Ionising radiation and bleomycin induce direct DNA breakage resulting in chromosome-type aberrations in G_0/G_1 cells and chromatid-type aberrations in S/G_2 cells (Evans and O’Riordan, 1975). The induced aberrations may persist throughout the cell cycle and are detected in the following mitosis. In non-cycling cells such as mature lymphocytes, re-entry into proliferation can be induced by *in vitro* stimulation with agents such as PHA (Albertini *et al*, 2000). Most other clastogens induce chromatid-type aberrations after cells have entered S-phase. Aberrations resulting from inhibition of DNA synthesis may occur when the clastogen, e.g. hydroxyurea, is present in high concentrations during the S-phase of the cell cycle.

Numerical chromosomal aberrations refer to changes in the number of chromosomes due to abnormal cellular division. Aneuploid cells contain either more or less than the normal number of chromosomes while polyploid cells contain multiples of the normal complement of chromosomes. Structural chromosome aberrations are visible changes in the shape of chromosomes, such as reciprocal changes, dicentric chromosomes, centric and acentric rings, interstitial and terminal deletions. They are further subdivided as “stable aberrations”, i.e

regularly propagated into the daughter cells and “unstable aberrations” i.e. leading to reproductive cell death in the first or a following mitosis after irradiation (Albertini *et al*, 2000). During chronic exposure to genotoxic agents, the number of observed aberrations is dependant on the dose, duration and frequency of exposure to the agent and may be influenced by the extent of DNA repair subsequent to exposure.

Mononuclear cells are separated from whole blood and cultured in medium containing PHA as the mitogen. It is essential that cells are arrested during the first metaphase to reduce the dilution of chromosomal damage. Cells are arrested using a cytokinesis blocking agent and allowed to continue culturing for a short period. After harvesting, cells are treated with a hypotonic solution, fixed and dropped onto glass slides. Metaphase spreads are examined for simple chromosomal aberrations e.g. breaks, deletions, gaps, ring chromosomes and dicentric chromosomes (Sumner, 1972).

In addition to classical aberration scoring, fluorescent *in situ* hybridisation (FISH) can be used to identify structural aberrations (Smith *et al*, 1998). Cells are stained with whole chromosome paint probes of different colours. FISH allows for the chromosome-specific centromeric DNA probes to be used in identification of whole chromosomes observed in micronuclei.

There is evidence that an increased frequency of structural chromosomal aberrations is associated with an increased risk of cancer (Sachs *et al*, 1996).

Sister chromatid exchanges arise from exposure to genotoxic agents that induce DNA damage that interferes with DNA replication. The exchange of the damaged DNA template involves breakage and rejoining. As the mechanism for sister chromatid exchange is unclear and the intra-individual variability of results is high, the assay is not used routinely as an endpoint. Mononuclear cells are cultured in the standard manner and arrested in the second metaphase cycle of cellular division. Slides are stained with Giemsa and sister chromatid exchanges are identified according to the banding pattern of chromosomes.

1.1.6 Apoptosis studies

Apoptosis is characterised by cellular shrinkage, marked condensation and margination of chromatin, nuclear and cellular fragmentation (Darzynkiewicz *et al*, 1992) and has been recognised as a feature of radiation-induced damage as early as 1955 and also reported by Falkvol (1990), Stephens *et al* (1991), Stephens *et al*, (1993) and Meyn *et al* (1993). Over the past few years a number of assays have been developed to quantify apoptosis. Flow cytometry is a quick and reliable method of evaluating apoptosis in peripheral leukocytes (Crompton and Ozsahin, 1997) and can be used to evaluate low dose radiation induced apoptosis (Hertveldt *et al*, 1997). Up to six different cell populations can be characterised simultaneously for DNA content. Cytotoxicity can then be defined as cell populations with reduced fluorescent intensity. Many markers for apoptosis have been reported e.g. Annexin V and 3,3 dihexyloxacarbocyanine iodide (Hertveldt *et al*, 1997). Apoptotic cells can also be identified using a modification of the comet assay namely the “ghost assay”. As apoptotic cells are devoid of DNA, traditional staining methods with ethidium bromide are not intense enough to detect “ghosts”. The use of YOYO-1

dye is used to identify apoptotic cells.

1.2 Ionising radiation and thorium exposure

Ionisation is the process whereby atoms usually lose electrons and thus become electrically charged and are known as ions. Ionising radiation is the term used to describe the transfer of energy in the form of either electromagnetic waves or subatomic particles that are capable of causing ionisation in matter (Smith, 1993). When ionising radiation passes through matter, energy is transferred to matter as ions are formed.

Cancer is the main long-term consequence of exposure to ionising radiation (Sali *et al*, 1996), with leukaemia being most strongly related to radiation exposure, usually manifesting between two and five years after exposure. The effects of high doses of short duration have been well documented (Sali *et al*, 1996), whereas the effects of continuous exposure to low doses of ionising radiation are not as clearly understood. Current risk estimates of continuous exposure to low doses are largely extrapolated from data from atomic bomb survivors in Hiroshima and Nagasaki. As these survivors received acute high-dose-rate exposures, these models are subject to uncertainty (Cardis *et al*, 1995).

Monazite is the primary ore of several rare earth metals (Figure 1), most notably thorium and the rare earth elements. Thorium is a naturally occurring radioactive metal present in rocks, soil, above- and underground water, plants and animals, contributing to weak background radiation of such substances. Rocks in underground mines may contain more concentrated forms of

thorium, usually in the form of thorium dioxide. The US Department of Health has determined that thorium dioxide is a known carcinogen and inhalation of thorium dust may result in increased risk of developing lung disease and lung cancer (ATSDR Public Health Statement: Toxicological Profile for Thorium, 1990). Occupational and experimental studies have shown that the lung, liver and haematopoietic system are the target organs following inhalation exposure to thorium.



Figure 1. Photograph of a 10 mm sample of the rare earth metal, monazite showing a characteristic crystal morphology. Thorium-bearing Monazite is radioactive and is mined for its uses in the aerospace and nuclear industries. (*Minerals of the World*, Spring Books, London, 1989)

More than 99 % of natural thorium exists as thorium-232 which is not stable and decays into a small “alpha” particle and a larger decay product which is also unstable and decays until a stable product is formed. During these decay processes, a series of new substances e.g. radium

and radon, alpha particles, beta particles and gamma radiation are formed. The alpha particle emission rate from thorium is low and the particle cannot penetrate human skin deeply, but can travel short distances in the body, whereas the emission rate for gamma radiation from thorium is very low and can penetrate human skin and tissue (Smith, 1993). Daughter products from thorium, viz. radium and thoron emit more gamma radiation than thorium-232. The radioactive half life of thorium-232 is 14 billion years and uses of thorium include ceramics, lantern mantels, metals used in the aerospace industry and in nuclear reactions.

The field of radiation physics is complex and is not within the scope of this study. The reader is referred to the International Commission for Radiological Protection (Smith,1993) recommendations for additional information. Briefly, the quantities used to measure the amount of ionising radiation have been based historically on the number of ionising events or the total amount of energy deposited in a defined mass of tissue. Although these measurements purposely provide the assessment of the average values of the total ion charge respectively, the total energy deposited in small samples of matter, irrespective of the actual discontinuities of these quantities due to the ionising particle tracks and the atomic interaction along these tracks, they have been shown to correlate well with the resultant biological effects (Smith, 1993). The decay rate of the number of nuclei in an amount of a radioactive isotope is called the “activity” of this radioactive substance. The old unit of activity is the Curie (Ci), equating to $3,7 \times 10^{10}$ disintegrations (decay events) per second. Thorium is expressed in pCi. The SI unit for activity is the Bequerel (Bq) which is equal to 1 disintegration per second or 27 pCi. The fundamental dosimetric quantity is the absorbed dose which measures the energy absorbed per unit mass expressed as joule per

kilogram or Gray (Gy) or rad. The old unit rad equals 0.01 Gy. The effects of radiation depend not only on the absorbed dose, but also the type and energy of the particular radiation. A weighting factor, q , is applied to the absorbed dose, depending on the quality of the radiation and this product is referred to as the dose equivalent e.g. alpha radiation carries a quality factor (q) of 20 to convert absorbed dose to dose equivalent. The unit of dose equivalent is also the joule per kilogram since q is a dimensionless factor, but for distinction from the absorbed dose, it is referred to as the Sievert (Sv) or rem (roentgen-equivalent-man). In radiological protection, it is the dose equivalent that is of interest.

As the process of ionisation changes atoms or molecules, it may cause damage to cells. If cellular damage occurs, and the cell is not adequately repaired, the cell may not survive or reproduce or it may result in a modified cell. Two effects may result from these changes. Most organs may be unaffected by the loss of a substantial number of cells, however, if the number is large enough, there will be harm resulting in a loss of tissue function of that organ. These effects are known as deterministic effects (Smith, 1993). If the irradiated cell is modified rather than killed, the clone of cells resulting from proliferation of the modified cell may manifest in a malignancy. The probability of cancer resulting from exposure usually increases with dose and these effects are known as stochastic effects. If damage occurs in a cell which transmits genetic information to future generations and the effects are expressed in the progeny, the effects are known as hereditary effects (Smith, 1993).

Large and small amounts of radiation are damaging to health. Current scientific consensus is that

radiation increases the probability of cancer and it is assumed that no threshold level exists below which there is no additional risk of cancer. Although there is some experimental evidence that radiation stimulates a number of cellular functions including the immunological response, repair of previous radiation damage and modification of hormone balances, the data has been inconclusive due to statistical difficulties at low doses. This phenomenon is termed “hormesis” and is addressed by Luckey (1991).

At present, there is considerable debate regarding the cancer risks to people chronically exposed to low and very low levels of radiation. Since there is a continuous exposure to small amounts of radiation in the environment, the minimum level that constitutes a health hazard is still unclear. Very little is known on specific long-term or short-term exposure levels to thorium that result in harmful effects on humans and animals (ATSDR Public Health Statement: Toxicological Profile for Thorium, 1990).

Radiation is a health risk as radioactive elements emit electromagnetic radiation that damage cells. Although the mechanism of toxicity for all effects is not well understood, evidence exists that the effects of thorium are due to the radiological and not chemical effects. Two epidemiological studies (Polednak *et al*, 1983; Albert *et al*, 1955) examined mortality rates among thorium workers exposed to between 0.001-0.007 Bq/m³ and neither study conclusively found a significant increase from controls. In both studies, workers were exposed to other toxic compounds as well as other radioactive materials. It was also concluded that the increase may have been attributable in part to smoking. The most comprehensive estimate of the carcinogenic

effects of low doses of ionising radiation was reported by Cardis *et al* (1995) where a significant increase in leukaemia, especially myeloid leukaemia, was shown among nuclear industry workers in the U.S., U.K. and Canada. Specific cancer type investigation showed an increase only in multiple myeloma.

Hartley and Hewson (1993) showed that current assessment of the internal dose received by thorium workers is complicated and accompanied by considerable uncertainty. The conversion of intake to effective dose is based on limited experimental studies and that development of biological modelling parameters is vital to improve estimation of internal dose following internal thorium inhalation.

1.3 Histology of radiation exposed tissues

Experimental studies have shown that exposure to radiation may lead to the onset of fibrosis and an inflammatory response in the lung and other tissues. The vascular response to radiation in the lungs of rats exposed to doses of between 11 and 18 Gy of gamma radiation is a decreased blood flow due to the development of pneumonitis (Peterson *et al*, 1992). The results suggested that endothelial as well as other cellular damage contributes to the development of post-irradiation fibrosis in the lung. In a study undertaken to determine individual radiosensitivity using lymphocytes of breast cancer patients with excessive normal tissue damage after radiotherapy, ten of the sixteen patients showed late complications such as fibrosis and telangiectasia. Experimental studies on effects of intracoronary beta-irradiating stents, showed no evidence of

necrosis, inflammation or excess fibrosis at doses of between 7 and 56 Gy in (Waksman *et al*, 1995 and Laird *et al*, 1996) arteries respectively. Tolerance of rat rectum to radiation was investigated by van der Kogel *et al* (1998) and showed late type injuries characterised by vascular injury, fibrosis and mucosal cysts at doses of between 6.5 Gy of X-rays and 13 Gray of pions. van Kleef *et al* (2000) demonstrated mild histological changes in kidneys of Rhesus monkeys 6-8 years after whole body exposure to between 4.5 - 8.5 Gy. Changes were generally mild and seen only in kidneys exposed to more than 7 Gy and included capillary dilation, fibrosis and slightly increased numbers of macrophages, indicating a mild inflammatory response.

Miller *et al* (1986) used sheep antibodies to bovine type I collagen to detect type I collagen expression in lung sections of irradiated mice. After immunohistochemical staining, an increasing dose response curve was observed in the alveolar walls of the mice exposed to between 0 and 10 Gy of ^{60}Co , with reproducible results at doses of 5 Gy and higher. The authors suggest the use of this technique to investigate the role of connective tissue macromolecules in the development of radiation pneumonitis and fibrosis.

Progressive lung damage was observed by Likhachev (1973), in a study where rats were exposed to varying concentrations of thorium dioxide. The severity of the damage and the time taken to observe the effects was directly related to the radiation dose received. At doses of up to 150 rad, reticulosarcoma was reported while at lung exposures of 100 - 2700 rad, glandular cancerous tumours were reported. Hodge and co-workers (1960) found no haematological nor histopathological effects on the lungs and bones of rats, guinea pigs, rabbits or dogs exposed

to 20 Bq/m³ of thorium dioxide. Although Xhing-an *et al* (1993) reported no excess lung cancers in a group of rare earth mineworkers exposed to between 0.85 and 5.56 Bq thorium, the incidence of respiratory symptoms, lung function disorders and pneumoconiosis were significantly increased among the miners exposed to thorium dust. It was suggested, however, that the observed respiratory tract disorders may have been due to other chemicals present in the dust.

1.4 The role of p53 in radiation exposure

Cancer has two heritable properties, viz to proliferate against normal constraints and to invade normal healthy tissues (Malkin, 1994). If clustered in a single mass which can be removed surgically, it is known as a benign tumour whereas if it enters the blood stream or the lymphatics and metastasises to other sites, it is malignant. Malignant tumours can often be traced to a single cell that has been changed i.e. there is a clonal origin of tumours. Carcinogenesis and mutagenesis has been well established with three main causative agents, viz. chemical carcinogens which cause changes in the DNA sequence, viruses which introduce foreign DNA into a cell and ionising radiation which results in chromosome breaks and induces DNA translocations (Malkin, 1994).

The most frequently encountered genetic event in human malignancy is the alteration of the p53 gene and its encoded protein (Levine *et al*, 1991). p53 was located by McBride *et al* (1986) and Miller *et al* (1986) on the short arm of chromosome 17, band 13 and is approximately 20 kb in length, encoding a 53 kD nuclear phosphoprotein containing 393 amino acids with 11 exons. DNA sequence analysis showed that the p53 gene has five highly conserved domains contained

in exons 1, 4, 5, 7 and 8, which are thought to be essential for normal functioning of p53. Figure 2 shows the structural features of the p53 tumour suppressor gene and the changes induced by ionising radiation.

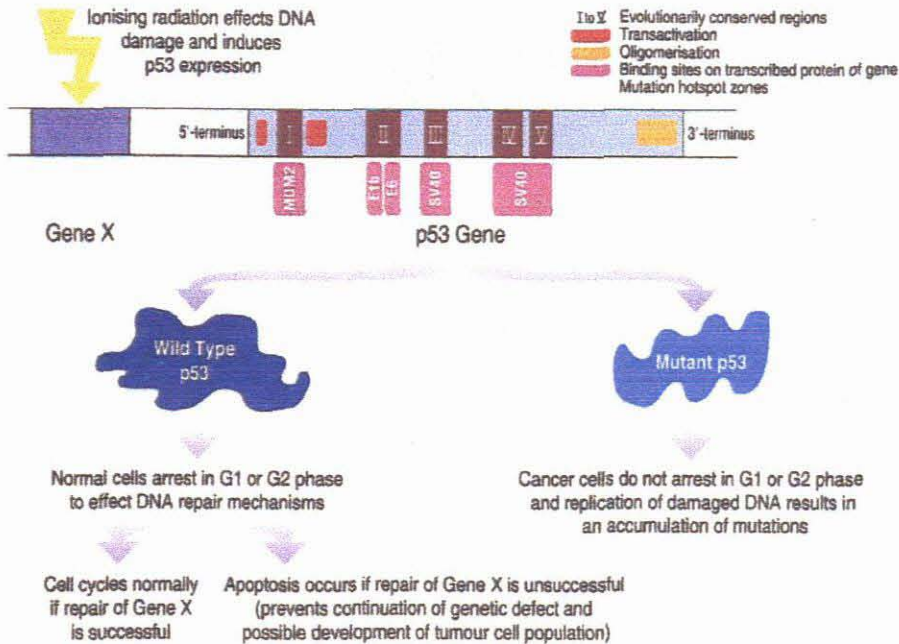


Figure 2. Diagrammatic representation of the structural features of the p53 gene and possible pathways after ionising radiation induced p53 gene expression. Normal cells arrest in G1 or G2 phase and may either continue if gene repair is successful or apoptosis occurs if gene repair is unsuccessful. Cancer cells do not arrest and replication of damaged DNA occurs and results in mutations.

p53 frequently mutates or is lost in human tumours and when wildtype (wt) is introduced into tumours, it results in the reversal of transformed cell growth in some instances. p53 regulates cell division by arresting cells in the G₁ phase of the cell cycle to allow for DNA repair. Should repair be unsuccessful, p53 is triggered and apoptosis (programmed cell death) is mediated. The importance of an intact p53 gene and its protein is therefore vital in normal cell proliferation.

Mutant p53 can act in a dominant fashion once mutated and the mutant proteins have a longer half-life than wild-type p53 and are known to accumulate to high levels in tumour cells compared to the low levels seen in normal cells. The elevated p53 is often located in the cell nucleus (Harris and Hollstein, 1993).

Takahashi *et al* (1989) found mutated or inactivated p53 genes in all types of human lung cancers and Iggo *et al* (1990) also suggested that p53 is the gene that most commonly undergoes mutation in lung cancer. In 1994, Kemp and co-workers reported that a single dose of 4 Gy radiation dramatically decreased the latency time for tumour development in p53 heterozygous mice and that at a lower dose of 1 Gy, tumour latency was also greatly reduced in preweanling p53 null mice, suggesting that p53 is a target for radiation-induced malignancy. Lumniczky *et al* (1998) reported allelic losses at the p53 locus in mouse liver and lung tumours induced by *in utero* exposure to 0.2 - 2 Gy of gamma radiation suggesting that oncogenic pathways are activated during *in utero* exposure to ionising radiation.

Mutations produce abnormal p53 proteins that are far more stable than wild-type p53. The half-life is increased from around twenty minutes to several hours due to the increased stability of the protein, and as a result, mutant and not wild-type p53 can be readily detected by conventional immunohistochemical techniques in the cell nucleus (Allred, 1993, Vojtseek, *et al*, 1992). Macallum *et al* (1996) used immunohistochemistry to demonstrate the accumulation of high levels of p53 in murine tissues after exposure to ionising radiation which may lead to the development of lung cancer.

1.5 Radiation effects on the haematopoietic system

Chronic radiation exposure may give rise to a number of haematological defects which are collectively termed “preleukaemia” or the myelodysplastic syndrome (MDS) which is irreversible and may lead to the onset of acute non-lymphocytic leukaemia over a period of months to years. The syndrome is characterised by a number of features including refractory peripheral blood cytopenias with dysplastic morphology and the presence of abnormal progenitor cells in the bone marrow (Oscier, 1997). The precise relationship between leukaemia risk and low-dose radiation exposure is unclear, but increased evidence for radiation exposure in the development of MDS is emerging (Bowen and Yoshida, 1998). Estimates had previously been extrapolated from high dose exposure, however, the cellular response to chronic low-dose exposure appears to be different to that of medium to high dose exposure.

Experimental studies suggest that the induction of mutations by ionising radiation follows a complex dose-response with enhanced mutagenesis at low to medium dose exposure and a lower response at higher doses due to enhanced cellular killing (Sankaranarayan, 1993). As the rate of mutation increases, so does the propensity for neoplastic cellular transformation. The bone marrow is therefore amongst the tissues most susceptible to the neoplastic effects of ionising radiation. Although the increased incidence of acute leukaemias in humans exposed to radiation is well documented (Roesch, 1987), the relationship between radiation dose and leukaemia risk is not well defined. Early studies on Japanese atomic-bomb survivors suggested a linear regression dose-response curve for medium to high dose exposure (Rotblat, 1988), whereas current studies indicate that the cellular response to chronic low-dose radiation is fundamentally

different from that of medium to high dose exposure over shorter time periods (Roesch, 1987). The complex relationship appears also to be influenced by the type of radiation (Rotblat, 1988).

Haematopoietic progenitor cells in the bone marrow appear to be capable of an adaptive response to chronic low-dose radiation in that cells have an ability to repair sub-lethal damage with an increase in radioresistance and an ability to continue proliferating with accumulating radiation dose (Seed and Meyers, 1993). However, associated with this, is a loss of normal DNA fidelity. Yau *et al*, (1979) showed that radiosensitive lymphoid cells (L 5178y) showed increased radioresistance after chronic low dose radiation as well as an increased mutation rate and an increased tendency toward proliferative clonal expansion.

Exposure to ionising radiation may produce distinct morphological changes in the bone marrow which may vary with respect to the quality, dose, dose-rate and age at the time of radiation exposure (Seed *et al*, 1987). MDS is an irreversible and progressive clonal alteration to the stem cell population which results in progenitor cells that initially mature but are structurally and functionally defective. The abnormal cells eventually replace the normal population and cause a defective haematopoiesis and decrease in the number of peripheral cells (Countenay, 1969). An increased rate of mutation appears to be characteristic of MDS due to progressive dysplastic cell maturation over time. Features of MDS have been well documented by the French American British Cooperative Group (FAB) (Bennett *et al*, 1985). Peripheral blood findings indicate microcytic as well as nucleated erythrocytes. A characteristic finding is a dimorphic picture with

normocytic or microcytic erythrocytes and macrocytes. Leukocyte abnormalities in the peripheral blood include immature as well as dysplastic granulocytes that may show defective granulation. Hyposegmented forms are common as well as pseudo-Pelger-Huet cells. Cytochemical staining of granulocytes may show a deficiency of myeloperoxidase. Platelet abnormalities include large platelets and circulating megakaryocyte fragments, megakaryocytes in the bone marrow may show hypo- and/or hypersegmented nuclei and micromegakaryocytes may be seen as well (Ruutu, 1986). The type, intensity and the duration of radiation exposure as well as the age of the irradiated individual will determine the severity of the bone marrow damage. The damaged bone marrow may follow one of four patterns viz. complete recovery, early post-irradiation change without complete restitution, the development of MDS with or without complete restitution or the development of MDS with or without subsequent leukaemia as a later event (Ruutu, 1986). Repeated marrow injury usually leads to permanent hypocellularity with dysplastic changes. Most individuals chronically exposed to a significant dose of radiation will develop hypoplastic or dysplastic marrow changes, yet only some will develop leukaemia. The increased risk of developing leukaemia has been associated with the occurrence of chromosomal abnormalities (Pierre, 1978).

The tendency of α -emitters to have a strong affinity for bone and bone marrow where they become incorporated and accumulate, leads to this type of radiation being a potent cause of bone cancer and leukaemia (Lord and Henry, 1995).

Small animals are more tolerant of whole-body irradiation than large animals such as man. The

LD_{50/30} (death of 50% of animals within 30 days) ranges from 15 Gy for small animals to 3-4 Gy for larger animals. A likely reason may be that small animals may be able to tolerate higher levels of depletion of progenitor cells better than larger animals (Lord and Henry, 1995). It is clear that long-term malformation of haematopoietic tissue may result from maternal contamination during pregnancy. Injection of plutonium-239 into pregnant mice showed a 2500-fold difference in the radiation levels in the liver and 500-fold difference in the bone marrow between contamination of the mother during embryonic development compared with direct contamination after weaning. From the extent of haematopoietic damage, it is clear that embryonic haematopoiesis is considerably more sensitive to α -particle irradiation than adult haematopoiesis (Lord and Henry, 1995). In contrast, a Relative Biological Efficiency (RBE) of 300 of γ -radiation dose was required to match the damage caused by α -particle damage to the bone marrow, showing that foetal haematopoiesis is extremely sensitive to this form of radiation. Neonatal animals have also been found to absorb 20-40 times more thorium than adult animals (Sullivan, 1980 and Sullivan *et al*, 1983).

Precise factors in leukaemogenesis is unknown and controversial. Leukaemia progression is associated with chromosomal abnormalities. Studies of radiation on haematopoietic tissue have indicated that not all responses are as a result of direct damage to the stem cell but also the effects on the regulatory control of the micro-environment. In combination with specific chromosomal changes, damage to the micro-environment may induce haematopoietic cells to develop in an uncontrolled manner. Endothelial cells are a critical component of the stroma in the regulation of haematopoiesis and dysfunction of these cells is a classic consequence of

radiation damage. Gaugler *et al* (1998) demonstrated changes in bone marrow epithelial cells after *in vitro* irradiation.

Foetal bones are formed around the sixth week of gestation by endochondrial ossification where cartilage is laid down and begins to proliferate. By the twelfth week, chondrocytes are hypertrophic and begin to calcify the cartilage. Intramembranous periosteal bone then forms around the shaft of the long bones and perivascular cells invade the hypertrophied chondrocytes and erode the cartilage, leaving spicules of calcified cartilage. Osteoblasts then align themselves and are responsible for production and deposition of the bone matrix and calcium. Spicules of calcified cartilage grow to form bone trabeculae. Osteoblasts then become enclosed in the bone matrix and become mature osteocytes, responsible for maintaining the bone matrix. Haematopoietic cells migrate to the ossifying cavities around the twelfth week of gestation. Trabecular spaces in the bone marrow are relatively small and are within α -particle range of a bone surface. As there are no fat cells in foetal bone marrow, there are more target cells for leukaemogenesis. There is evidence that the total equivalent dose of α -radiation received by the bone marrow rises sharply after birth due to the higher breathing rate and lung development in the young (Henshaw, 1995). The steady rise after the age of twenty is associated with the increase of fat in the marrow as some α -emitters such as the radon isotope have a high affinity for fat.

A full blood count on a cohort of 273 male workers at a monazite refinery was undertaken by Conibear (1983) to determine the effect of thorium on the haematopoietic system. It was

reported that the full blood counts did not correlate with the thorium doses received by the workers and as the workers were also exposed to cigarette smoke, other toxic compounds and other sources of radioactivity, the toxic effects could not be attributed to thorium. Xhing-an and co-workers (1993), also reported that miners exposed to thorium in a rare earth mine exhibited no changes in the peripheral blood. However, no additional investigations into haematological parameters were undertaken in these studies. Effects on haematological parameters were, however, found in dogs exposed to thorium e.g. thorium dioxide (150 Bq/m^3) for 6 hours per day, 5 days per week (Hall *et al*, 1951). These changes included abnormal forms of leukocytes, hypoplastic bone marrow, red cell count depression and an increase in immature granulocytes (Hall *et al*, 1951). Hodge *et al* (1960) observed no change in haematological parameters in rats, guinea pigs and dogs exposed to a dose of 20 Bq/m^3 of thorium dioxide. A significant increase in the incidence of haematopoietic cancers was found in uranium mill workers (Archer, 1973) where the radioactivity was attributed to α -emissions from thorium-230. Concentrations of thorium isotopes in bone and other tissues of autopsy samples was investigated in three areas viz Grand Junction, USA (Ibrahim *et al*, 1983), Colorado, USA (Wrenn *et al*, 1981) and Washington DC, USA (Singh *et al*, 1982). The maximum concentration of all isotopes was found in the tracheobronchal lymph nodes, with lungs and bones containing the next highest concentration. Autopsy data of individuals exposed to thorium in the environment showed that pulmonary lymph nodes contained the highest concentrations of thorium, followed by the lungs and then bones (Sunta *et al*, 1987). Sullivan *et al* (1983) showed that 50 % of absorbed thorium was retained in the skeleton of neonatal rats and 75 % in the skeleton of adult mice.

Very little data exists on the health effects due to inhalation exposure to humans and animals (ATSDR Public Health Statement :Toxicological Profile for Thorium, 1990). The existing data suggests that thorium may pose a potential health threat to exposed populations. The main issue regarding thorium is the potential radiological effect since thorium is an alpha-emitting bone seeker and the small amount that enters the body migrates to bone surfaces.

1.6 Assays to evaluate radiation induced DNA damage

1.6.1 The micronucleus assay in peripheral lymphocytes

The micronucleus assay was first described by Fliedner *et al* (1964) as an important tool in the field of radiation biological dosimetry and continues to be used as an effective biological indicator for radiosensitivity (Schmidt, 1975; Countryman and Heddle, 1976; Almassy et al, 1987). Chromosomal damage to lymphocytes results in augmentation of cells containing a micronucleus. Fenech and Morley (1985) introduced the cytokinesis blocking agent, cytochalasin B thus enabling discrimination of cells that had undergone one mitotic division (binucleated) from those that had not (mononucleated). Bat lymphocytes that had not undergone mitosis were therefore excluded from the analysis. Micronuclei enclose acentric chromosome fragments or whole chromosomes that have not been incorporated in the main nucleus at cell division. Trinucleated and tetranucleated lymphocytes represent lymphocytes that have undergone more than one division and these cells were also excluded from the analysis. The nucleation index, as described by Imamura and Edgreen (1994), reflects the distribution of the number of nuclei per lymphocyte and is an important indicator of the success of the lymphocyte culture. Indices for bat cultures are therefore reported in this investigation.

1.6.2 The micronucleus assay in peripheral reticulocytes

Historically, the rodent micronucleus assay has been widely used to evaluate chemical clastogenicity using bone marrow polychromatic erythrocytes as target cells (Heddle *et al*, 1983 and Mavournin *et al*, 1990). The use of mouse peripheral blood was introduced by MacGregor *et al* (1980), but since discrimination between young and mature erythrocytes was not clear with conventional staining methods, the use of peripheral blood was not pursued as a screening technique. Supravital staining of mouse peripheral blood was introduced by Hayashi *et al* (1990) and Hayashi and Sofuni (1994) in which reticulocytes were easily identified after acridine-orange staining by their red fluorescing reticulum structure, resulting in a less subjective assay. Micronuclei, on the other hand are easily identified by their strong green fluorescence due to the presence of chromatin. Although the use of mouse peripheral erythrocytes had been reported by MacGregor *et al* (1980), until recently, bone marrow erythrocytes were still the target cells used in mutagenicity testing. The results of Hayashi *et al* (1992) demonstrated the validity and reliability of this simple and inexpensive assay. Kolanko and co-workers (1999) described the development of a mouse specific probe to verify micronuclei in reticulocytes without the use of fluorescent microscopy resulting in permanent colour and indefinite storage of slides. To date, the assay used in this study has not been applied to evaluate potential clastogenicity resulting from radiation exposure.

1.6.3 The single cell gel electrophoresis (comet) assay

The single cell gel electrophoresis assay, or comet assay, was first described by Östling and Johanson (1984) to detect DNA damage using neutral electrophoretic conditions. A later

modification of the assay using alkaline conditions (pH >13) allowed detection of single-strand breaks and alkali-labile lesions (Singh *et al*, 1988). While biomonitoring studies using cytogenetic assays are limited to circulating lymphocytes and proliferating cell populations, the SCGE assay may be applied to any cell population and cells of tissues being the first site of contact with mutagenic or carcinogenic substances e.g. the oral and nasal mucosa cells (Kassie *et al*, 2000). The assay is rapid, sensitive and simple (Fairbairn *et al*, 1995) and is widely used to detect DNA damage at the individual cell level caused by physical and chemical genotoxic agents (McKelvey-Martin *et al*, 1993). Since exposure to radiation in the workplace or in the environment is usually low or even close to background level, Olive *et al* (1990) and Vijayalaxmi *et al* (1992) documented the usefulness of the assay in the detection of low dose radiation-induced DNA damage.

1.7 Radiation - induced chromosomal aberrations

The formation of chromosomal aberrations was reported over 50 years ago, but the relationship between primary DNA damage and visible chromosome aberrations remains unclear. It is acknowledged though, that a DNA double-strand break (dsb) leads to chromosome aberrations (Bryant, 1997). After ionising radiation has induced the double-strand break, illegitimate unions and rearrangement of fragments causes aberrations in the chromosome that have been considered as the causes of most radiobiological effects (Sachs *et al*, 1996). Aberrations have been used in biodosimetry, as indicators of radiosensitivity and some are strongly linked with haematopoietic cancers (Ban *et al*, 1997). High linear energy transfer (LET) radiation is more effective at producing dsb than low LET radiation.

The most commonly observed chromosome aberrations are “exchange-type” aberrations that result from misjoining of two or more dsb regions. Radiation damage to chromosomes can be measured at a number of levels. Classically, metaphase spreads can be examined using conventional brightfield microscopy and the number of dicentric or centric ring chromosomes per cell will be an indication of the extent of DNA damage (Sachs *et al*, 1996). Gaps and breaks may also be identified as shown in Figure 3.

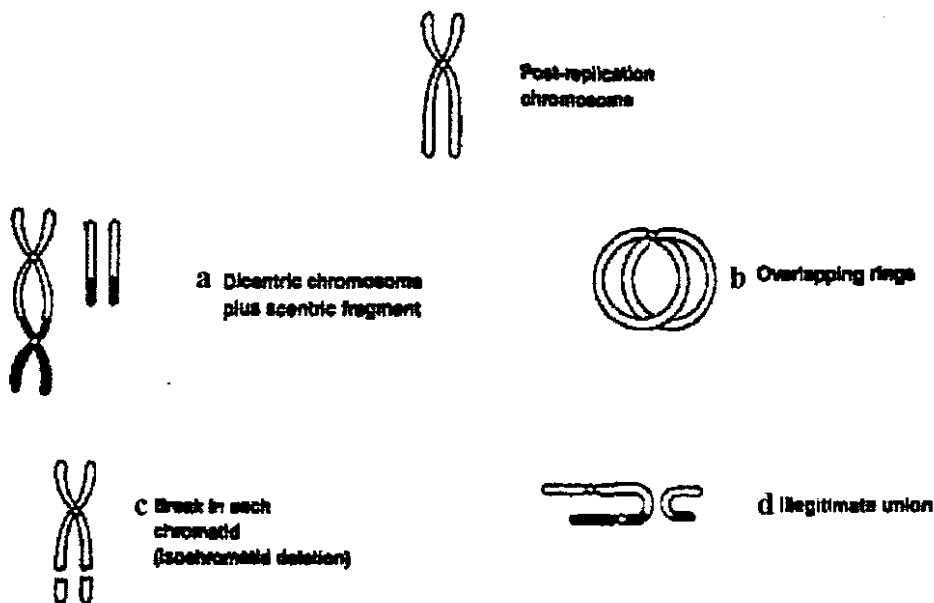


Figure 3. Diagram showing chromosome aberrations induced by ionising radiation e.g. a dicentric chromosome and an acentric fragment (a), an overlapping ring chromosome (b), a break in each chromatid (c) and an illegitimate union giving rise to a gap (d). Metaphase spreads can be examined and the number of aberrations observed serves as an indication of the extent of DNA damage.

Other aberrations e.g. translocations and inversions require detailed banding analysis. Although scoring of stable aberrations such as translocations is the method of choice after acute exposure to radiation, but not unstable aberrations such as dicentrics (Tanaka *et al*, 1996), classical

methods are widely used for chronic exposures. With the advent of fluorescent *in situ* hybridisation (FISH), chromosome painting with probes specific for a particular chromosome number has dramatically increased the scope of aberration studies where many simple and complex aberrations have been reported, including studies conducted after radiation exposure (Stephan and Pressel, 1996, Lindholm *et al*, 1996 and Bauchinger *et al*, 1996). By using FISH, chromosome 4 was shown to exhibit the highest frequency of translocations induced after radiation exposure (Knehr *et al* 1996).

1.8 Steenkampskraal monazite mine

The Namaqualand metamorphic complex in South Africa is host to a number of monazite deposits. The largest of these is at Steenkampskraal, 350 km north of Cape Town (Figure 4), and has been mined intermittently for thorium since the 1950's (Andrioli *et al*, 1994). After commencing operation in 1952, the first radiation survey was undertaken in 1953 using a portable gamma ray detector. Underground gamma radiation levels monitored 25 mr/h (1.2 r/48h week) and dust levels of 14 mg/m³ were reported (Du Toit, 1964). After another survey in 1955, the mine authorities took steps to reduce the levels of employee exposure by improving the ventilation. A third radiation survey was conducted in 1958 by using an ionisation-chamber dose-rate meter calibrated against radium where radiation levels of up to 10 mr/h was measured (Du Toit, 1964). Production ceased shortly after this survey.

In 1962 the mine was reopened with more stringent safety control measures, notably reduction

of exposure time and short contract employment periods. Gamma ray intensities were similar to those measured previously, however, doses received by employees did not exceed 7 rad/year. An alpha radiation estimation was also conducted in 1962 where thoron daughters were measured through millipore filters and were measured with a scintillometer. Between 1952 and 1963, Steenkampskraal represented the world's leading producer of thorium and rare earth elements (Andrioli *et al*, 1994). The mine ceased operation in 1963, but renewed interest since the 1980's in rare earth metals as a valuable resource has resulted in investigations into the viability of the mine becoming operational again.

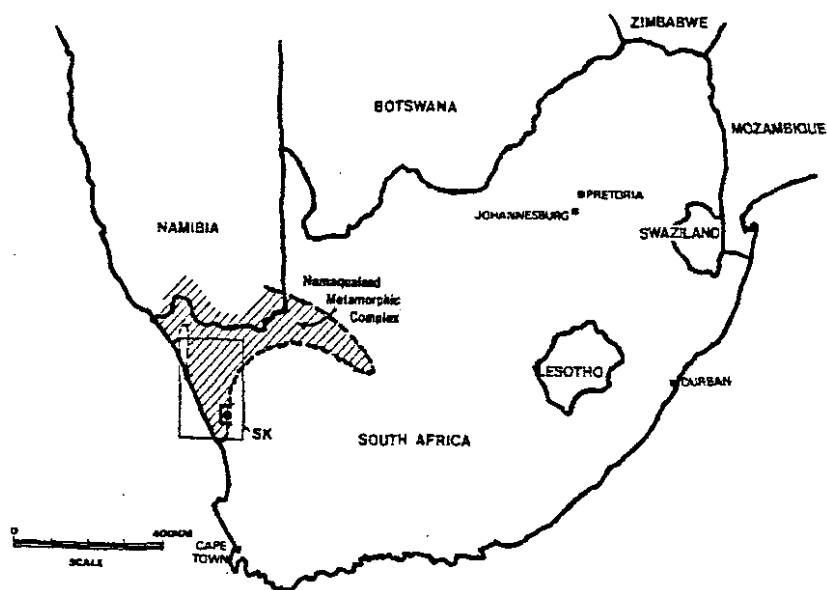


Figure 4. Locality map of the monazite mine at Steenkampskraal, approximately 350 km north of Cape Town, South Africa. Steenkampskraal forms part of the Namaqualand metamorphic complex which is host to a number of monazite deposits.

During the inactive period since 1963, a population of bats (*Chiroptera*), *Rhinolophus capensis*,

(Figure 5) have inhabited the abandoned mine and have been roosting there for a number of years. The bats hibernate during the winter months and are therefore exposed to continuous low levels of ionising radiation. It is of particular interest that the bats mate during autumn and store the sperm over winter, conceiving and gestating young at the beginning of spring (Nowack, 1994). Germline DNA is therefore exposed to the radiation for approximately three months before foetal development. This study presented a unique opportunity to study the effects of continuous exposure to low doses of ionising radiation.



Figure 5. Photograph of a *Rhinolophus capensis* bat residing in the abandoned monazite mine. All Rhinolophids have leaf-like protuberances on their noses and are dull-brown to reddish brown in colour. *Rhinolophus capensis* bats weigh approximately 10g and have a wingspan of 22 cm. (Courtesy Prof. Brock Fenton, Professor of Biology, York University, Canada)

CHAPTER TWO

MATERIALS AND METHODS

2.1 Sample Collection

Adult *Rhinolophus Capensis* bats (Chiroptera) (Figure 5) weighing between 9 and 14 g were collected from the abandoned radioactive monazite mine at Steenkampskraal in Namaqualand, South Africa (Figure 4). The radioactivity in two areas of the mine where the bats were found to be roosting were measured for levels of total external radioactivity by means of a portable gamma ray detector Ludlum 14C (Ludlum Measurements Inc., Sweetwater, Texas) and measured to be around 20 $\mu\text{Sv/h}$ and 100 $\mu\text{Sv/h}$ respectively. The same species of bat was collected approximately 500 km from Steenkampskraal in a cave at the de Hoop Nature Reserve where no detectable levels above normal background radiation ($< 2 \mu\text{Sv/h}$) were measured.

As Chiroptera are a protected species in South Africa, a permit was granted by the Department of Nature Conservation to collect and sacrifice a limited number of bats.

Prior to commencing the study, five bats exposed to radiation were screened for traces of Na-22, K-40, Sr-85, Tl-208, Pb-212, Ra-224, Ac-228 and Th-228 by means of a TNI GammaTrac Browser (Oxford Instruments - Nuclear Measurements Group) to ensure the absence of internal, ingested radioactivity.

Bats were anaesthetised with halothane gas and blood was collected aseptically by cardiac

puncture. Tissues were collected post mortem and fixed in either 10 % formal saline, snap frozen in liquid nitrogen or placed in Zenkers acetic fixative (See appendix).

2.2 Histological methodology

2.2.1 Tissue preparation

The liver and lungs were removed post mortem from each bat under aseptic conditions. Representative samples of each organ were taken and placed in a solution of 10% buffered formal saline, pH 7.4. Samples were placed in cassettes and processed in an automated tissue processor. After embedding in wax, tissue blocks were sectioned to 3 μm using a Riechert Jung 2040 rotary microtome. Sections were collected on clean glass slides and prepared for staining.

The remainder of the tissue was immediately snap frozen in liquid nitrogen and stored in Eppendorf tubes at -80 °C until required.

2.2.2 Staining techniques

A section of lung and liver tissue from control and radiation exposed bats was stained using the Haematoxylin and Eosin technique (see Appendix) for investigation of general histological architecture. Liver and lung samples from bats exposed to radiation were then stained using the Verhoef van Gieson technique (see Appendix) to identify fibrosis. Liver samples were stained using the Alcian Blue PAS technique (see Appendix) for the identification of mucin. Tissues were examined microscopically at 400x magnification. Control bat tissue was compared to tissue from bats exposed to radiation.

2.3 Immunohistochemistry using a monoclonal p53 antibody

3µm sections of formalin-fixed, paraffin embedded lung and liver samples from control and radiation-exposed bats were mounted on positively charged silanised slides to ensure adhesion of sections during heat mediated antigen retrieval (HMAR) and incubated at 56°C for 1 hour to facilitate drying. After dewaxing in xylol and hydrating through graded alcohols, HMAR was performed in a Presto pressure cooker for 2 minutes at full pressure (15 lbs at 121 °C) in a 3M urea solution (see Appendix).

After thorough washing in water, sections were processed on the Nexes automated immunostainer (Ventana Medical Systems, Tuscon, Arizona, USA). Briefly, slides were exposed to an aqueous solution of 3 % hydrogen peroxide to inhibit endogenous peroxidase activity and washed in buffer supplied by the manufacturer. The primary p53 antibody (Mouse monoclonal - Code M7001 DAKO A/S Copenhagen, Denmark) was applied at a 1:10 dilution for 32 minutes at 42 °C. and washed in buffer supplied by the manufacturer. The secondary biotinylated IgG antibody was added and the slides incubated for a further 8 minutes at 42 °C. After washing, samples were incubated with Streptavidin - Horseradish peroxidase (HRP) for 8 minutes at 42° C.

Visualisation and development of the chromogenic substrate was as recommended by the manufacturers; DAB Basic Detection Kit (Code M760-001, Ventana Medical Systems). Sections were counterstained briefly with Haematoxylin (see Appendix), blued in Scott's tap water, dehydrated through graded alcohols to xylol and then mounted in Entellan.

Positive human breast tumour samples were included with each batch as an internal control. Negative controls, both human and test material, were also included by omitting the p53 antibody.

Examination of sections was by light microscopy at 400x magnification. One hundred bronchiolar lining cells, one hundred alveolar cells and one hundred liver cells were examined per sample and cell nuclei exhibiting a brown precipitate, which represented antigen/antibody complexes, were graded as 1+ (weakly positive), 2+ (moderately positive) and 3+ (strongly positive).

2.4. Haematological methodology

2.4.1 Peripheral blood analysis

Approximately 300 μ l of blood was collected from each bat by means of a cardiac puncture and placed into Eppendorf tubes containing 1 mg/ml EDTA as the anticoagulant. Full blood counts were performed immediately using a Coulter counter (Model T890) set on the veterinary mode to account for the small size of bat erythrocytes. Each batch of bats collected was assigned a batch number viz. H1 - H3 (control), S1 - S4 (20 μ Sv/h) and S5 - S7 (100 μ Sv/h). A normal range for the sampled control population was determined for White Cell Count (WCC); Red Cell Count (RCC); Haemoglobin (Hb); Haematocrit (Hct) and Mean Cell Volume (MCV) and compared to bats exposed to radiation. Due to the inclination of the bat thrombocytes to clump, platelet counts were not included in the analysis. A peripheral blood smear was made on a clean glass slide and stained using the Wright's Romanowsky staining technique (see Appendix) and

a differential count was performed on each bat blood sample. One hundred white blood cells were counted per bat and the percentage of neutrophils, lymphocytes, monocytes, eosinophils and basophils (Figure 6) were reported. Pseudo-Pelger Huet cells which are a characteristic feature of radiation exposure were observed (Figure 6) and expressed as a percentage of the total neutrophil count.

The WCC was used to determine the absolute counts for each cell type. As morphological changes were evident in bats exposed to radiation, subsequent bat blood samples were also subjected to specialised stains. A non-specific esterase stain (see Appendix) was performed to identify leukocytes of the monocytic lineage. Monocytes stained moderately to strongly positive as they contain esterases which hydrolyse naphthalene. A naphthyl compound is liberated and couples with a diazonium salt present in the mixture, resulting in a brightly coloured precipitate at or near the site of enzymatic activity. Monocytic cells were expressed as a percentage of all cells.

A myeloperoxidase stain (DAB) was performed to differentiate between neutrophils and monocytes (see Appendix). Peroxidases are haematopoietic enzymes which, in the presence of hydrogen peroxide catalyze the oxidation of substrates including phenols, several amino acids and some aromatic acids.

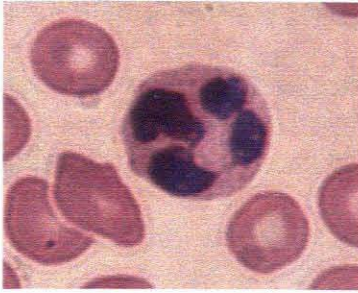
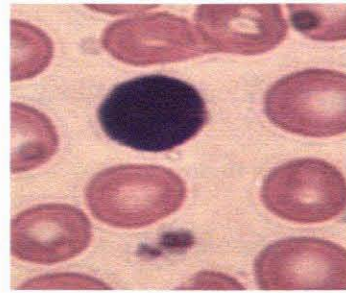
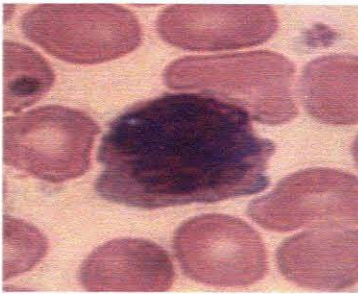
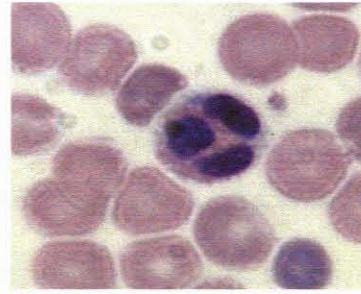
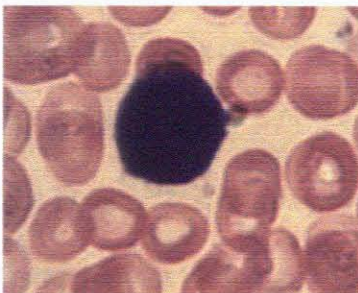
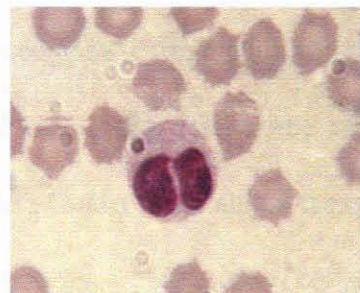
**a) Neutrophil****b) Lymphocyte****c) Monocyte****d) Eosinophil****e) Basophil****f) Pseudo-Pelger Huet**

Figure 6. Photomicrographs of leukocytes identified in bat peripheral blood showing characteristic morphological features of a neutrophil with polymorphonuclear morphology and agranular cytoplasm (**a**), a lymphocyte with mononuclear morphology and condensed chromatin (**b**), a monocyte with mononuclear, large and irregular morphology (**c**), an eosinophil with polymorphonuclear morphology and orange-red cytoplasmic granules (**d**), a basophil with violet cytoplasmic granules (**e**) and a pseudo-Pelger Huet cell with unique binucleated nuclear morphology (**f**).

Golden brown positive granules precipitate and fill the cytoplasm of neutrophils from the promyelocyte stage to the segmented forms whereas most cells from the monocytic lineage are peroxidase negative, but can be weakly positive. Granular precipitation in the cytoplasm of control neutrophils was compared to neutrophils from the radiation-exposed bats.

2.4.2 Trephine Biopsies

As differences in peripheral blood analysis in control and radiation exposed bats were evident, subsequent sample collections included collection of the breast bone from control and test bats. After removal, breastbone samples were placed in Zenkers acetic fixative (see Appendix) for four hours and washed overnight in tap water. Samples were decalcified the following day with Formalin decalcifying solution (see Appendix) and processed in an automated tissue processor. After embedding in wax, 7 μ m sections were cut on an Ames Rotary microtome and stained using the Haematoxylin and Eosin technique (see Appendix). Control and radiation exposed bat breastbone sections were examined microscopically for cellularity, architecture of cells and bone structure. Attempts at retrieving bone marrow aspirates from the wing bones of bats in order to perform a myelogram was unsuccessful as no representative smear could be made due to inadequate amounts of marrow.

2.4.3 Bone mineralisation using image analysis

As the architecture of bone sections from radiation exposed bats appeared abnormal, Haematoxylin and Eosin stained breast bone biopsy samples from control and radiation-exposed bats were examined for mineralisation of bone osteoid using an Image Analysis System

(OPTIMAS 6.1) whereby mineralisation was determined by a variation in intensity of light absorbed by the osteoid and was digitally graded according to predetermined parameters and expressed as a percentage. Bone mineralisation of control bats was compared to that of radiation-exposed bats.

2.5 DNA damage evaluation

2.5.1 Micronucleus assay in peripheral lymphocytes

Bat lymphocytes were cultured using the method of Paul and Chakravarty (1987). Whole blood was collected aseptically into EDTA tubes. As a volume of 3-5 ml is recommended for human lymphocyte culture and only approximately 350 μ l blood was obtained per bat, blood from six bats were pooled into one tube. Blood was diluted with phosphate buffered saline (PBS) (see Appendix) and layered on Ficoll Histopaque (Sigma Co., USA). After centrifugation at 100 xg for 30 minutes, the erythrocytes sedimented and the lymphocyte layer was carefully removed. Lymphocytes were washed twice in PBS by centrifugation at 100 x g for 7 minutes and resuspended in up to 5ml RPMI medium containing 10% Foetal Calf Serum (FCS). Phytohaemagglutinin (Gibco) was selected as the mitogen and added to a final concentration of 10 μ g/ml to stimulate bat lymphocytes into cell division. Samples were incubated at 37°C in an incubator containing 5% CO₂ and 95% air. A culture time of 90 hours proved to be optimal to stimulate the bat lymphocytes into cellular division. After 90 hours, Cytochalasin B (Sigma), a cytokinesis blocking agent, was added to the lymphocyte culture to a final concentration of 3 μ g/ml and incubated for a further 30 hours. Samples were then centrifuged to pellet the lymphocytes which were resuspended in 500 μ l of the supernatant, placed on clean glass slides

and fixed with methanol/acetic acid (3:1). Slides were prepared for fluorescent microscopy after staining with a 10µg/ml acridine orange solution as described by Hayashi *et al* (1983). Nucleation indices were determined for each slide before micronuclei were scored. Tetranucleated and quatanucleated lymphocytes were excluded from the analysis as they had undergone more than one cellular division. According to the criteria of Heddle (1973), micronucleus scoring included sharply bordered nuclei and a spatial separation between the main, or macronucleus, and the micronuclei. Micronuclei had to be more than 20% but less than 50% of the macronucleus diameter, and fluoresce with the same intensity as the main nuclei. The number of micronuclei per lymphocyte were recorded and the micronuclei frequencies per 500 binucleated lymphocytes in test and control groups compared.

2.5.2 Micronucleus assay in peripheral reticulocytes

Acridine orange coated slides were prepared according to the method of Hayashi *et al* (1990). Briefly, 20 µl of a 1 mg/ml acridine orange aqueous solution was spread homogeneously on a glass slide pre-warmed to 70°C. 5 µl of peripheral whole blood was drawn by means of cardiac puncture and placed in the centre of the pre-warmed slide. The slide was covered immediately with a coverslip and placed overnight at 4°C to allow the cells to settle and take up the stain. The supravitaly stained reticulocytes were examined the next day by fluorescence microscopy. Young reticulocytes were examined as described by Vander *et al* (1963). The nuclei of nucleated cells fluoresced strongly green whereas reticulum structures of reticulocytes fluoresced strongly red. Micronuclei were identified as being round in shape and exhibiting a strong yellow-green fluorescence due to the presence of chromatin. One thousand reticulocytes were observed per

bat sample and the frequency of micronuclei in test and control samples were scored.

2.5.3 Single cell gel electrophoresis (comet) assay

The Single Cell Gel (SCGE) assay, first described by Östling and Johanson (1984) to assess DNA damage on an individual cell basis, was adapted by Singh *et al* (1988) to an alkaline technique which is able to detect single-strand breaks. Slides were dipped in a hot 1% normal melting agarose (NMA) (see Appendix) solution made up in calcium/magnesium- free phosphate buffer and allowed to cool completely. 75µl of bat whole blood (~ 10 000 leukocytes) was mixed with a 0.5% solution of low melting point agarose (LMPA) (see Appendix), cooled to 37°C and spread on the coated slide. The slide was covered with a coverslip and placed on ice to set. The coverslip was removed and a third layer of 75µl of LMPA agarose was applied. The coverslip was replaced and the slide was placed on ice to set. After the agarose had set, the slides were placed in freshly prepared cold lysing solution (see Appendix). Slides were left overnight at 4°C to ensure complete lysis of erythrocytes. Preparation of the slides and lysis was performed in the dark to prevent any additional DNA damage. After lysis, slides were placed in an alkaline electrophoresis buffer (see Appendix) for 30 minutes to allow the DNA to unwind. Slides were then electrophoresed for 30 minutes at 25V and 300mA. After electrophoresis, slides were washed with neutralisation buffer (see Appendix), dipped briefly in cold 100% ethanol and allowed to dry. Slides were prepared for fluorescence microscopy by staining with 100µl of 2µg/ml ethidium bromide (see Appendix). For visualisation of DNA damage, observations were made using a 40x objective and a fluorescence microscope equipped with an excitation filter of 515-560nm and a barrier filter of 590nm. In this procedure, one is able to visualise the nuclear

matrix with a fluorescent halo formed by undamaged, non-migrating DNA. Damaged cells appear as “comets”, consisting of a “head” (the nuclear matrix) and a “tail” (damaged DNA fragments migrating in the electric field) as shown in Figure 7. DNA damage is directly proportional to the length of the comet tail. One hundred comets were analysed per sample and graded from 1 to 4 according to the length of the comet tails using the criteria of Lebailley *et al* (1997). A sample of normal human lymphocytes was run with each assay as an internal control.

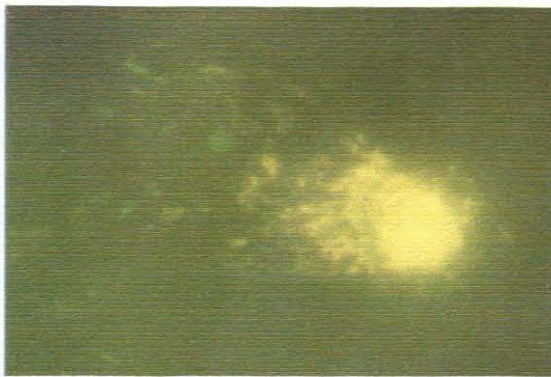


Figure 7. Photograph of DNA damage as shown by the comet assay, indicating the head and the tail of the “comet”. Lymphocytes are suspended in agarose and electrophoresed under alkaline conditions. DNA damage is proportional to the length of the “comet” tail. (magnification : 600x)

2.6 Cytogenetic techniques

Bat lymphocytes were cultured using the method of Paul and Chakravarty (1987). Whole blood was collected aseptically into EDTA tubes. As a volume of 3 - 5 ml is required for human lymphocyte culture and only approximately 350 μ l blood was obtained per bat, blood from six bats were pooled into one tube. Blood was diluted with phosphate buffered saline (PBS) (see Appendix) and layered on Ficoll Histopaque (Sigma Co., USA). After centrifugation at 100 x g

for 30 minutes, the erythrocytes sedimented and the lymphocyte layer was carefully removed. Lymphocytes were washed twice in PBS by centrifugation at 100 x g for 7 minutes and resuspended in up to 5 ml RPMI medium containing 10 % Foetal Calf Serum (FCS). Phytohaemagglutinin (Gibco) was selected as the mitogen and added to a final concentration of 10 µg/ml to stimulate bat lymphocytes into cell division. Samples were incubated for 90 hours at 37°C in an incubator containing 5 % CO₂ and 95 % air. For the last five hours of culture time, Colcemid (Gibco) was added to a final concentration of 0.1 µg/ml to block the dividing lymphocytes in the metaphase. Lymphocytes were therefore cultured for a total of 95 hours. The method described by Sumner (1972) was used to prepare chromosomes for staining. Briefly, cultures were centrifuged at 100 x g for 5 minutes and the supernatant discarded. After gently resuspending the cells, 3 ml of a 0.56 % KCl solution was added dropwise, while vortexing, to the tubes and left to stand for 20 minutes. The tube was then centrifuged at 150 x g for 5 minutes, the supernatant discarded and the lymphocytes resuspended. The same procedure was carried out twice using Carnoy's fixative as 3 parts methanol : 1 part acetic acid. After the final spin, the supernatant was discarded leaving approximately 0.5 ml to resuspend the lymphocytes.

Glass slides were cleaned and placed at -4° C until required. A retort stand was set up with a Pasteur pipette and cells were drawn into the pipette and dropped from a distance of 20 cm onto a cold slide. Slides were allowed to dry overnight and stained with Giemsa staining method (see Appendix). 100 metaphases per group were viewed using a 100 x objective with ordinary light microscopy for the presence of dicentric chromosomes, ring chromosomes, breaks and gaps as shown in Figure 3 (Pg 28).

CHAPTER 3

RESULTS

3.1 Histology

Tissue sections were examined by light microscopy and included lung and liver samples of control and radiation exposed bats. Liver samples of control and radiation exposed bats stained with Haematoxylin and Eosin showed normal liver lobules with large, polyhedral hepatocytes arranged as plates converging upon the central vein (Figure 8(a)). Cell nuclei stained blue-black by haematoxylin and the cytoplasm and most connective tissue stained varying shades of pink, orange and red.

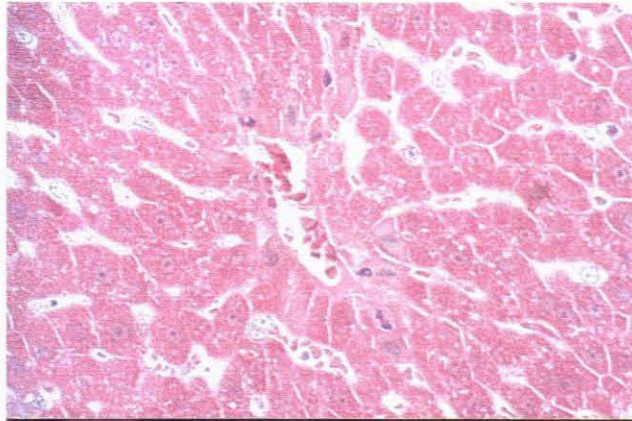


Figure 8(a). Photomicrograph of a liver sample from a radiation exposed bat stained with Haematoxylin and Eosin as described in Materials and Methods. Normal morphology was observed and showed normal liver lobules with hepatocytes converging upon the central vein. (Magnification : x 400).

Figure 8(b) demonstrates the presence of glycogen in the hepatocytes after staining with Alcian Blue PAS, indicating normal, well-nourished bats. The remaining cytoplasm was strongly eosinophilic due to a high content of cell organelles. Acid mucins stained blue, neutral mucins magenta and nuclei pale blue. There appeared to be no difference in the presence of mucin between control and radiation exposed bats.

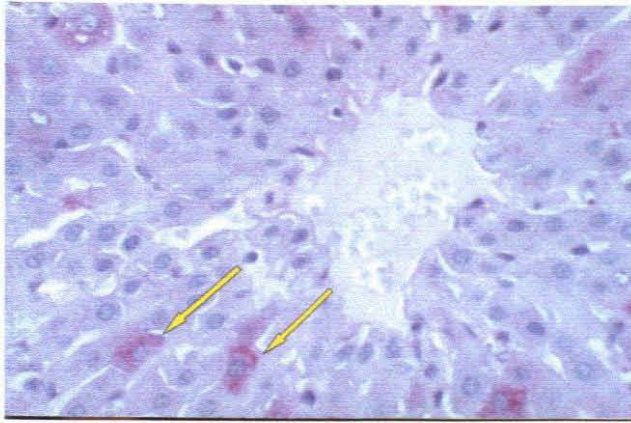


Figure 8(b). Photomicrograph of a liver sample from a radiation exposed bat stained with Alcian Blue PAS as described in Materials and Methods. The presence of glycogen in hepatocytes (shown by arrows) indicated normal, well-nourished bats. (Magnification: x400)

Liver samples stained with the Verhoef van Gieson showed no fibrosis in control and radiation exposed bat liver sections (Figure 8(c)) Elastic fibres and nuclei stained black, collagen red and muscle, red cells and background stained yellow.

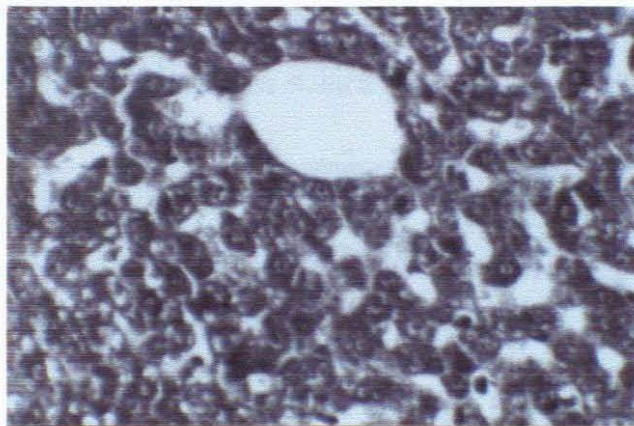


Figure 8(c). Photomicrograph of a liver sample from a radiation exposed bat stained with Verhoef van Gieson as described in Materials and Methods. Cell nuclei stained black and no collagen (red staining) was observed, indicating normal morphology. (Magnification: x 400).

Lung samples of control and radiation exposed bats stained with Haematoxylin and Eosin showed normal histology with no pathology of the terminal portion of the respiratory tree. The

alveolar ducts, respiratory bronchioles and alveoli appeared to be normal (Figure 9(a)).

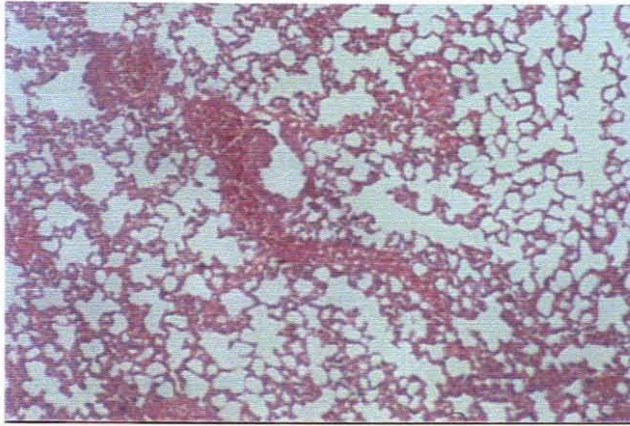


Figure 9(a). Photomicrograph of a lung sample from a radiation exposed bat stained with Haematoxylin and Eosin as described in Materials and Methods. Alveolar ducts, respiratory bronchioles and alveoli showed normal lung morphology (Magnification: x 100).

No obvious fibrosis was found to be present in lung sections from both control and radiation exposed bats when stained with Verhoef van Gieson as demonstrated in Figure 9(b). Elastic fibres and nuclei stained black and collagen stained red.

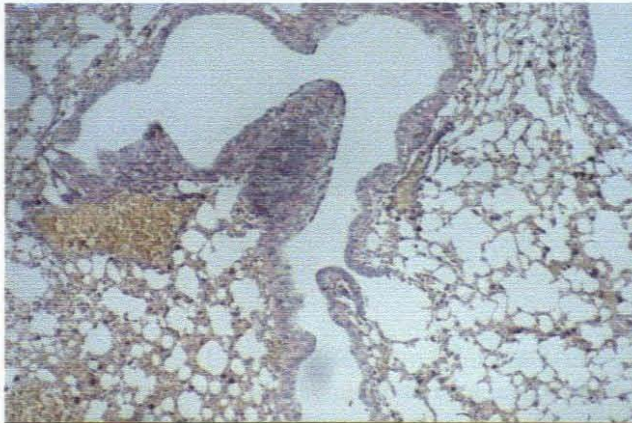


Figure 9(b). Photomicrograph of a lung sample from a radiation exposed bat stained with Verhoef van Gieson as described in Materials and Methods showing normal staining of elastic fibres (black) and collagen in blood vessels (red) and no visible lung fibrosis. (Magnification: x 100).

3.2 p53 immunohistochemistry

Sections of lung and liver tissue were examined for the presence of a brown precipitate in the nuclei of the cells which represented the presence of p53 antigen / antibody complex formation as described in materials and methods. An internal control was included in the staining procedure as shown in Figure 10. Two areas of the lung, viz. bronchiolar lining cells and alveolar cells were examined as there appeared to be a difference in the degree of precipitation as shown in Figure 11(a). Cells from lung sections from control bats appeared normal and stained blue (Figure 11(b)) whereas bronchiolar lining cells from radiation exposed bats showed positive immunohistochemical staining (Figure 11(c)) as did the alveolar cells (Figure 11(d)).

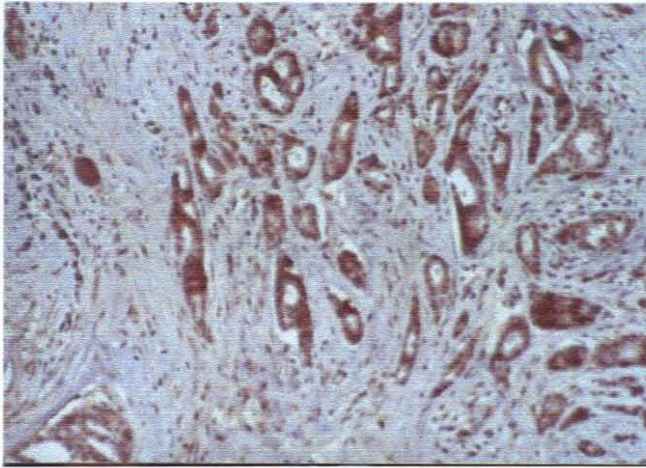


Figure 10. Photomicrograph of a tissue section from a human breast cancer used as the internal p53 positive control. Brown immunohistochemical staining indicates the presence of p53 antigen/antibody complexes. (Magnification : x 100)

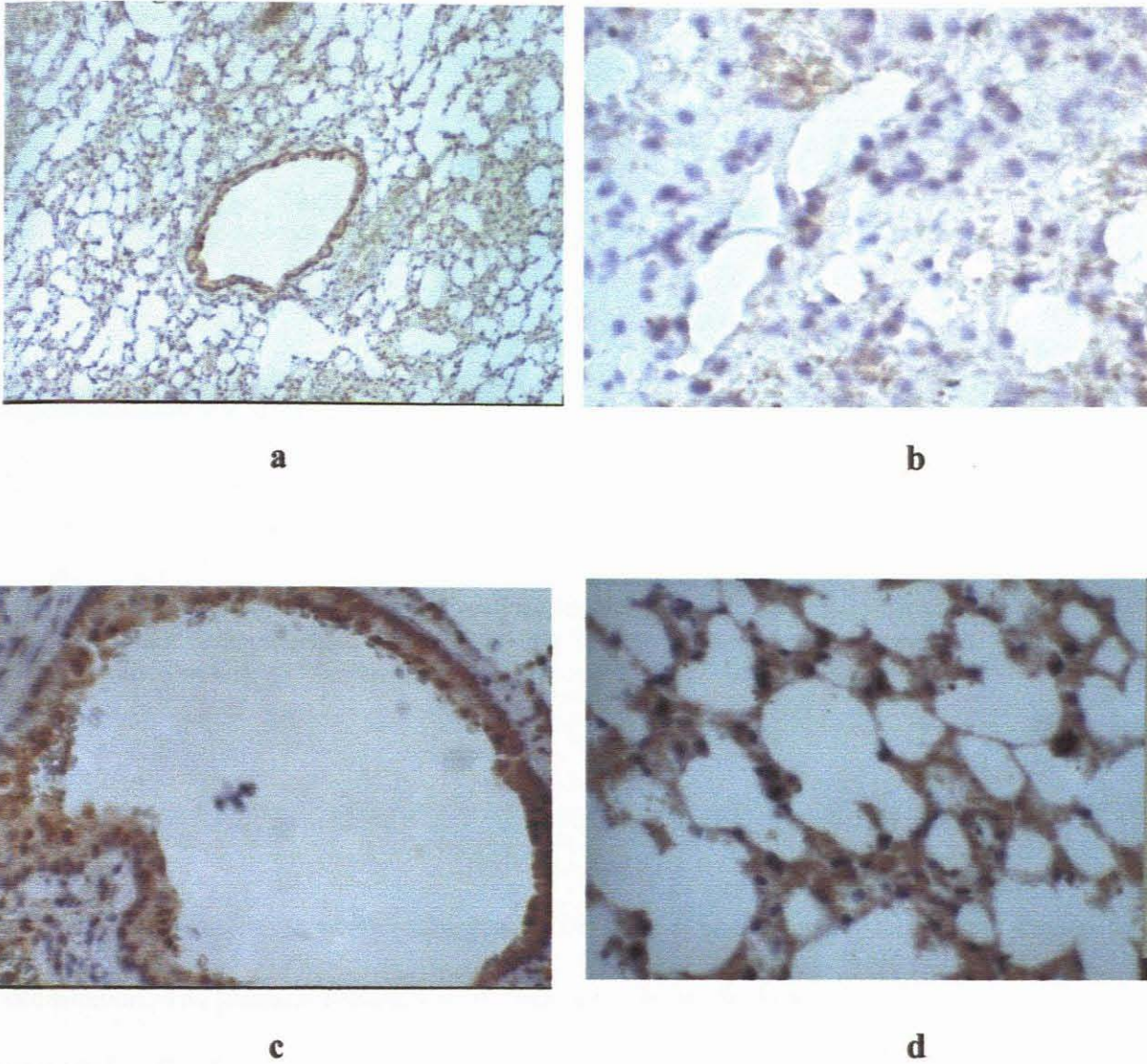


Figure 11. Photomicrographs of bat lung samples stained with a monoclonal p53 antibody as described in Materials and Methods showing the difference in the degree of positivity between bronchiolar lining cells and alveolar cells (a) (Magnification: x 100); a lung section from a control bat (b) (Magnification: x 100); positive p53 immunohistochemical staining of the bronchiolar lining cells of a radiation exposed bat (c) (Magnification: x 400) and positive p53 immunohistochemical staining of alveolar cells in a radiation exposed bat (d) (Magnification: x 400)

Liver sections from control bats appeared normal (Figure 12(a)) whereas sections from radiation exposed bats showed an increased immunohistochemical staining of p53 protein as shown in

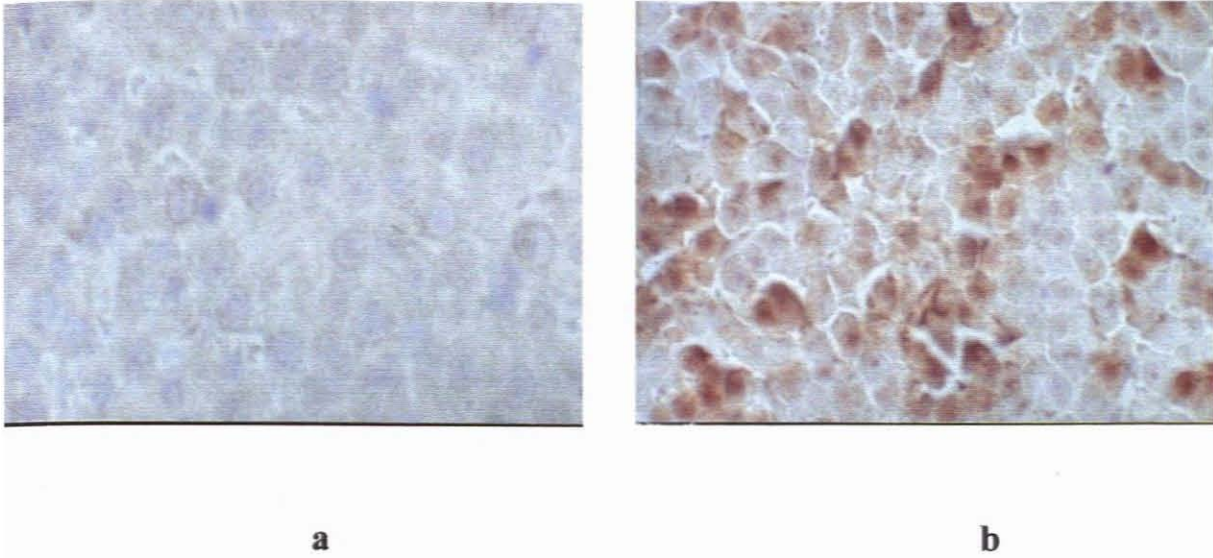


Figure 12. Photomicrographs of bat liver samples showing a section from a control bat showing no positive immunohistochemical staining for p53 **(a)** and a radiation exposed bat showing positive nuclear p53 immunohistochemical staining **(b)** (Magnification: x 400).

Figure 12(b).

100 cells per tissue were scored and graded between 0 and 3+ according to the degree of precipitation. The average percentage of negative cells in the bronchiolar lining was 94.9 % compared to 22.1 % in the control group. The average of 1+, 2+ and 3+ cells in the same area was 5.1 %, 0 % and 0 % respectively in the control group and 33 %, 41 % and 4 % respectively in the radiation exposed group (Table I).

The alveolar lining of the control bats showed 97 % negative cells compared to 36.1 % in the radiation exposed bats and 5.2 %, 0 % and 0 % compared to 33 %, 26 % and 4.4 % of 1+, 2+ and 3+ cells (Table I). Examination of liver sections showed similar findings as 99.4 % cells were negative and 0.6 %, 0% and 0% were 1+, 2+ and 3+ respectively compared to radiation exposed

samples which showed an average of 62.5 % negative cells and 23 %, 13 % and 2.1 % showing 1+, 2+ and 3+ positivity (Table I). Graphic comparisons are shown in Figure 13.

p53 immunohistochemistry

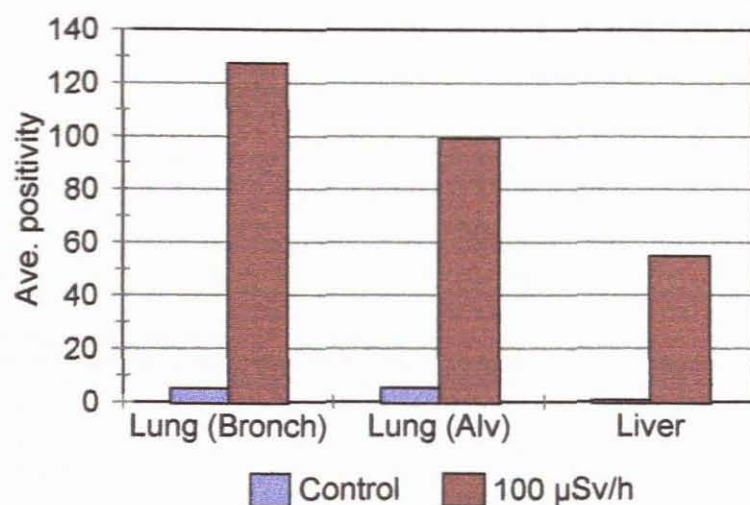


Figure 13. Graphic representation of p53 immunohistochemistry total positivity from lung and liver sections of control and 100 $\mu\text{Sv/h}$ exposed bats. In the bronchiolar lining cells (bronch), the total positivity of the control bats was 5.08 compared to 127.35 in the radiation exposed bats. The alveolar cells (alv) showed a total positivity of 5.23 in the control group compared to 99.12 in the radiation exposed bats and the liver cells showed a total positivity of 0.62 compared to 54.71 in radiation exposed bats. These results show a significant increase in p53 protein in tissues from radiation exposed bats.

Table I. Results of p53 immunohistochemistry in lung and liver sections from control and 100 $\mu\text{Sv/h}$ exposed bats. 100 cells were counted per tissue and graded according to the intensity of precipitation observed. Total positivity was calculated as described in materials and methods. Statistical analysis showed a highly significant increase ($p < 0.001$) in p53 protein expression in lung and liver sections from radiation exposed bats.

SAMPLE #	LUNG (BRONCH)					LUNG (ALV)					LIVER				
	NEG	1+	2+	3+	TOTAL	NEG	1+	2+	3+	TOTAL	NEG	1+	2+	3+	TOTAL
H 032	99	1	0	0	1	100	0	0	0	0	100	0	0	0	0
H 033	100	0	0	0	0	100	0	0	0	0	100	0	0	0	0
H 035	100	0	0	0	0	98	2	0	0	2	100	0	0	0	0
H 036	100	0	0	0	0	100	0	0	0	0	99	1	0	0	1
H 037	70	30	0	0	30	65	35	0	0	35	100	0	0	0	0
H 038	80	20	0	0	20	75	25	0	0	25	100	0	0	0	0
H 039	98	2	0	0	2	100	0	0	0	0	98	2	0	0	2
H 040	100	0	0	0	0	100	0	0	0	0	100	0	0	0	0
H 041	90	10	0	0	10	97	3	0	0	3	100	0	0	0	0
H 042	97	3	0	0	3	97	3	0	0	3	95	5	0	0	5
H 043	100	0	0	0	0	100	0	0	0	0	100	0	0	0	0
H 044	100	0	0	0	0	100	0	0	0	0	100	0	0	0	0
H 045	100	0	0	0	0	100	0	0	0	0	100	0	0	0	0
AVERAGE	94.92	5.1	0	0	5.08	94.77	5.2	0	0	5.23	99.38	0.6	0	0	0.62
SAMPLE #	LUNG (BRONCH)					LUNG (ALV)					LIVER				
100 $\mu\text{Sv/h}$	NEG	1+	2+	3+	TOTAL	NEG	1+	2+	3+	TOTAL	NEG	1+	2+	3+	TOTAL
S 065	20	10	50	20	170	30	10	30	30	160	90	5	5	0	15
S 066	0	80	20	0	120	0	70	30	0	130	40	0	50	10	130
S 067	0	80	15	5	125	10	40	40	10	150	40	40	20	0	80
S 068	10	75	10	5	110	40	60	0	0	60	90	5	5	0	15
S 069	75	15	10	0	35	90	10	0	0	10	90	10	0	0	10
S 070	50	40	10	0	60	60	30	10	0	50	70	30	0	0	30
S 071	5	20	75	0	170	10	40	50	0	140	80	20	0	0	20
S 072	10	10	75	5	175	15	30	50	5	145	80	10	10	0	30
S 073	5	10	80	5	185	25	5	60	10	155	40	25	30	5	100
S 074	0	70	30	0	130	45	53	0	3	62	0	70	30	0	130
S 075	0	10	75	15	205	10	20	70	0	160	50	35	15	0	65
S 076	50	0	45	5	105	20	60	10	10	110	80	10	10	0	30
S 077	35	0	60	5	135	30	10	60	0	130	70	30	0	0	30
S 080	95	5	0	0	5	90	10	0	0	10	100	0	0	0	0
S 081	10	10	70	10	180	70	5	20	5	60	40	25	20	15	110
S 082	0	85	15	0	115	50	50	0	0	50	40	30	25	5	95
S 083	10	40	50	0	140	19	60	20	1	103	60	40	0	0	40
AVERAGE	22.08	33	41	4.4	127.35	36.12	33	28	4.4	98.12	62.35	23	13	2.1	54.71

Bronch : Bronchiolar lining

Alv : Alveolar

p values - p53 immunohistochemistry
Control vs 100 $\mu\text{Sv/h}$

Lung - Bronch	6.1E-08
Lung - Alv	1.1E-06
Liver	0.0001

These highly significant results were confirmed by p-values calculated by statistical analysis assuming unequal variance on the total score of each tissue examined in control and 100 $\mu\text{Sv/h}$ exposed bats. Results of bronchiolar lining cells, alveolar cells and liver tissues were compared and highly significant p-values ($p < 0.001$) indicated a significant increase in p53 protein in tissues from radiation exposed bats when compared to the control group (Table I).

3.3 Haematology

3.3.1 Peripheral blood analysis

Each group of bats collected were assigned a batch number e.g. H1 - H4 for control groups, S1-S4 for 20 $\mu\text{Sv/h}$ and S5 - S7 for 100 $\mu\text{Sv/h}$ exposed bats. Full blood counts were performed on blood samples collected into EDTA of control bats and 1SD and 2SD values were reported to indicate a normal range for the White Cell Count (WCC), Red Cell Count (RCC), Haemoglobin (Hb), Haematocrit (Hct) and Mean Cell Volume (MCV) (Table II(a)). Full blood counts of each group of radiation-exposed bats was compared to the control group. Averages for each group as well as the cumulative average for the low radiation (20 $\mu\text{Sv/h}$) and high radiation (100 $\mu\text{Sv/h}$) groups were also reported (Table II(b) and II(c)). Samples which coagulated during collection were omitted from analysis.

Table II(a). Full blood counts of control bats, H1 - H3, showing results for white blood cell counts (WBC), red cell counts (RCC), haemoglobin (Hb), haematocrit (HCT) and mean cell volume (MCV). Averages were calculated for each batch and a cumulative average for the control bats was reported. 1 SD and 2 SD values are given to indicate the normal range.

SAMPLE #	WBC (x 10 ⁹ /l)	RCC (x 10 ¹² /l)	HB (g/dl)	HCT (%)	MCV (fl)
Control					
H1					
H 003	6.59	5.10	10.4	26.8	52.6
H 004	7.44	4.33	13.3	20.9	48.2
H 005	5.16	4.85	11.9	26.9	52.4
H 008	5.68	5.05	12.0	27.6	51.7
H 010	6.39	5.24	10.5	26.5	50.5
H 011	3.74	4.13	14.8	21.6	52.5
AVERAGE	5.83	4.78	12.15	25.05	51.32
H2					
H 013	4.76	4.12	15.2	15.7	44.2
H 015	6.64	4.76	17.8	18.4	45.9
H 016	5.00	4.49	12.8	16.8	47.4
H 018	5.41	4.68	14.3	18.4	49.3
H 020	4.21	3.85	14.2	15.7	40.8
AVERAGE	5.20	4.38	14.86	17.00	45.52
H3					
H 033	3.93	3.42	15.2	15.6	45.6
H 034	6.09	4.93	13.4	23.3	47.3
H 035	7.36	5.53	11.7	25.1	45.4
H 036	4.08	3.68	15.7	17.2	46.8
H 037	6.37	5.11	14.6	22.5	43.9
H 038	6.77	5.20	13.2	26.9	51.7
H 040	3.97	3.57	16.2	16.2	45.5
H 042	4.17	3.74	15.8	17.0	45.4
H 044	5.35	4.59	14.1	21.2	46.3
AVERAGE	5.34	4.42	14.43	20.56	46.43
CUM AVE	5.34	4.53	13.91	21.22	47.76
1 SD	1.12	0.59	1.72	4.19	3.13
2 SD	2.24	1.18	3.45	8.39	6.25

Table II(b). Full blood counts of 20 $\mu\text{Sv/h}$ bats, S3 - S4, showing results for white blood cell counts (WBC), red cell counts (RCC), haemoglobin (Hb), haematocrit (HCT) and mean cell volume (MCV). Averages were calculated for each batch and a cumulative average for the 20 $\mu\text{Sv/h}$ exposed bats was reported.

SAMPLE # 20 $\mu\text{Sv/h}$	WBC ($\times 10^9/\text{l}$)	RCC ($\times 10^{12}/\text{l}$)	HB (g/dl)	HCT (%)	MCV (fl)
S3					
S 085	4.88	4.34	13.5	21.3	49.0
S 086	4.41	3.83	15.0	17.5	45.6
S 087	5.55	4.47	14.7	21.2	47.5
S 088	5.34	4.46	14.4	20.7	46.4
S 089	5.37	4.46	14.9	21.1	47.3
S 090	6.48	5.09	12.5	23.7	46.5
S 091	5.77	4.71	13.8	21.9	46.5
S 092	4.79	4.04	15.7	19.2	47.6
S 093	4.49	3.93	15.6	18.4	46.8
S 094	6.65	5.16	11.9	24.4	47.4
S 095	6.82	5.41	12.4	25.1	46.3
AVERAGE	5.50	4.54	14.0	21.3	47.0
S4					
S 111	6.72	5.04	11.0	22.6	44.8
S 112	6.35	4.94	12.0	22.3	45.1
S 114	5.86	4.70	11.7	19.7	44.9
S 115	6.89	5.29	9.7	21.2	45.1
S 116	5.53	4.33	12.9	19.6	45.3
S 117	3.57	3.15	15.1	14.8	44.9
S 119	3.78	3.31	14.9	14.8	43.7
S 120	4.02	3.53	14.3	15.8	44.8
AVERAGE	5.34	4.29	12.70	18.85	44.83
CUM AVE	5.44	4.43	13.47	20.28	46.08

Table II(c). Full blood counts of 100 $\mu\text{Sv/h}$ bats, S5 - S7, showing results for white blood cell counts (WBC), red cell counts (RCC), haemoglobin (Hb), haematocrit (HCT) and mean cell volume (MCV). Averages were calculated for each batch and a cumulative average for the 100 $\mu\text{Sv/h}$ exposed bats was reported.

SAMPLE # 100 $\mu\text{Sv/h}$	WBC ($\times 10^9/\text{l}$)	RCC ($\times 10^{12}/\text{l}$)	HB (g/dl)	HCT (%)	MCV (fl)
S5					
S 003	5.94	4.85	14.3	22.4	46.1
S 004	4.98	4.16	12.2	19.0	45.6
S 005	6.45	5.06	12.7	23.4	46.2
S 006	4.70	4.18	13.4	17.9	42.8
S 009	4.37	3.85	13.4	18.4	47.8
S 010	3.23	3.01	14.7	15.1	50.4
S 012	3.59	3.38	14.9	15.3	45.3
AVERAGE	4.75	4.07	13.7	18.8	46.3
S6					
S 069	5.54	3.65	15.8	15.4	42.0
S 073	4.28	3.95	13.4	17.2	43.6
S 076	6.47	5.30	12.9	23.8	44.9
S 077	5.09	3.54	14.7	15.5	43.7
S 078	4.60	4.13	15.8	18.9	45.7
S 079	4.98	3.41	13.0	16.3	47.7
S 080	6.09	4.14	11.2	19.1	46.2
AVERAGE	5.29	4.02	13.8	18.0	44.8
S7					
S 096	3.99	3.49	13.9	15.0	43.1
S 097	4.67	3.07	13.5	15.2	43.2
S 098	6.14	4.88	11.5	20.4	41.8
S 099	5.81	4.60	12.2	20.8	45.3
S 100	4.03	3.54	13.8	15.1	42.6
S 101	4.23	3.66	15.1	16.4	45.0
S 104	7.15	5.23	10.5	22.8	43.5
S 106	3.97	3.49	14.1	15.6	44.6
S 107	5.49	4.50	12.3	20.6	45.8
S 108	3.08	2.79	15.4	12.3	44.0
S 109	4.05	3.50	14.3	15.5	44.3
S 110	5.21	4.31	12.3	18.0	41.8
AVERAGE	4.82	3.92	13.24	17.31	43.75
CUM AVE	4.93	3.99	13.51	17.90	44.73

Figure 14 shows a graphic representation of the data obtained. Paired t-test analysis assuming unequal variance was performed on the full blood counts and showed that the WCC, RCC and Hb values from all radiation-exposed bats (S3-S7) did not differ significantly from the control group. S4 and S7 showed a significant decrease in the MCV when compared to the control group, indicating the presence of microcytic red blood cells as demonstrated in Table III.

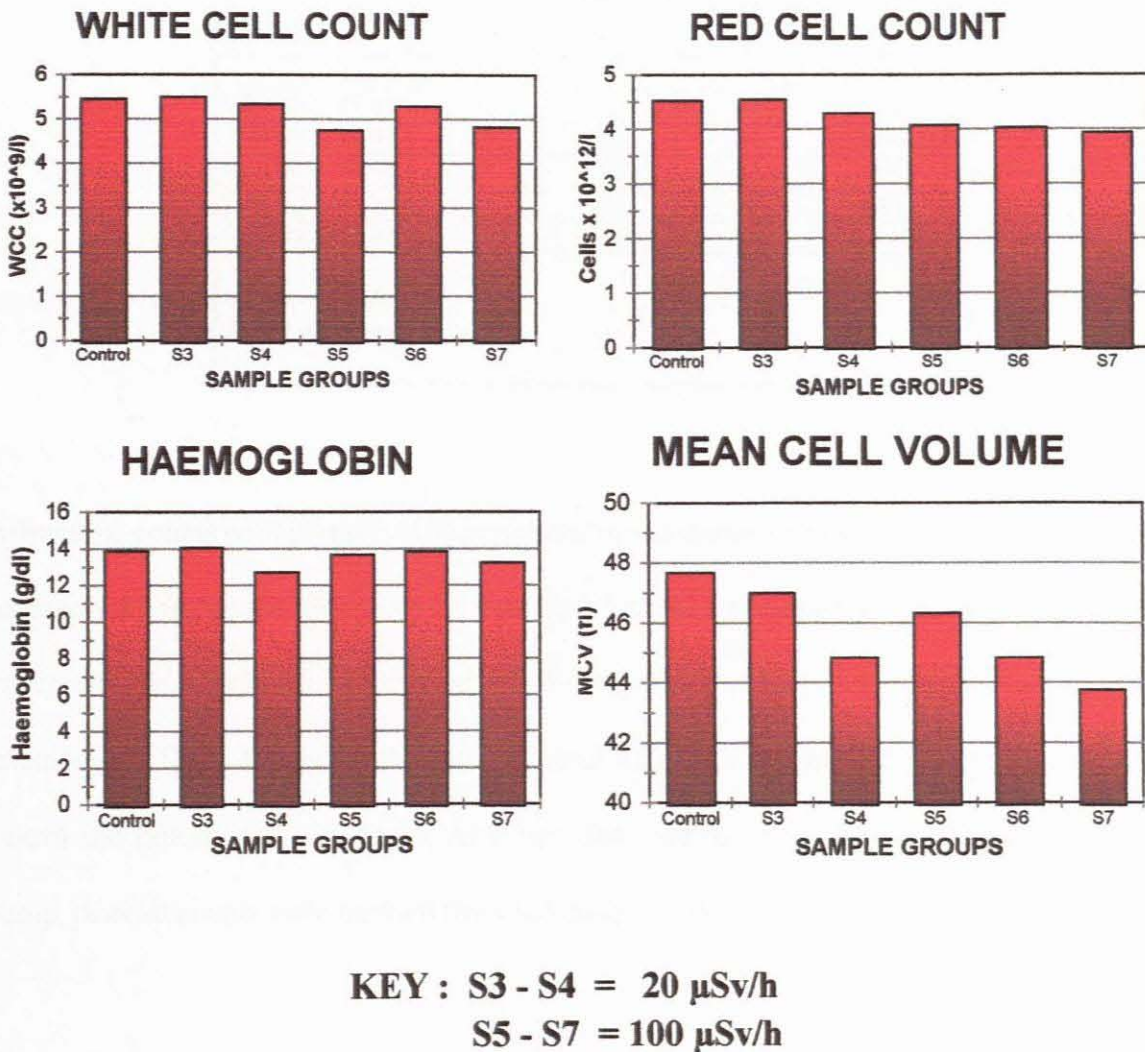


Figure 14. Graphical representation of average WCC, RCC, Hb, and MCV counts from control, 20 μ Sv/h (S3 - S4) and 100 μ Sv/h (S5 - S7) exposed bats. WCC, RCC and Hb values from radiation exposed bats did not differ significantly from the control group whereas the MCV values showed a significant decrease in radiation exposed bats when compared to the control group, indicating the presence of microcytic red blood cells. See Table II(a) for normal range.

Table III. Statistical analysis of full blood counts from control vs radiation exposed bats. Significant p-values ($p < 0.05$) are shown in bold typeface. There was no significant difference between control and radiation-exposed bats for the WCC, RCC or Hb parameters. S4 (20 $\mu\text{Sv/h}$) and S7 (100 $\mu\text{Sv/h}$) showed a statistically significant decrease in the MCV when compared with control group, indicating the presence of microcytic red blood cells and are shown in bold typeface.

P VALUES - FULL BLOOD COUNTS				
GROUPS	WCC	RCC	HB	MCV
CONTROL VS S3	0.9	0.9	0.8	0.4
CONTROL VS S4	0.8	0.5	0.2	0.001
CONTROL VS S5	0.2	0.2	0.7	0.3
CONTROL VS S6	0.7	0.1	0.7	0.01
CONTROL VS S7	0.2	0.03	0.3	7.2E-05
S3 - S4 = 20 $\mu\text{Sv/l}$ S5 - S7 = 100 $\mu\text{Sv/l}$				

Differential counts were performed on peripheral blood smears of bats after staining by Wright's Romanowsky technique. Erythrocytes from both control and radiation-exposed bats exhibited polychromasia which was confirmed by the supravital New Methylene blue stain for reticulocytes. There did not appear to be a marked difference between reticulocyte counts in the control and radiation-exposed bats. As it was observed that thrombocytes had a tendency to clump, platelet counts were omitted from full blood counts.

One hundred white blood cells were counted per bat viz. neutrophils, lymphocytes, monocytes, eosinophils and basophils (Figure 6, pg 37). As it was apparent that dyplastic neutrophils were present in radiation-exposed bats, pseudo-Pelger Huet cells were observed (Figure 6f) and

expressed as a percentage of the total neutrophil count (Table IV(a), (b) and (c)).

The average total neutrophil count observed in the control bats was 37 %, whereas the average in the low radiation group was 17 % and the high radiation group, 18 %. Scores for each group are shown in Table IV(a), (b) and (c). Statistical analysis assuming unequal variance showed a highly significant decrease ($p < 0.001$) in neutrophil counts between control bats and those exposed to radiation except for S2 as shown in Table V.

The average lymphocyte count of the control group was 58 %, whereas the average for both the low radiation group and the high radiation group were 78 %. Scores for each group are shown in Table IV (a), (b) and (c). Statistical analysis assuming unequal variance showed highly significant decrease ($p < 0.001$) between control bats and those exposed to radiation except for S2 as shown in Table V. Similarly, the percentage of pseudo-Pelger Huet cells expressed as a percentage of the total neutrophil count for the control group was 0.27 %. Only two bats showed pseudo-Pelger Huet cells (Table IV(a)). The average percentage for the low radiation group was 12.67 % whereas the average percentage for the high radiation group was 22.66 %. Statistical analysis showed a significant ($p < 0.05$) or highly significant ($p < 0.001$) increase in the percentage of pseudo-Pelger Huet cells in all groups of radiation-exposed bats compared to control bats (Table V). Figure 16 shows graphic representation of the data of differential counts on bat peripheral blood. Neutrophils observed in radiation-exposed bats were noted to be dyplastic and either hypo- or hypersegmented. Due to the low numbers of eosinophils and basophils, statistical analysis was not performed on these cell types. No marked difference however was observed

between the control and radiation-exposed bats. It was of interest that the higher eosinophil count in S3 correlated to the presence of parasitic worms.

The neutrophils of control bats appeared to be hypogranular (Figure 6a) however cytochemical staining of peripheral blood using DAB myeloperoxidase showed that although neutrophilic granules in the control group were weakly positive (Figure 15(a)) neutrophils from radiation-exposed bats were largely agranular (Figure 15(b)).

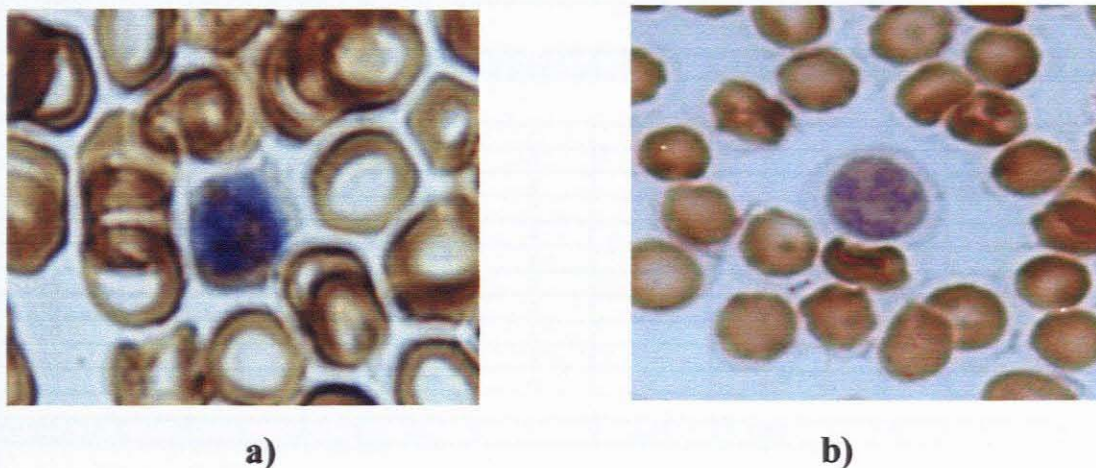


Figure 15. Photomicrograph of DAB myeloperoxidase staining of bat peripheral blood showing the presence of a brown granular precipitate in the cytoplasm of a neutrophil from a control bat (a) compared to the agranular appearance of a radiation exposed bat (b).

Table IV(a). Differential counts from control bats (H1 - H3) showing results for total neutrophils, normal neutrophils, lymphocytes, monocytes, eosinophils , basophils stab cells, pseudo Pelger-Huet (PH) cells and the percentage PH cells of the total neutrophil count. Averages for each cell type are given for each batch as well as the cumulative average for the control bats.

SAMPLE #	TOT NEUT	NEUT	LYMPHS	MONOS	EOSIN	BASO	STAB	PH	% PH
Control									
H1									
H 001	26	26	70	4	0	0	0	0	0
H 002	33	33	61	5	1	0	0	0	0
H 003	35	28	59	5	1	0	0	7	20
H 004	39	39	57	3	0	1	0	0	0
H 005	24	24	69	5	1	1	0	0	0
H 006	44	44	48	5	1	1	1	0	0
H 007	30	30	66	4	0	0	0	0	0
H 008	58	58	38	3	0	0	1	0	0
H 009	31	31	65	3	1	0	0	0	0
H 010	41	41	56	2	0	0	1	0	0
H 011	31	29	62	5	0	0	0	2	6.4
AVERAGE	36	35	59	4	0.45	0.27	0.27	0.82	2.40
Control									
H2									
H 012	30	30	64	5	1	0	0	0	0
H 013	34	34	61	4	1	0	0	0	0
H 014	27	27	69	4	0	0	0	0	0
H 015	36	36	62	2	0	0	0	0	0
H 016	44	44	52	4	0	0	0	0	0
H 017	37	37	58	4	1	0	0	0	0
H 018	34	34	61	5	0	0	0	0	0
H 019	34	34	64	2	0	0	0	0	0
H 020	41	41	55	4	0	0	0	0	0
H 022	42	42	54	3	0	1	0	0	0
H 023	31	31	63	4	2	0	0	0	0
AVERAGE	35	35	60	4	0.45	0.09	0.00	0.00	0.00
Control									
H3									
H 033	44	44	51	4	0	0	1	0	0
H 036	24	24	71	5	0	0	0	0	0
H 037	42	42	54	4	0	0	0	0	0
H 038	35	35	61	4	0	0	0	0	0
H 039	61	61	34	5	0	0	0	0	0
H 040	33	33	61	5	0	1	0	0	0
H 041	49	49	47	4	0	0	0	0	0
H 042	29	29	68	2	1	0	0	0	0
H 043	58	58	38	4	0	0	0	0	0
H 044	26	26	70	4	0	0	0	0	0
H 045	44	44	52	4	0	0	0	0	0
AVERAGE	40	40	55	4	0.09	0.09	0.09	0.00	0.00
CUM AVE	37	37	58	4	0.33	0.15	0.12	0.27	0.80

Table IV(b) Differential counts from 20 $\mu\text{Sv/h}$ exposed bats (S1- S2) showing results for total neutrophils, normal neutrophils, lymphocytes, monocytes, eosinophils, basophils, stab cells, pseudo Pelger-Huet (PH) cells and the percentage PH cells of the total neutrophil count. Averages for each cell type are given for each batch as well as the cumulative average for the 20 $\mu\text{Sv/h}$ exposed bats.

SAMPLE #	TOT NEUT	NEUT	LYMPHS	MONO	EOSIN	BASO	STAB	PH	% PH
20 $\mu\text{Sv/h}$									
S1									
S 028	15	12	82	2	0	1	0	3	20.00
S 029	6	6	91	2	1	0	0	0	0.00
S 030	16	14	78	5	0	0	1	2	12.50
S 031	15	13	79	6	0	0	0	2	13.33
S 032	15	14	81	4	0	0	0	1	6.67
S 033	16	13	79	3	0	2	0	3	18.75
S 034	10	9	86	4	0	0	0	1	10.00
S 035	12	10	84	3	1	0	0	2	16.67
S 036	13	12	81	5	0	0	1	1	7.69
S 037	11	11	87	2	0	0	0	0	0.00
S 038	14	12	82	4	0	0	0	2	14.29
S 039	8	7	90	1	0	1	0	1	12.50
S 040	10	9	88	2	0	0	0	1	10.00
S 041	18	14	79	2	0	1	0	4	22.22
S 042	15	14	82	2	1	0	0	1	6.67
S 043	17	15	77	5	0	1	0	2	11.76
S 044	11	9	87	2	0	0	0	2	18.18
S 045	12	9	85	3	0	0	0	3	25.00
S 046	17	14	82	1	0	0	0	3	17.65
S 047	16	14	79	4	0	1	0	2	12.50
S 048	12	12	85	3	0	0	0	0	0.00
AVERAGE	13	12	83	3	0.14	0.33	0.10	1.71	12.21
20 $\mu\text{Sv/h}$									
S2									
S 049	38	32	57	4	0	0	1	6	15.79
S 050	36	33	57	4	0	0	3	3	8.33
S 051	37	34	56	5	1	1	0	3	8.11
S 052	30	25	59	7	1	2	1	5	16.67
S 053	20	19	76	4	0	0	0	1	5.00
S 054	21	17	72	6	0	0	1	4	19.05
S 056	28	25	64	6	0	1	1	3	10.71
S 057	27	25	66	3	1	1	2	2	7.41
S 059	10	10	83	4	1	1	1	0	0.00
S 060	62	60	36	2	0	0	0	2	3.23
S 061	38	34	58	4	0	0	0	4	10.53
AVERAGE	32	29	62	4	0.36	0.55	0.91	3.00	9.53

Table IV(b) cont. Differential counts from 20 $\mu\text{Sv/h}$ exposed bats (S3-S4) showing results for total neutrophils, normal neutrophils, lymphocytes, monocytes, eosinophils, basophils, stab cells, pseudo Pelger-Huet (PH) cells and the percentage PH cells of the total neutrophil count. Averages for each cell type are given for each batch as well as the cumulative average for the 20 $\mu\text{Sv/h}$ exposed bats.

SAMPLE #	TOT NEUT	NEUTS	LYMPHS	MONO	EOSIN	BASO	STAB	PH	% PH
20 $\mu\text{Sv/h}$									
S3									
S 084	8	6	86	6	0	0	0	2	25.00
S 085	15	12	80	3	1	1	0	3	20.00
S 086	20	17	72	3	5	0	0	3	15.00
S 087	15	14	81	2	1	1	0	1	6.67
S 088	23	19	74	2	1	0	0	4	17.39
S 089	11	8	84	4	0	1	0	3	27.27
S 090	13	11	82	4	1	0	0	2	15.38
S 091	12	10	83	2	2	1	0	2	16.67
S 092	5	4	89	4	1	1	0	1	20.00
S 093	22	20	70	2	5	1	0	2	9.09
S 094	22	21	70	2	5	1	0	1	4.55
S 095	14	13	82	4	0	0	0	1	7.14
AVERAGE	15	13	79	3	1.83	0.58	0.00	2.08	14.47
20 $\mu\text{Sv/h}$									
S4									
S 111	12	12	85	2	1	0	0	0	0.00
S 112	15	12	79	4	1	0	1	3	20.00
S 113	7	7	92	1	0	0	0	0	0.00
S 114	7	5	91	2	0	0	0	2	28.57
S 115	22	20	74	2	2	0	0	2	9.09
S 116	6	4	91	2	1	0	0	2	33.33
S 117	10	9	88	2	0	0	0	1	10.00
S 118	12	10	79	5	1	3	0	2	16.67
S 119	10	9	87	2	1	0	0	1	10.00
S 120	9	8	88	2	1	0	0	1	11.11
AVERAGE	11	10	85	2	0.80	0.30	0.10	1.40	13.88
CUM AVE	17	15	78	3	0.69	0.43	0.24	2.00	12.67

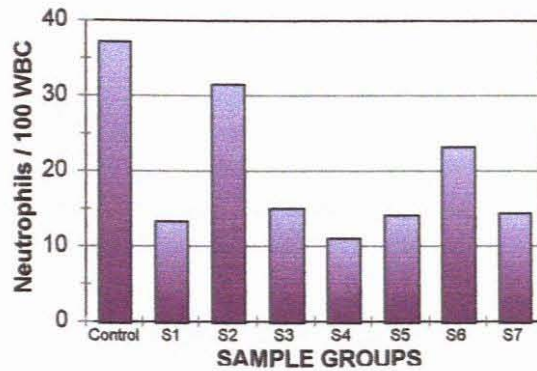
Table IV(c). Differential counts from 100 $\mu\text{Sv/h}$ exposed bats (S5-S6) showing results for total neutrophils, normal neutrophils, lymphocytes, monocytes, eosinophils, basophils, stab cells, pseudo Pelger-Huet (PH) cells and the percentage PH cells of the total neutrophil count. Averages for each cell type are given for each batch as well as the cumulative average for the 100 $\mu\text{Sv/h}$ exposed bats.

SAMPLE #	TOT NEUT	NEUTS	LYMPHS	MONO	EOSIN	BASO	STAB	PH	% PH
100 $\mu\text{Sv/h}$									
S5									
S 001	11	9	81	5	3	0	0	2	18.18
S 002	21	18	74	3	1	1	0	3	14.29
S 003	7	5	85	4	2	2	0	2	28.57
S 004	14	13	81	4	1	0	0	1	7.14
S 005	11	9	85	2	2	0	0	2	18.18
S 006	10	8	85	3	2	0	0	2	20.00
S 007	13	11	78	3	4	0	2	2	15.38
S 008	15	12	82	1	1	0	1	3	20.00
S 009	9	8	86	5	0	0	0	1	11.11
S 010	20	19	74	4	2	0	0	1	5.00
S 011	8	7	85	2	4	0	1	1	12.50
S 012	18	15	78	2	1	0	1	3	16.67
S 013	30	29	62	5	2	1	0	1	3.33
S 014	10	7	86	3	1	0	0	3	30.00
AVERAGE	14	12	80	3	1.85	0.29	0.36	1.93	15.74
SAMPLE #									
100 $\mu\text{Sv/h}$									
S6									
S 065	11	8	86	3	0	0	0	3	27.27
S 066	22	14	73	4	0	0	1	8	36.36
S 068	22	22	76	2	0	0	0	0	0.00
S 069	24	16	70	4	0	0	2	8	33.33
S 070	33	22	61	5	0	0	1	11	33.33
S 071	28	27	67	5	0	0	0	1	3.57
S 072	33	24	62	4	0	0	1	9	27.27
S 073	24	22	72	3	0	0	1	2	8.33
S 074	21	14	74	5	0	0	0	7	33.33
S 075	18	13	80	2	0	0	0	5	27.78
S 076	20	6	74	6	0	0	0	14	70.00
S 077	15	10	82	3	0	0	0	5	33.33
S 078	24	12	74	2	0	0	0	12	50.00
S 079	22	17	75	3	0	0	0	5	22.73
S 080	18	5	78	4	0	0	0	13	72.22
S 081	36	16	58	5	0	0	1	20	55.56
S 082	27	22	68	5	0	0	0	5	18.52
S 083	20	6	74	6	0	0	0	14	70.00
AVERAGE	23	15	72	4	0.00	0.00	0.39	7.89	37.57

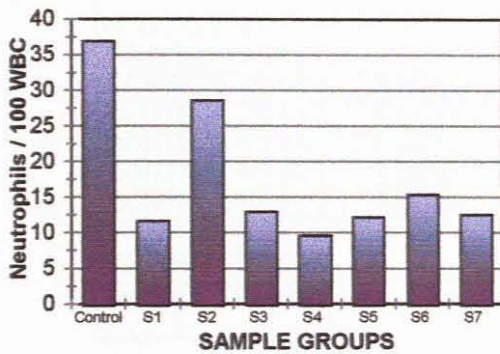
Table IV(c) cont. Differential counts from 100 $\mu\text{Sv/h}$ exposed bats (S7) showing results for total neutrophils, normal neutrophils, lymphocytes, monocytes, eosinophils, basophils, stab cells, pseudo Pelger-Huet (PH) cells and the percentage PH cells of the total neutrophil count. Averages for each cell type are given for each batch as well as the cumulative average for the 100 $\mu\text{Sv/h}$ exposed bats.

SAMPLE #	TOT NEUT	NEUTS	LYMPHS	MONO	EOSIN	BASO	STAB	PH	% PH
100 $\mu\text{Sv/h}$									
S7									
S 096	10	10	84	6	0	0	0	0	0.00
S 097	10	9	84	6	0	0	0	1	10.00
S 098	12	6	82	3	1	0	2	6	50.00
S 099	14	10	81	2	0	0	3	4	28.57
S 100	9	7	88	2	1	0	0	2	22.22
S 101	35	35	61	3	1	0	0	0	0.00
S 102	8	6	90	2	0	0	0	2	25.00
S 103	13	10	81	3	1	0	2	3	23.08
S 104	17	12	80	3	0	0	0	5	29.41
S 105	6	6	90	3	1	0	0	0	0.00
S 106	6	6	93	1	0	0	0	0	0.00
S 107	24	22	73	2	1	0	0	2	8.33
S 108	34	34	61	4	1	0	0	0	0.00
S 109	9	9	85	5	1	0	0	0	0.00
S 110	8	6	87	5	0	0	0	2	25.00
AVERAGE	14	13	81	3	0.53	0.00	0.47	1.80	15.83
CUM AVE	18	13	78	4	0.72	0.09	0.40	4.17	22.66

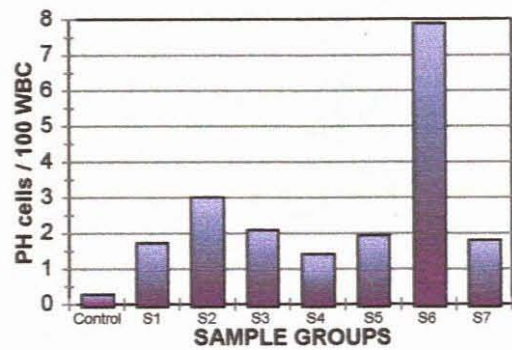
TOTAL NEUTROPHIL COUNTS



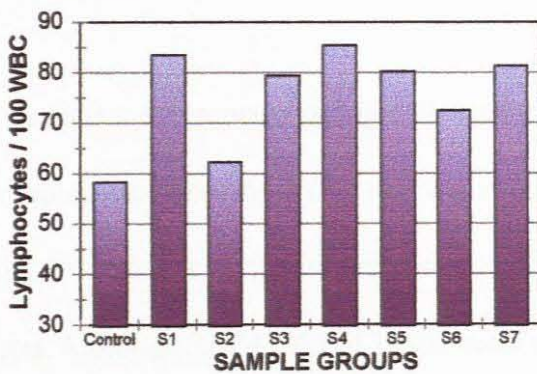
NORMAL NEUTROPHIL COUNTS



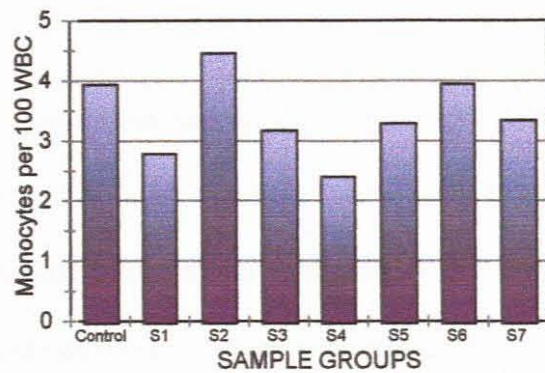
PSEUDO-PELGER HUET CELLS



LYMPHOCYTE COUNTS



MONOCYTE COUNTS



**KEY: S1 - S4 = 20 μ Sv/h
S5 - S7 = 100 μ Sv/h**

Figure 16. Histograms of neutrophil, lymphocyte and monocyte counts from control, 20 μ Sv/h and 100 μ Sv/h exposed bats. Results indicate a decrease in total neutrophil counts and normal neutrophil counts in radiation exposed bats with the exception of S2 and S6. Similarly, an increase in PH cells and lymphocytes was observed in radiation exposed bats with the exception of S2 and S6.

Table V. Statistical analysis of differential counts from control vs radiation exposed bats. Significant p-values ($p < 0.05$) and highly significant p-values ($p < 0.001$) are shown in bold typeface and indicate a significant decrease in neutrophil counts in radiation exposed bats when compared to the control group and an increase in lymphocyte counts and percentage pseudo-Pelger Huet cells in radiation exposed bats when compared to the control group. S2 and S6 showed the least significant differences when compared to the neutrophil and lymphocyte counts of the control group.

P VALUES - DIFFERENTIAL COUNTS				
GROUPS	NEUTROPHILS	LYMPHOCYTES	MONOCYTES	%PH
CONTROL VS S1	1.2E-16	1.4E-17	0.02	2.3E-07
CONTROL VS S2	0.2	0.3	0.3	4.5E-04
CONTROL VS S3	6.7E-11	1.8E-09	0.07	1.6E-05
CONTROL VS S4	6.4E-13	2.0E-10	0.002	0.004
CONTROL VS S5	1.2E-11	1.5E-10	0.1	5.6E-06
CONTROL VS S6	1.2E-07	3.7E-07	1.0	3.7E-06
CONTROL VS S7	1.8E-08	2.3E-08	0.2	0.004
S1 - S4 = 20 μ Sv/h				
S5 - S7 = 100 μ Sv/h				

To confirm a neutropenia and not a lymphocytosis in radiation exposed bats, absolute counts were calculated from the WCC, where available, from control and radiation exposed bats (Table VI(a), (b) and (c)). Statistical analysis assuming unequal variance was performed on absolute counts. Although S3, S4, S6 and S7 showed a significant increase in lymphocyte counts ($p < 0.05$) compared to the control group, the difference in neutrophil counts was highly significant in all groups ($p < 0.001$) and the results indicated a neutropenia (Table VII), which is a characteristic feature of patients with MDS. Figure 17 shows a graphic representation of absolute counts.

Table VI(a). Absolute neutrophil, lymphocyte, monocyte, eosinophil, basophil and stab cell counts of control bats calculated from the WBC as described in Materials and Methods. Averages for each group as well as the cumulative average for the control bats is given.

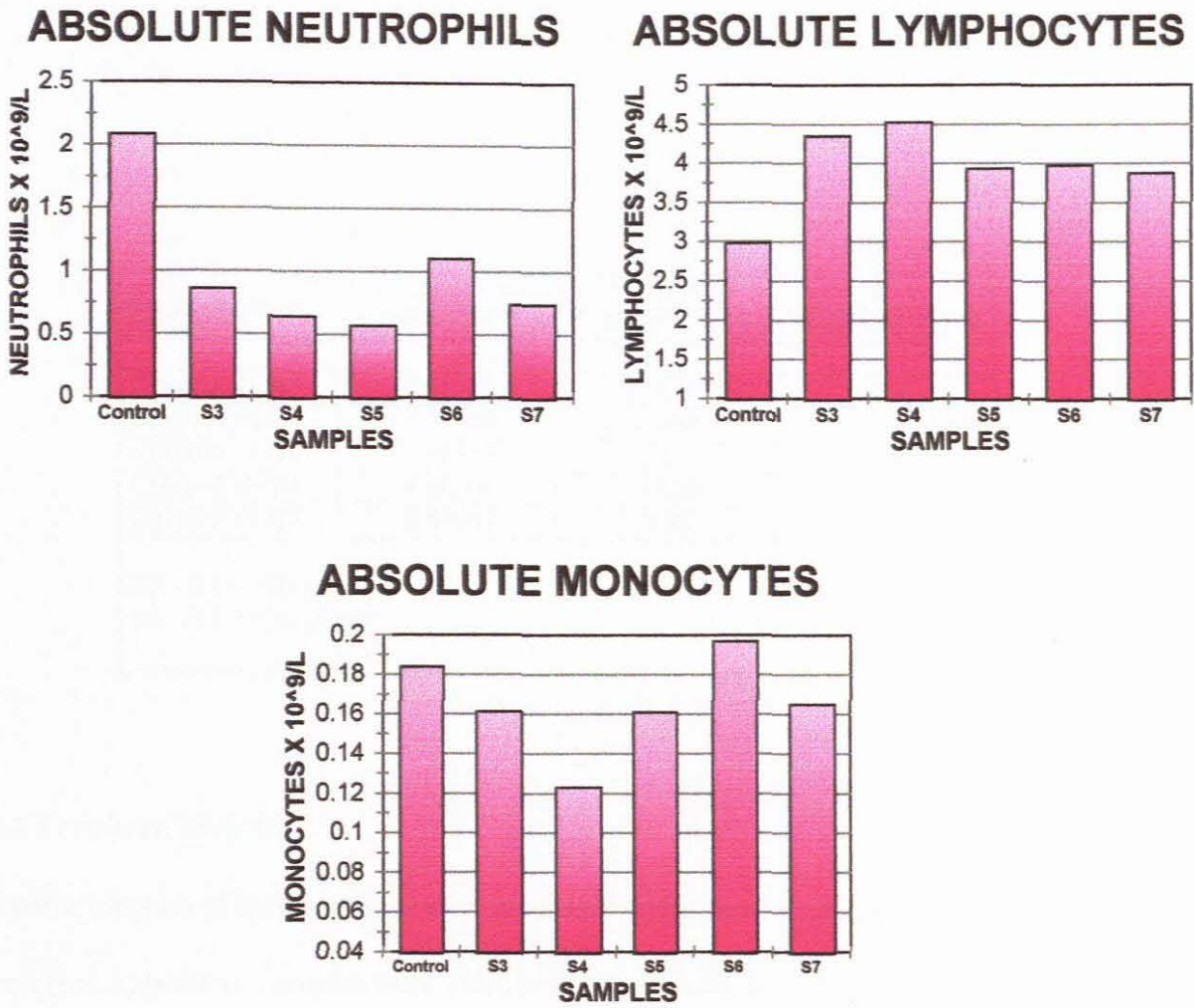
SAMPLE #	A NEUT	A LYMPH	A MONO	A EOSIN	A BASO	A STAB
Control						
H 003	2.31	3.89	0.33	0.07	0.13	0.00
H 004	2.90	4.24	0.22	0.00	0.07	0.00
H 005	1.24	3.56	0.25	0.05	0.05	0.00
H 008	3.29	2.15	0.17	0.00	0.00	0.06
H 010	2.58	3.58	0.13	0.00	0.00	0.00
H 011	1.14	2.32	0.19	0.00	0.00	0.00
AVERAGE	2.24	3.29	0.22	0.02	0.04	0.01
H 013	1.61	2.90	0.19	0.09	0.00	0.05
H 015	2.39	4.12	0.13	0.00	0.00	0.00
H 016	2.20	2.60	0.20	0.00	0.00	0.00
H 018	1.84	3.30	0.27	0.00	0.00	0.00
H 020	1.73	2.31	0.17	0.00	0.00	0.00
AVERAGE	1.95	3.05	0.19	0.02	0.00	0.01
H 033	1.77	1.93	0.16	0.00	0.00	0.00
H 036	2.94	0.98	0.16	0.00	0.00	0.00
H 037	3.06	3.06	0.25	0.00	0.00	0.00
H 038	2.37	3.99	0.00	0.41	0.00	0.00
H 040	1.55	2.18	0.20	0.00	0.00	0.00
H 042	1.21	2.84	0.08	0.04	0.00	0.00
H 044	1.39	3.75	0.21	0.00	0.00	0.00
AVERAGE	2.04	2.68	0.15	0.06	0.00	0.00
CUM AVE	2.08	2.98	0.18	0.04	0.01	0.01

Table VI(b). Absolute neutrophil, lymphocyte, monocyte, eosinophil, basophil and stab cell counts of 20 $\mu\text{Sv/h}$ exposed bats calculated from the WBC as described in Materials and methods. Averages for each group as well as the cumulative average for the 20 $\mu\text{Sv/h}$ exposed bats is given.

SAMPLE # 20 $\mu\text{Sv/h}$	A NEUT	A LYMPH	A MONO	A EOS	A BAS	A STAB
S3						
S 085	0.73	3.90	0.15	0.05	0.05	0.00
S 086	0.88	3.18	0.13	0.22	0.00	0.00
S 087	0.83	4.50	0.11	0.06	0.06	0.00
S 088	1.23	3.95	0.11	0.05	0.00	0.00
S 089	0.59	4.51	0.21	0.00	0.05	0.00
S 090	0.84	5.31	0.26	0.06	0.00	0.00
S 091	0.69	4.79	0.12	0.12	0.06	0.00
S 092	0.24	4.26	0.19	0.05	0.05	0.00
S 093	0.99	3.14	0.09	0.22	0.04	0.00
S 094	1.46	4.66	0.13	0.33	0.07	0.00
S 095	0.95	5.59	0.27	0.00	0.00	0.00
AVERAGE	0.86	4.34	0.16	0.11	0.03	0.00
S4						
S 111	0.81	5.71	0.13	0.07	0.00	0.00
S 112	0.95	5.02	0.25	0.06	0.00	0.06
S 114	0.41	5.33	0.12	0.00	0.00	0.00
S 115	1.52	5.10	0.14	0.14	0.00	0.00
S 116	0.33	5.03	0.11	0.06	0.00	0.00
S 117	0.36	3.14	0.07	0.00	0.00	0.00
S 119	0.38	3.29	0.08	0.04	0.00	0.00
S 120	0.36	3.54	0.08	0.04	0.00	0.00
AVERAGE	0.64	4.52	0.12	0.05	0.00	0.01
CUM AVE	0.77	4.42	0.14	0.08	0.02	0.00

Table VI(c). Absolute neutrophil, lymphocyte monocyte, eosinophil, basophil and stab cell counts of 100 $\mu\text{Sv/h}$ exposed bats calculated from the WBC as described in Materials and Methods. Averages for each group as well as the cumulative average for the 100 $\mu\text{Sv/h}$ exposed bats is given.

SAMPLE #	A NEUT	A LYMPH	A MONO	A EOS	A BAS	A STAB
100 $\mu\text{Sv/h}$						
S5						
S 003	0.42	5.05	0.24	0.12	0.12	0.00
S 004	0.70	4.03	0.20	0.05	0.00	0.00
S 005	0.71	5.48	0.13	0.13	0.00	0.00
S 006	0.47	4.00	0.14	0.09	0.00	0.00
S 009	0.39	3.76	0.22	0.00	0.00	0.00
S 010	0.65	2.39	0.13	0.06	0.00	0.00
S 012	0.65	2.80	0.07	0.04	0.00	0.04
AVERAGE	0.57	3.93	0.16	0.07	0.02	0.01
S6						
S 069	1.33	3.88	0.22	0.00	0.00	0.11
S 073	1.03	3.08	0.13	0.00	0.00	0.04
S 076	1.29	4.79	0.39	0.00	0.00	0.00
S 077	0.76	4.17	0.15	0.00	0.00	0.00
S 078	1.10	3.40	0.09	0.00	0.00	0.00
S 079	1.10	3.74	0.15	0.00	0.00	0.00
S 080	1.10	4.75	0.24	0.00	0.00	0.00
AVERAGE	1.10	3.97	0.20	0.00	0.00	0.02
S7						
S 096	0.40	3.35	0.24	0.00	0.00	0.00
S 097	0.47	3.92	0.28	0.00	0.00	0.00
S 098	0.74	5.03	0.18	0.00	0.00	0.12
S 099	0.81	4.71	0.12	0.00	0.00	0.17
S 100	0.36	3.55	0.08	0.00	0.00	0.00
S 101	1.48	2.58	0.13	0.00	0.00	0.00
S 104	1.22	5.72	0.21	0.00	0.00	0.00
S 106	0.24	3.69	0.04	0.00	0.00	0.00
S 107	1.32	4.01	0.11	0.00	0.00	0.00
S 108	1.05	1.88	0.12	0.00	0.00	0.00
S 109	0.36	3.44	0.20	0.00	0.00	0.00
S 110	0.42	4.53	0.26	0.00	0.00	0.00
AVERAGE	0.74	3.87	0.16	0.00	0.00	0.02
CUM AVE	0.79	3.91	0.17	0.02	0.00	0.02



KEY: S1 - S4 = 20 μ Sv/h
S5 - S7 = 100 μ Sv/h

Figure 17. Graphic representation of absolute neutrophil, lymphocyte and monocyte counts of control, 20 μ Sv/h and 100 μ Sv/h exposed bats indicating a significant decrease in absolute neutrophil counts of radiation exposed bats compared to the control group. Although absolute lymphocytes counts from radiation exposed bats were decreased, the results indicate a less significant difference.

Table VII. Statistical analysis of absolute counts from control vs radiation-exposed bats. Significant p-values ($p < 0.05$) and highly significant p-values ($p < 0.001$) are shown in bold typeface. p-values for lymphocyte counts in S3, S4, S6 and S7 radiation exposed bats were significantly increased and the difference in neutrophil counts was highly significant in all groups and indicated a neutropenia.

P VALUES - ABSOLUTE COUNTS			
GROUPS	NEUTROPHILS	LYMPHOCYTES	MONOCYTES
Control vs S3	6.4E-07	2.3E-04	0.4
Control vs S4	1.7E-06	0.003	0.04
Control vs S5	1.9E-08	0.07	0.4
Control vs S6	1.3E-05	0.008	0.8
Control vs S7	3.5E-07	0.03	0.5
S3 - S4 = 20 μ Sv/h S5 - S7 = 100 μ Sv/h			

3.3.2 Trephine biopsies

Trephine biopsies of bat breastbone were processed and stained with Harris' Haematoxylin and Eosin (see Appendix). Samples were examined from control bats as well as from bats exposed to high dose radiation (100 μ Sv/h). Bone marrow was examined for general architecture, cellularity, the granulocyte: lymphocyte: erythrocyte (GLE) ratio as well as the megakaryocyte morphology. Bone marrow from control bats showed a normocellular picture with normal granulocytic, lymphocytic and erythrocytic maturation, few sinusoid spaces and multilobulated megakaryocytes (Figure 18a). Bone marrow from radiation exposed bats on the other hand showed a marked decrease in the cellularity of the bone marrow, an increase in sinusoid spaces and hypolobulated and micro-megakaryocytes. Granulocytic maturation was markedly decreased as shown in Figure 18b.

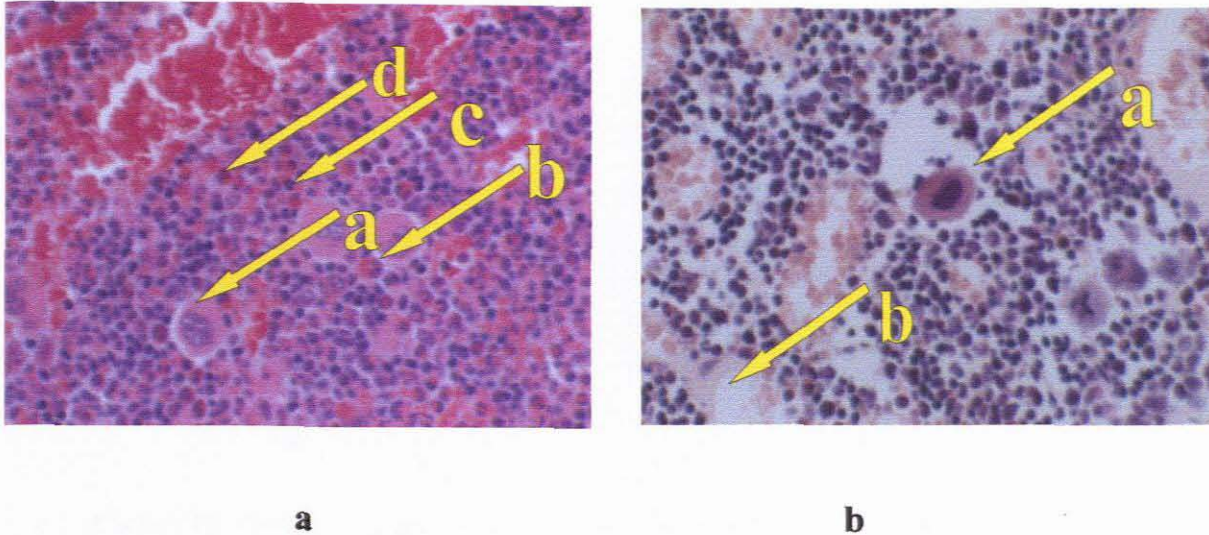


Figure 18. Photomicrographs of bone marrow samples from a control bat (a) showing a normocellular picture with a multilobulated megakaryocyte (a); granulocytic development (b); lymphocytic development (c) and normocytic development (d) and a 100 $\mu\text{Sv/h}$ exposed bat (b) showing an increase in sinusoid spaces (a); a monolobulated megakaryocyte (b) and a decrease in granulocytic development (Magnification : x 400).

The bone architecture of control bats appeared normal with a normal distribution of osteocytes (Figure 19(a)) compared to the bone architecture of radiation exposed bats where an excess of osteocytes was observed (Figure 19(b)). These findings indicated bone resorption which has been reported in patients exposed to radiation.

An additional finding in the bone marrow of some radiation exposed bats was the presence of islands of osteoblasts. The presence of these immature cells, as shown in Figure 20, indicate the severe marrow stress of the radiation exposed bats as new cartilage deposition takes place in order to compensate the failing marrow.

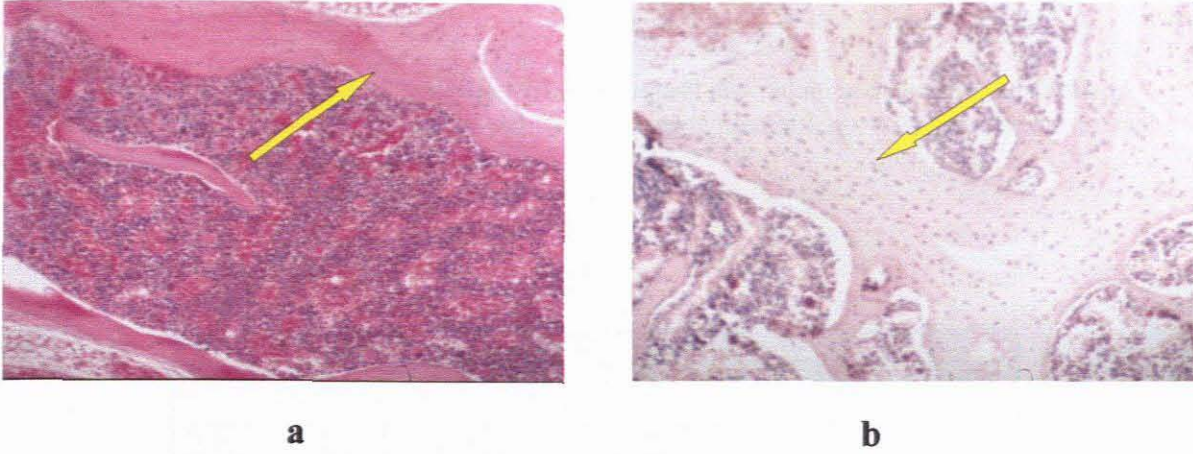


Figure 19. Photomicrograph showing normal osteocyte distribution in the bone of a control bat (a) and an increased osteocyte distribution in a radiation exposed bat indicating bone resorption (b) as shown by the arrows. (Magnification: x 100)

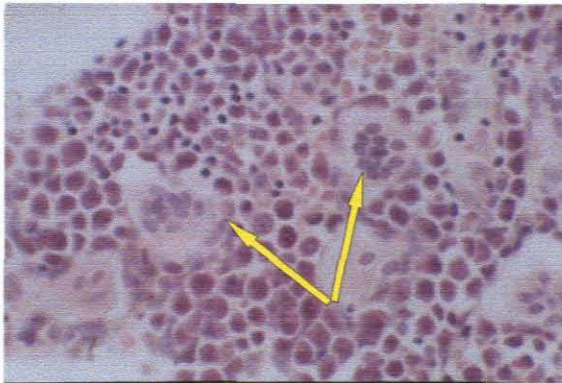


Figure 20. Photomicrograph showing islands of osteoblastic development (shown by arrows) indicating severe marrow stress in the bone marrow of a radiation exposed bat. (Magnification : x 400)

The average percentage cellularity of the control group was 73% and 56 % for the radiation-exposed group as shown in Table VIII. The GLE ratio showed a decrease in granulocytes and an increase in lymphocytes in the radiation-exposed bats whereas the erythrocyte ratio remained constant (Table VIII). Statistical analysis showed highly significant differences ($p < 0.001$) in the results of radiation exposed bats when compared to the control group (Table IX).

Table VIII. Analysis of bone marrow from control and radiation exposed bats showing percentage cellularity, GLE ratio and megakaryocyte morphology. Averages for the control and radiation exposed bats are shown.

SAMPLE # Control	CELL %	RATIO			MEGAKARYOCYTES		
		G	L	E	MULTI	MONO	MICRO
H 032	70	60	25	15	3	0	0
H 034	70	60	25	15	6	0	0
H 035	80	60	20	20	3	0	0
H 036	70	60	20	20	12	0	0
H 038	75	60	20	20	4	0	0
H 039	70	60	20	20	3	0	0
H 041	70	60	20	20	11	0	0
H 042	70	60	25	15	4	0	0
H 043	80	60	25	15	7	0	0
H 044	80	60	20	20	4	0	0
H 045	70	60	25	15	6	0	0
AVERAGE	73	60	22	18	6	0	0
SAMPLE # 100 μ S/h	CELL %	RATIO			MEGAKARYOCYTES		
		G	L	E	MULTI	MONO	MICRO
S 065	60	50	30	20	5	3	2
S 066	50	60	30	10	8	1	1
S 067	60	50	30	20	9	0	1
S 068	50	50	30	20	7	1	2
S 069	50	50	30	20	2	3	5
S 070	65	60	25	15	7	1	2
S 071	60	50	30	20	8	1	1
S 072	50	50	30	20	6	1	3
S 073	60	50	30	20	6	2	2
S 074	60	50	25	15	5	1	4
S 075	50	50	30	20	7	2	1
S 076	60	50	35	15	8	1	1
S 077	50	50	30	20	7	1	2
S 078	50	50	30	20	3	3	4
S 079	60	50	30	20	6	2	2
S 080	60	50	35	15	5	2	3
S 081	60	50	35	15	4	4	2
S 083	60	50	30	20	6	1	3
AVERAGE	56	51	30	18	6	2	2

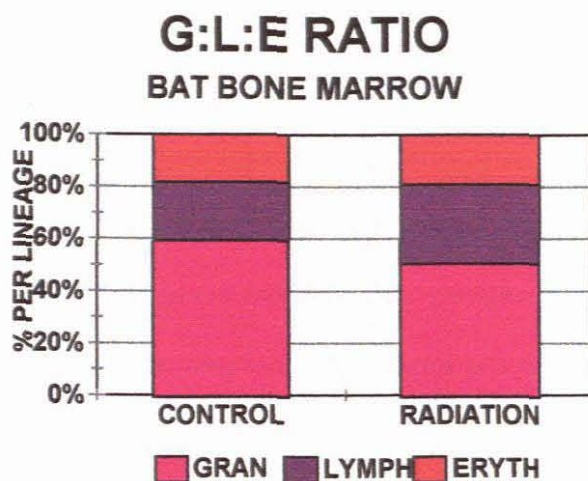


Figure 21. Graphic representation of G:L:E ratio of bone marrow from control and 100 $\mu\text{Sv/h}$ exposed bats showing a decrease in the granulocytic development (gran) and a relative increase in lymphocytic development (lymph). No difference was observed in erythrocytic development (eryth) between the two groups.

Table IX. Statistical analysis of bone marrow investigation in control vs 100 $\mu\text{Sv/h}$ exposed bats showing highly significant differences ($p < 0.001$) between cellularity, granulocytic and lymphocytic development and megakaryocyte morphology.

P VALUES - BONE MARROW	
Control vs 100 $\mu\text{Sv/h}$	
CELLULARITY	4.4E-09
GRANULOCYTIC %	1.6E-09
LYMPHOCYTIC %	7.1E-08
ERYTHROID %	0.8
MULTIMEGS	0.8
MONOMEGS	2.7E-06
MICROMEGS	2.6E-07

3.3.3 Bone mineralisation using image analysis

Due to the abnormal appearance of bone samples from radiation exposed bats, qualitative examination of the percentage mineralisation of the bone osteoid was undertaken on Haematoxylin and Eosin stained trephine biopsies using the OPTIMAS 6.1 image analyser. Variations in the intensity of the light absorbed were calculated by means of digitally graded parameters and radiation exposed bats showed a marked decrease in osteoid mineralisation when compared to the control bats as shown in Figure 22.

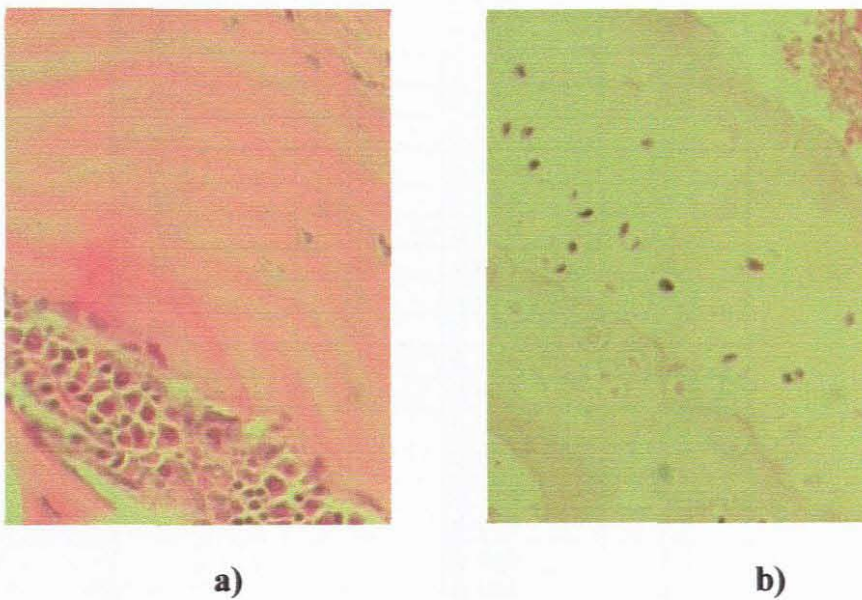


Figure 22. Photomicrographs of bat bone sections stained with Haematoxylin and Eosin and examined qualitatively for the percentage mineralisation of bone osteoid. Control bats showed normal mineralisation as indicated by the eosinophilic staining (a) compared to radiation exposed bats which showed a marked decrease in the mineralisation of the bone osteoid (b). (Magnification : x 400)

The average bone mineralisation of the control bats was 80.57 % compared to 27.4 % mineralisation in the exposed bats as shown in Table X. Statistical analysis assuming unequal variance showed a highly significant decrease ($p < 0.001$) in mineralisation of osteoid in radiation exposed bats when compared to the control group.

Table X. Results of bone mineralisation using image analysis from control and 100 $\mu\text{Sv/h}$ exposed bats showing a marked decrease in radiation exposed bats when compared to the control group. The highly significant p-value ($p < 0.001$) supports these findings.

BONE MINERALISATION			
Control		100 $\mu\text{Sv/h}$	
SAMPLE #	%	SAMPLE #	%
H 032	72.0	S 031	4.2
H 034	84.6	S 032	32.7
H 035	80.6	S 065	34.4
H 036	92.2	S 066	5.9
H 037	88.0	S 067	13.4
H 038	93.4	S 068	29.4
H 039	87.4	S 069	51.5
H 040	75.8	S 070	22.2
H 041	86.5	S 071	39.0
H 042	78.4	S 072	50.4
H 043	52.7	S 073	24.2
H 044	80.4	S 074	30.2
H 045	75.4	S 075	2.0
		S 076	85.3
		S 077	7.6
		S 078	46.9
		S 079	2.0
		S 080	8.4
		S 081	4.3
		S 082	3.8
		S 083	70.0
AVERAGE	80.57	AVERAGE	27.04
P value : 5.2E-10			

3.4 DNA damage evaluation

3.4.1 Micronucleus assay in peripheral lymphocytes

A total culture time of 120 hours using PHA as the mitogen appeared to be a suitable method to stimulate bat lymphocytes into cellular division. Nucleation indices confirmed that culturing was successful (Table XI). Five hundred binucleated lymphocytes (BNL's) were examined per culture for the presence of micronuclei (Figure 23).

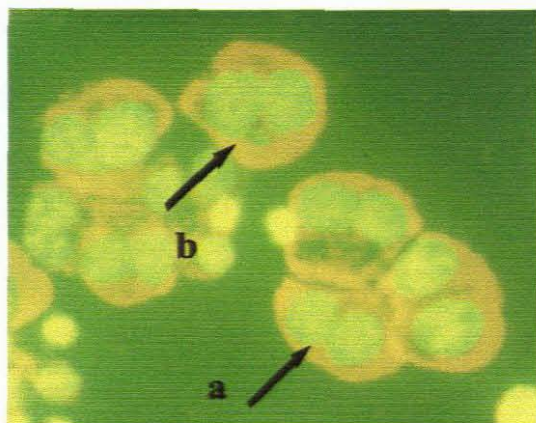


Figure 23. Photomicrograph showing bat lymphocytes cultured for a total of 120 hours using PHA as the mitogen and Cytochalasin B as a cytokinesis blocking agent. After staining with acridine orange, 500 binucleated lymphocytes (BNL's) (a) were counted per bat culture using fluorescence microscopy and examined for the presence of micronuclei (b).

The number of lymphocytes containing micronuclei increased as the radiation dose increased suggesting a dose response curve. Table XI shows that in bats exposed to 20 $\mu\text{Sv/h}$, samples 2 binucleated lymphocytes with 2 micronuclei. The lymphocyte culture from bats exposed to 100 $\mu\text{Sv/h}$ had a total of 4 binucleated lymphocytes containing 2 micronuclei and one binucleated and 3 each contained one binucleated lymphocyte with two micronuclei while sample 9 showed 2 lymphocyte containing 4 micronuclei. These results support published data (Thierens *et al*, 1991), that the number of micronuclei per binucleated lymphocyte increases with the radiation

dose. The control lymphocyte culture showed binucleated lymphocytes containing only one micronucleus. Cultures from bats exposed to 20 $\mu\text{Sv/h}$ had an average of 17.7 micronuclei per 500 binucleated lymphocytes (MN / 500 BNL's), those from the 100 $\mu\text{Sv/h}$ had 27.1 MN / 500 BNL's and the control group, 5.3 MN / 500 BNL's as shown in Table XI.

Not only was there a significant difference between the test and control groups, but a significant difference between the lower and higher radiation exposure groups was also observed (Figure 24) indicating an increasing dose response curve. This assay therefore is sensitive enough to detect DNA damage at low doses of radiation exposure in bats and the results are in agreement with the findings of Almassy *et al* (1987) and Thierens *et al* (1991) that the frequency of micronuclei is higher in individuals exposed to higher radiation doses than those exposed to lower doses.

Table XI. Nucleation indices indicating culture success; number of BNL's containing n number of micronuclei indicating an increase in micronuclei as the dose increased and micronuclei per 500 BNL's for control, 20 μ Sv/h and 100 μ Sv/h exposed bat lymphocytes cultured in PHA. One parameter SD values are shown.

SAMPLE #	NUCLEATION INDEX	NUMBER OF BINUCLEATED LYMPHOCYTES CONTAINING N NUMBER OF MICRONUCLEI					TOTAL No. OF BNL'S* ANALYSED	TOTAL No. OF MN* OBSERVED	MN PER 500 BNL'S*
		N=0	N=1	N=2	N=3	N=4			
Control									
1	1.1	744	8	0	0	0	752	8	5.3 \pm 1.9
20μSv/h									
1	1.4	798	22	0	0	0	820	22	13.4 \pm 2.9
2	1.4	953	45	1	0	0	1,000	47	23.5 \pm 3.4
3	1.4	974	35	1	0	0	1,011	37	18.3 \pm 3.0
4	1.5	234	8	0	0	0	242	8	16.5 \pm 5.8
5	1.7	813	29	0	0	0	842	29	17.2 \pm 3.2
6	1.7	838	31	0	0	0	869	31	17.8 \pm 3.2
7	1.7	938	33	0	0	0	971	33	17.0 \pm 2.9
8	1.7	826	28	0	0	0	854	28	16.4 \pm 3.1
9	1.7	974	35	2	0	0	1,013	39	19.2 \pm 3.1
AVERAGE									
	1.58	816	30	0.44	0.00	0.00	847	30	17.70
100μSv/h									
1	1.3	1,100	51	4	0	1	1,163	63	27.1 \pm 3.4

* BNL - Binucleated lymphocyte

* MN - Micronuclei

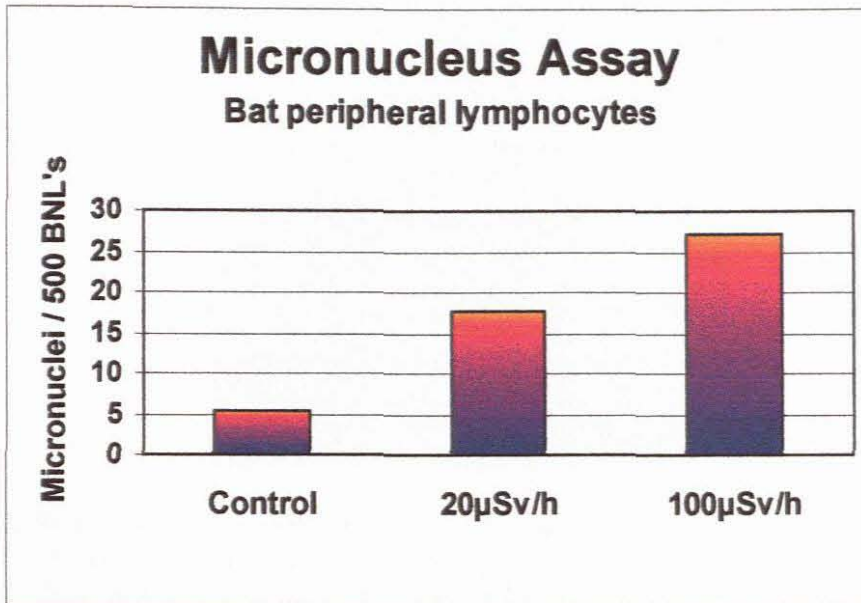


Figure 24. Graphic representation of micronuclei per 500 binucleated lymphocytes (BNL's) observed in control, 20 $\mu\text{Sv/h}$ and 100 $\mu\text{Sv/h}$ exposed bats. Bat lymphocytes were cultured with PHA as described in Materials and Methods. The average for the control group was 5.3, 20 $\mu\text{Sv/h}$ exposed bats showed an average of 17.7 and 100 $\mu\text{Sv/h}$ exposed bats showed an average of 27.1. The results show a significant increased dose response curve.

3.4.2 Micronucleus assay in peripheral reticulocytes

Analysis of bat peripheral reticulocytes for the presence of micronuclei (Figure 25) showed that control bat samples had between 0 and 3 micronuclei per 1 000 peripheral reticulocytes (Table XII). Bats exposed to low dose radiation of 20 $\mu\text{Sv/h}$ had between 0 and 7 micronuclei whereas those exposed to higher doses of 100 $\mu\text{Sv/h}$ had between 6 and 17 micronuclei per 1 000 peripheral reticulocytes.

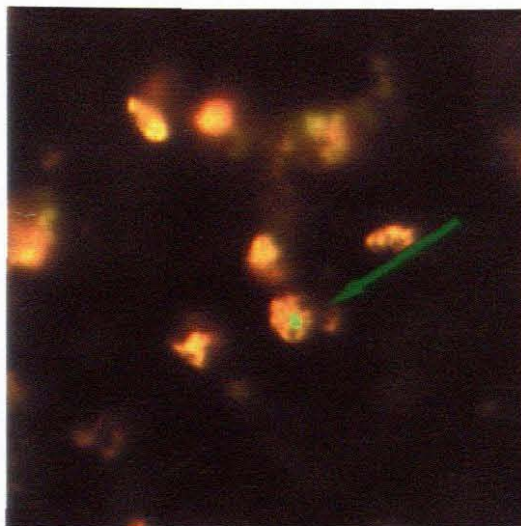


Figure 25. Photomicrograph of peripheral bat reticulocytes. Peripheral whole blood was sampled from bats, supravivally stained on a glass slide with acridine orange and examined using fluorescence microscopy. Micronuclei were identified as being round in shape and exhibiting a strong yellow-green fluorescence due to the presence of chromatin as indicated by the arrow. (Magnification : x 1000)

The average number of micronuclei in the control group, the 20 $\mu\text{Sv/h}$ group and the 100 $\mu\text{Sv/h}$ group were 1.7, 2.88 and 10.75 respectively and are shown graphically in Figure 26. Paired t-test analysis assuming unequal variance showed not only significant differences between the control and low radiation groups ($p = 0.002$) and between the control and higher radiation groups ($p < 0.001$), but also a statistically significant difference between the 20 $\mu\text{Sv/h}$ and the 100 $\mu\text{Sv/h}$ radiation exposure groups ($p < 0.001$), suggesting dosage dependent DNA damage (Table XII).

Table XII. Results of micronuclei observed in 1 000 supravivally stained peripheral reticulocytes of control, 20 μ Sv/h and 100 μ Sv/h exposed bats. The average micronuclei observed in control bats was 1.26, 2.88 in 20 μ Sv/h exposed bats and 9.45 in 100 μ Sv/h exposed bats. Statistical analysis showed all p-values to be significant ($p < 0.05$) indicating an increased dose response curve.

Control Sample #	MN/1000 Retics
H012	2
H013	2
H014	0
H015	2
H016	2
H017	0
H018	1
H020	2
H021	1
H022	0
H023	3
H024	0
H025	1
H026	1
H027	2
H028	0
H029	1
H030	2
H031	2
AVERAGE	1.26

20 μ Sv/h Sample #	MN/1000 Retics
S028	4
S029	1
S030	1
S031	4
S032	3
S033	3
S034	1
S035	7
S036	2
S037	3
S038	2
S039	0
S040	3
S049	2
S051	4
S052	5
S053	4
AVERAGE	2.88

100 μ Sv/h Sample #	MN/1000 Retics
S025	10
S026	11
S027	13
S050	9
S065	10
S066	15
S067	6
S068	12
S069	12
S071	6
S073	6
S074	6
S075	7
S076	6
S077	7
S078	17
S079	12
S081	6
S082	7
S083	11
AVERAGE	9.45

p Values	
Control vs Low	0.002
Control vs High	2.6E-08
Low vs High	1.4E-06

Low : 20 μ Sv/h
 High : 100 μ Sv/h

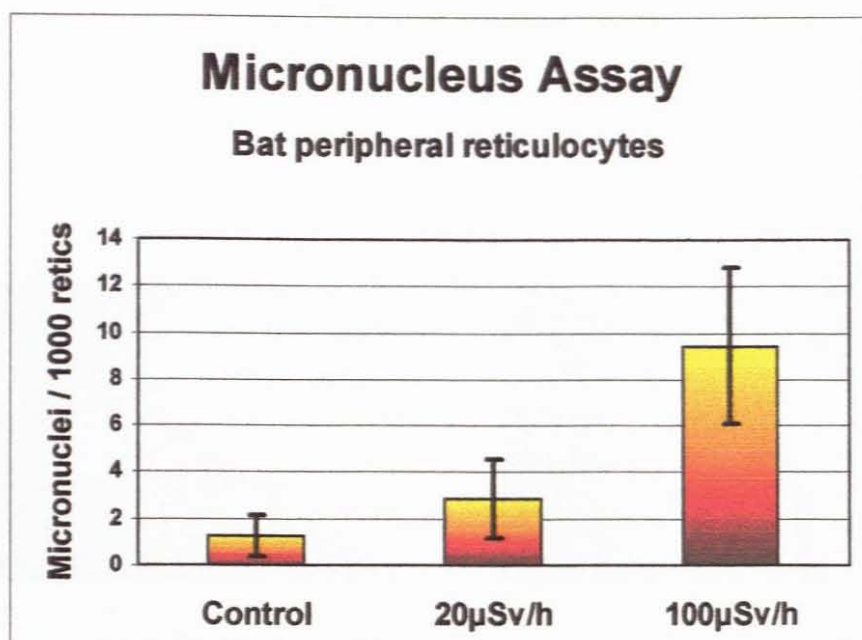


Figure 26. Graphic representation of average micronuclei per 1 000 peripheral bat reticulocytes of control, 20 $\mu\text{Sv/h}$ and 100 $\mu\text{Sv/h}$ exposed bats. The average for the control bats was 1.26, 20 $\mu\text{Sv/h}$ exposed bats showed an average of 2.88 and 100 $\mu\text{Sv/h}$ exposed bats showed an average of 9.45. The results suggest a significant increased dose response curve. Error bars of 1SD are indicated and show values of 0.9 for control bats, 1.7 for 20 $\mu\text{Sv/h}$ exposed bats and 3.3 for 100 $\mu\text{Sv/h}$ exposed bats.

3.4.3 Single cell gel electrophoresis (comet) assay

Comets were analysed according to the criteria of Lebailey *et al* (1997). Examples of grade 1 (undamaged), grade 2 (slightly damaged) and grade 3 (damaged) comets are shown in Figure 27.

In control samples, an average of 30 % of the comets were grade 1 whereas no grade 1 comets were observed for either the 20 $\mu\text{Sv/h}$ or 100 $\mu\text{Sv/h}$ doses of radiation exposure. 91 % of comets observed in the 20 $\mu\text{Sv/h}$ exposure samples were grade 2 while 9 % were grade 3. Bats exposed

to 100 $\mu\text{Sv/h}$ radiation had 72 % of comets as grade 2 and 28 % as grade 3 (Table XIII). No grade 4 comets (highly damaged) were detected in any of the samples.

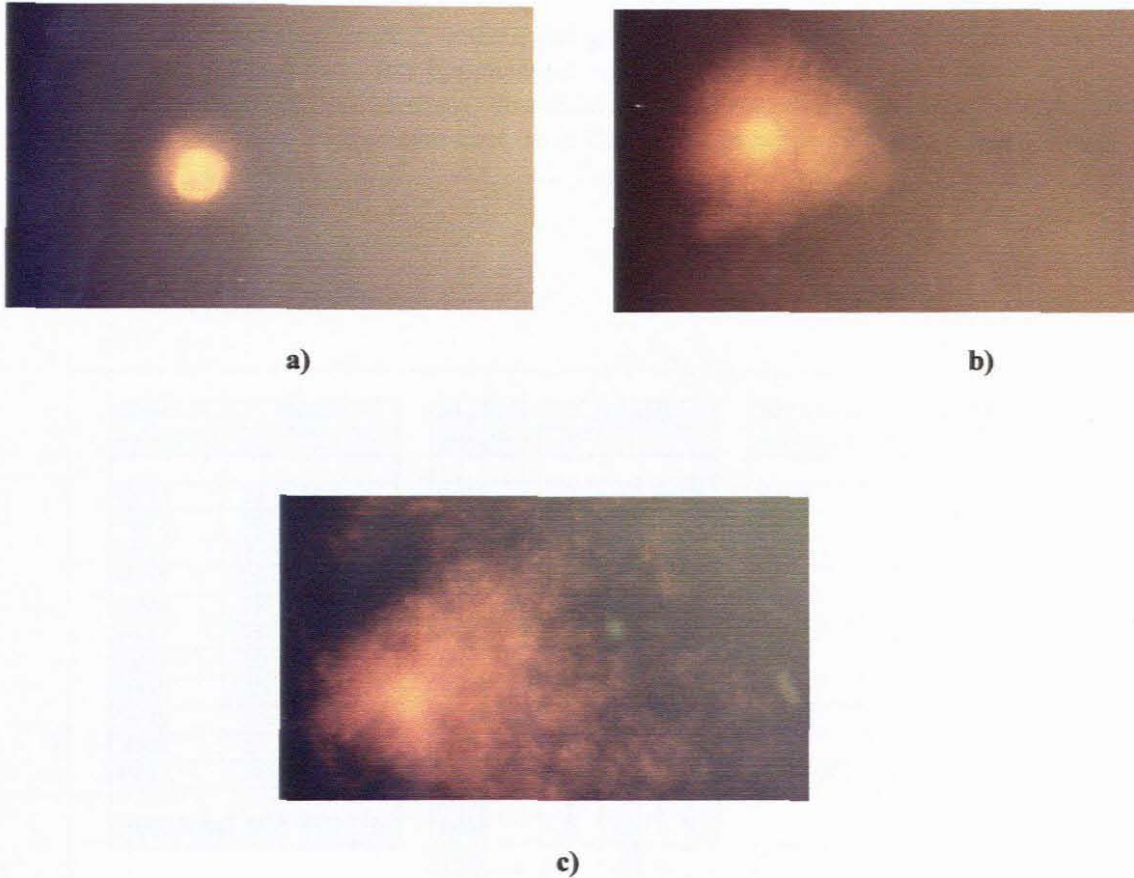


Figure 27. Photomicrographs of comets observed in bat lymphocytes after electrophoresis in an alkaline medium. After staining with Ethidium Bromide and using fluorescence microscopy, the characteristic nuclear matrix (“head”) and the “tail” can be seen and comets observed were graded as grade 1 - undamaged (a); grade 2 - slightly damaged (b) and grade 3 - damaged (c). (Magnification : x 600)

Mean damage per sample was calculated by assigning a value of 1 to grade 1 comets, 2 to grade 2 comets and 3 to grade 3 comets (Figure 28). The number of grade 3 comets clearly increased

as the radiation dose increased while the number of grade 1 comets clearly decreased. Paired t-test analysis assuming unequal variance was performed on the mean damage observed in control, 20 $\mu\text{Sv/h}$ and 100 $\mu\text{Sv/h}$ and p-values were recorded (Table XIII).

Table XIII. Results of grade 1, grade 2 and grade 3 comets observed in control, 20 $\mu\text{Sv/h}$ and 100 $\mu\text{Sv/h}$ exposed bats. Bat lymphocytes were electrophoresed in an alkaline medium as described in Materials and Methods.. Statistical analysis showed p-values to be highly significant ($p < 0.001$) indicating a significant increase in DNA damage as the radiation dose increased.

Control	GRADE			20 $\mu\text{Sv/h}$	GRADE			100 $\mu\text{Sv/h}$	GRADE		
Sample #	1	2	3	Sample #	1	2	3	Sample #	1	2	3
H012	32	59	9	S028	0	89	11	S015	0	69	31
H013	33	64	3	S029	0	87	13	S016	0	77	23
H014	33	60	7	S030	0	93	7	S017	0	76	24
H015	28	64	8	S031	0	90	10	S018	0	64	36
H016	39	49	12	S032	0	90	10	S019	0	70	30
H017	29	69	2	S033	0	88	12	S020	0	74	26
H018	30	53	17	S034	0	91	9	S021	0	72	28
H019	23	66	11	S035	0	88	12	S024	0	73	27
H020	25	59	16	S036	0	93	7	S050	0	71	29
H022	31	57	12	S037	0	89	11				
H023	24	66	10	S038	0	92	8	AVERAGE	0	72	28
AVERAGE	30	61	10	S039	0	91	9				
				S040	0	90	10				
				S041	0	93	7				
				S042	0	93	7				
				S043	0	91	9				
				S044	0	94	6				
				S045	0	90	10				
				S046	0	88	12				
				S047	0	89	11				
				S048	0	92	8				
				AVERAGE	0	91	9				

P-value (Mean Damage)	
Control vs Low	3.8E-08
Control vs High	2.0E-12
Low vs High	9.1E-08

Low : 20 $\mu\text{Sv/h}$
 High : 100 $\mu\text{Sv/h}$

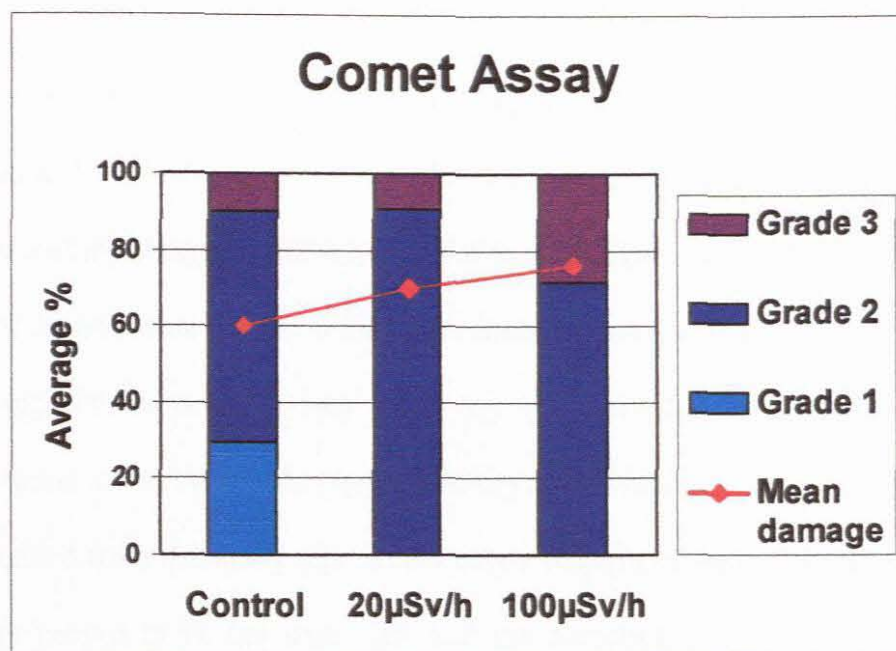


Figure 28. Graphic representation of grade 1, grade 2 and grade 3 comets observed in control, 20 $\mu\text{Sv/h}$ and 100 $\mu\text{Sv/h}$ exposed bats. Bat lymphocytes were electrophoresed in an alkaline medium as described in Materials and Methods. Mean damage per group was calculated as described in Materials and Methods and are indicated by the red bar. The results show a significant increased dose response curve.

Not only was there a highly significant increase in the DNA damage between the test and the control groups ($p < 0.001$), but there was also a statistically highly significant difference between the 20 $\mu\text{Sv/h}$ and the 100 $\mu\text{Sv/h}$ test groups ($p < 0.001$). The assay, therefore, is valuable in detecting cumulative DNA damage due to prolonged radiation exposure.

3.5 Cytogenetic Investigation

Bat chromosomes were successfully obtained by culturing bat lymphocytes as described in the materials and methods (page 39). One hundred metaphase spreads from control bats were analysed and the chromosomes were similar to those observed by Qumsiyeh *et al* (1988) in eleven of the sixty nine species in the genus, *Rhinolophus*. Qumsiyeh *et al* (1988) reported that identifying chromosomes in bats was “very difficult” due to the large number of bat chromosomes in the *Rhinolophus* species namely around fifty six to sixty chromosomes and that data obtained from that study represented only a fraction of the bats sampled. An additional difficulty proved to be the small size and the acrocentric nature of the majority of the chromosomes (Figure 29(a)). There were however no chromosomal aberrations observed in metaphase spreads from control bats.

One hundred metaphase nuclei were analysed from each group of radiation-exposed bats. However, as mentioned, analysis of chromosomes was extremely difficult. Very few dicentric chromosomes (Figure 29(b)) and ring chromosomes (Figure 29(c)) were observed and gaps and breaks could not be reported with confidence due to the small nature of the chromosomes.

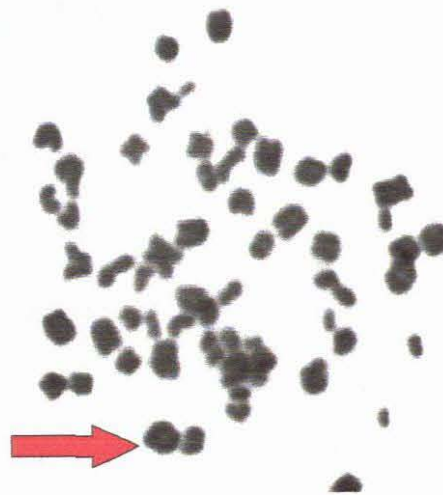
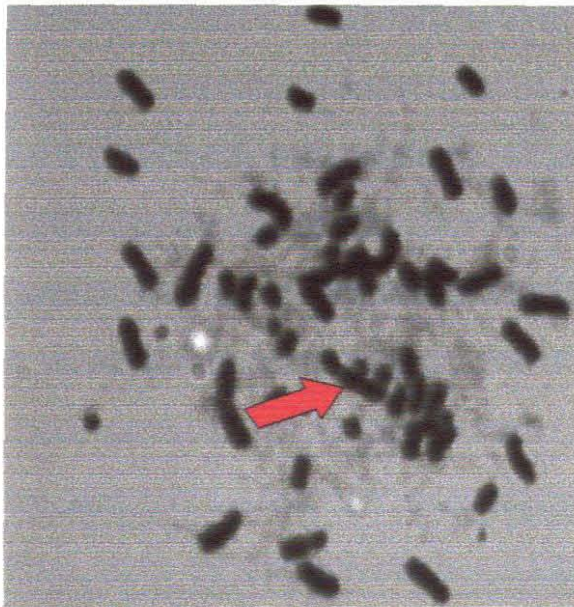
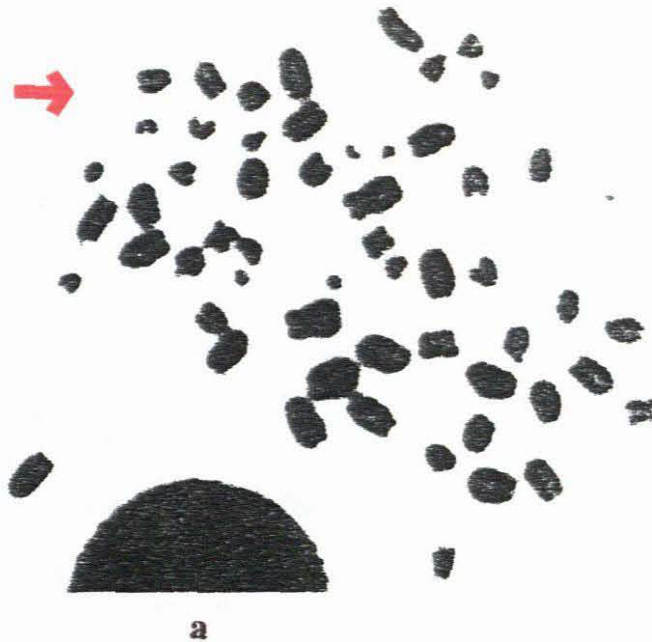


Figure 29. Metaphase spreads from bat lymphocytes cultured in PHA showing chromosomes from a control bat with many acrocentric chromosomes (arrows) and no aberrations (a) and from radiation exposed bats showing a dicentric chromosome (arrow) (b) and a ring chromosome (arrow) (c). (magnification : x 600)

CHAPTER 4

DISCUSSION

Histological investigation

Histological examination of bat lung and liver sections showed no morphological changes, fibrosis or inflammation nor increased collagen deposition in radiation exposed bats when compared to the control group. Although histological changes in radiation exposed tissue have been reported (Likhachev, 1973; Peterson *et al*, 1992; Waksman *et al*, 1995; Laird *et al*, 1996; van der Kogel *et al*, 1998 and van Kleef *et al*, 2000), the magnitude of the dose exposure was not comparable to this study. Current literature encompasses only experimental models where doses of up to 75 Gy were received and they were not limited to whole body exposure. There is, however, no published data to suggest that exposure to ionising radiation at doses of between 20 and 100 $\mu\text{Sv/h}$ may lead to tumour development, fibrosis or inflammation.

Miller *et al* (1986) showed a dose dependant increase in type 1 collagen in the lungs of irradiated mice to explore the role of connective tissue macromolecules in the development of radiation-induced pneumonitis and fibrosis. The use of this assay to detect an increase in collagen type I in lungs of radiation exposed bats may elucidate whether molecular changes may take place at low doses and it is envisaged that this aspect will be further investigated.

p53 Immunohistochemistry

Immunohistochemical results showed that the p53 protein had accumulated in the cells of the lungs and liver of radiation-exposed bats when compared to the same tissues of control bats. The results support previous findings that p53 accumulates to high levels in the tissues subsequent to radiation exposure (Harris and Hollstein, 1993). Not only was there a significant increase in the percentage of p53 positive cells, but also in the degree of p53 accumulation, especially in the cells lining the bronchiolar spaces. These cells are exposed to the environment and therefore more susceptible to the effects of α - radiation. As the penetration depth of α -radiation is very short (Smith, 1993), the p53 levels accumulated in the alveolar spaces were markedly decreased. p53 levels in the liver of radiation exposed bats were also increased, although not to the same extent as in the bronchiolar lining cells. As the liver is an organ of high metabolic activity, one would expect to find an increase in p53 levels. Although the p53 gene consists of highly conserved regions across many species (Malkin *et al*, 1994), the protocol for detection of p53 protein required standardisation for bat tissue and to our knowledge, identification of p53 mutations and subsequent increases in the expression of the gene in bat tissue has not been described elsewhere. The data, however, supports the current view that exposure to ionising radiation may lead to mutation of the p53 gene and subsequent progression to various cancers (Harris and Hollstein, 1993). As p53 mutations have not been described at doses of between 20 and 100 μ Sv/h, the results of this assay may prove to be invaluable in assessing the relationship between dose and risk of exposure to continuous low doses of ionising radiation. Future studies could focus on radiation induced mutations of the p53 and other germline genes.

Haematological investigation

It is well documented that exposure to ionising radiation may lead to the development of haematopoietic cancers, especially acute non-lymphocytic leukemia (Oscier, 1997). The relationship between risk and dose, however, remains unclear (Bowen and Yoshida, 1988). This study presented a unique opportunity to investigate a natural model where bats were exposed to continuous low doses of ionising radiation. Individuals exposed to radiation may develop myelodysplastic syndrome (MDS), the features of which include microcytic erythrocytes, a neutropenia with dysplastic neutrophils and cytoplasmic hypogranularity and a hypocellular bone marrow with abnormal progenitor development (Countenay, 1969 and Oscier, 1997).

As bone marrow damaged by irradiation may recover or persist with or without subsequent development of leukemia (Ruutu, 1986), it was reasonable that no bats presented with a leukaemic blood picture.

There was evidence of bone resorption in the marrow of some radiation-exposed bats which may be attributed to the effects of ionising radiation as described by Lord and Henry, (1995). As the bone structure of the radiation-exposed bats appeared abnormal, bone mineralisation using image analysis was investigated. Although the assay was qualitative, there was a marked decrease in osteoid mineralisation in radiation exposed bats. Although it would be recommended that radiodensity assays be done on control and radiation exposed bat bone samples, there was evidence suggesting a decrease in osteoid mineralisation subsequent to radiation exposure.

Throughout the investigation, samples S2 (20 $\mu\text{Sv/h}$) and S6 (100 $\mu\text{Sv/h}$) appeared to be less severely affected than the other groups within the dose range. Although the neutrophil count of S6 had not decreased to the same extent as the other samples in the group, the percentage of pseudo-Pelger Huet cells observed was the highest of all the groups. Bats in this group exhibited myelodysplastic syndrome that was not as advanced as in the other groups, however, neutrophil dysplasia was severe. S2 appeared to be the least affected as shown by the haematological investigation. As described earlier, a limitation of the study is that the precise age of each bat is not known, except that all bats sampled were adult and not juvenile. It is postulated that the bats from groups S2 and S6 may have been younger than those sampled in other groups and that the myelodysplastic syndrome had not progressed as yet to the same degree as in other sample groups.

Therefore, notwithstanding the limitations of the study, there is clear morphological evidence of dyshaemopoiesis, a relative neutropenia and a reduction in bone calcification. The above findings are clearly associated with secondary (radiation-induced) myelodysplastic syndrome in the human model. To our knowledge, new evidence now exists that exposure to such low doses of ionising radiation may lead to haematopoietic cancers.

DNA damage evaluation

It is important to develop simple and reliable techniques for biological dosimetry of exposure to radiation as such exposure is potentially carcinogenic and genotoxic (Fenech and Morley, 1985). The optimal sample time for any cell population is during a long-term chronic exposure

when induction and repair of DNA damage is presumed to be in equilibrium (Albertini *et al*, 2000). Careful selection of sample time will maximise the likelihood of identifying exposure to a DNA damaging agent. Should the exposure be of an acute nature, sample collection should be within a few hours of the exposure as DNA damage decreases with time due to activation of repair processes, loss of cells due to apoptosis, necrosis and cell turnover. As many experimental studies involve acute exposures, the limitations of these assays apply. This study therefore provided a unique opportunity to study a natural model where bats were continuously exposed to low-dose ionising radiation. The DNA damage and repair could therefore be assumed to be in equilibrium.

The micronucleus assay in peripheral lymphocytes has the potential for becoming a reliable technique for radiation-exposed population screening due to the simplistic nature of the technique (Fenech and Morely, 1995). Since exposure to genotoxins in the environment or in the workplace is usually close to background levels, conventional human biomonitoring studies e.g. chromosomal aberrations do not usually show unequivocal results (Olive *et al*, 1990). The comet assay however has shown to be extremely sensitive to low dose exposure to genotoxic agents (Kassie *et al*, 2000). The assay is not technically demanding and it may therefore be used to screen large population groups exposed to any potential carcinogen.

The methodologies employed in this study, namely micronuclei formation in peripheral lymphocytes and reticulocytes and the comet assay, showed that long term exposure to low doses of ionising radiation exposure resulted in a dose-dependent increase in DNA damage and these

results are in agreement with those of previous studies (Almassy *et al*, 1987, Hayashi *et al*, 1992). To our knowledge, micronuclei formation in peripheral reticulocytes has been documented after exposure to more than 400 different genotoxic chemicals, but not on radiation exposure.

The assays used in this study are clearly sensitive enough to detect DNA damage induced by prolonged exposure to low doses of ionising radiation.

Cytogenetic investigation

Although analysis of bat chromosomes proved to be more challenging than expected, Qumsiyeh (1988) observed and reported the difficulty in bat chromosome analysis. Aberrations were observed, albeit only in larger chromosomes, from bats exposed to radiation. Statistical analysis could not be performed and unequivocal conclusions could not be drawn. Detailed analysis of bat chromosomes could be undertaken using banding pattern techniques, however this was not within the scope of the study nor was the expertise required readily available in South Africa. It is envisaged that metaphase spreads will be forwarded to Qumsiyeh and co-workers for addition to the database of chromosome analysis of *Rhinolophus* species.

As chromosome aberrations have been statistically shown to occur in the smaller chromosomes (Sachs *et al*, 1996), it can be concluded that aberrations observed in this study may constitute only a fraction of the actual chromosomal damage induced by exposure of the bats to ionising radiation.

CHAPTER FIVE

CONCLUSIONS AND DIRECTIONS FOR FUTURE STUDIES

As far as we are aware, very few studies have been undertaken whereby a comparative analysis of more than one endpoint assay was performed after exposure to genotoxic agents. Gutierrez *et al* (1998) reported higher sensitivity of the micronucleus assay compared to the comet assay and Hartmann *et al* (1995) reported an increase in sister chromatid exchanges compared to the comet assay. These studies however were subsequent to acute exposure to ^{131}I and cyclophosphamide treated patients respectively. The present study appears to be the first study undertaken where the majority of all biomonitoring end point assays recommended by the ICRP (Albertini *et al*, 2000) were performed after continuous exposure to low doses of ionising radiation. In addition, histological and haematological investigations were also performed and the haematology proved to be of valuable interest elucidating the potential harmful effects of radiation on the haematopoietic system.

Many studies involving individuals exposed to low doses of ionising radiation have been subject to criticism due to inter-individual differences such as smoking, lifestyle, environmental factors and general health status thus unequivocal results could not be supported. This study, however, proved to be a unique model as all bats resided in the same location, had the same daily diet and, as far as the author is aware, did not partake in cigarette smoking. This is therefore the first study where a homogenous population exposed naturally to environmental or occupational ionising radiation for many years could be investigated. The study was also unique in that the subjects

were probably exposed as fertilised germ cells and furthermore *in utero* to the ionising radiation. The study has highlighted published data suggesting the increased susceptibility of embryonic tissue to the effects of ionising radiation.

It would be important to identify the molecular changes in type I collagen gene expression in the lungs of radiation exposed bats. As an increase in the expression of p53 protein in the lungs and liver of radiation exposed bats was observed, the bat (*Rhinolophus capensis*) p53 gene could be identified and sequenced. Once the sequence of control and radiation-exposed bats has been compared, possible mutation hotspots may be identified and documented. These studies may further elucidate the role of macromolecules in the development of radiation induced mutagenesis.

As the monazite mine at Steenkampskraal is likely to reopen in the near future, it will be in the best interest of the mining management to make use of a biodosimetry service. As it is known that inter-individual difference in radiosensitivity occurs (Thierens *et al*, 1991), the prospective employees will be exposed *in vitro* to various doses of ionising radiation and assays used in this study should be performed to verify the sensitivity of each endpoint. Employees that are more sensitive to radiation exposure can be placed in areas of the mine where the doses are lower. White (1996) stresses the importance of monitoring possible harmful exposure in the workplace as the South African Occupational Health and Safety Act (OHSA) of 1993 has established and broadened the right of all employees to a safe working environment. Occupational medical surveillance is defined in the OHSA as a planned programme of periodic examination (biological

monitoring) of employees. The screening element of medical surveillance aims to detect overexposure or an adverse effect of occupational exposure at a point earlier than that at which the individual would seek medical attention (Ehrlich, 1996). By screening the radiation exposed miners on a regular basis for early signs of DNA damage using e.g. micronuclei formation and the comet assay, this would be accomplished.

As indicated throughout the study, the assays described can be applied to any potential mutagen or carcinogen that an individual is exposed to and a biodosimetry service can therefore be extended to incorporate other industries such as paint, pesticide and plastics.

Wu and coworkers (1999) reported that scientists may have to alter risk estimates for people exposed to low levels of ionising radiation such as radon after discovering that cytoplasm hit with alpha particles may mediate a mutational event in the nucleus. Prior to this report, the cell nucleus has been considered the only target for carcinogenic mutations. Cells are usually killed when large portions of DNA are damaged, whereas non-lethal mutations persist and may accumulate, potentially leading to cancer. Cytoplasmic irradiation may therefore play a significant role in carcinogenesis. The results of the present study may be explained in the light of this discovery as doses of 100 $\mu\text{Sv/h}$ have historically been considered safe.

Although one has to be cautious about extrapolating data from bats to humans, the results of this study clearly indicate the potential risk of continuous exposure to low doses of ionising radiation.

REFERENCES

- ATSDR. (1990). Toxicological profile for thorium. US Department of Health and Human Services. Public Health Service. Agency for Toxic Substances and Disease Registry. Atlanta, GA.
- Adamkiewicz, J., Eberle, G., Huh, N., Nehls, P. and Rajewsky, M.F. (1985) Quantitation and visualisation of alkyl deoxynucleosides in the DNA of mammalian cells by monoclonal antibodies. *Environ. Health Perspect.* 62, 49-55.
- Albert, R., Klewin, P., and Fresco, J. (1955) Industrial hygiene and medical survey of a thorium refinery. *Arch. Ind. Health* 11, 234-242.
- Albertini, R.J. and Hayes, R.B. (1997) Somatic cell mutations in cancer epidemiology. International Agency for Research on Cancer, Lyons. 159-184.
- Albertini, R.J., Sullivan, L.S., Berman, K.J., Greene, C. J., Stewart, J.A., Silveira, J.M. and O'Neill, J.P. (1988) Mutagenicity monitoring in humans by autoradiographic assay for mutant T lymphocytes. *Mutat. Res.* 204, 481-492.
- Albertini, R.J., Anderson, D., Douglas, G.R., Hagmar, L., Hemminki, K., Merlo, F., Natarajan, A.T., Norppa, H., Shuker, D.E.G., Tice, R., Waters, M.D. and Aitio, A. (2000) IPCS guidelines for the monitoring of genotoxic effects of carcinogens in humans. (Special Issue) *Reviews in Mut. Res.* 463(2), 111-172.
- Allred, D.C., Clark, G.M., Elledge, R., Fuqua, S.W.A., Brown, R.W., Chamness, G.C., Osborne, C.K. and McGuire, W.L. (1993) Association of p53 protein expression with tumour cell proliferation rate and clinical outcome in node-negative breast cancer. *J. Nat. Cancer Inst.* 85(3), 200-206.

- Almassy, Z., Krepinsky, A., Bianco, A. and Koteles, G.J. (1987) The present state and perspectives of micronucleus assay in radiation protection. A Review. **Int. J. Radiat.** 38 (4), 241-249.
- Andrioli, M.A.G., Smith, C.B., Watkeys, M., Moore, J.M., Ashwal, L.D. and Hart, R.J. (1994) The geology of the Steenkampskraal Monazite deposit, South Africa : implications for REE-TH-Cu mineralization in Charnockite-Granulite Terranes. **Economic Geology** 89, 994-1016.
- Archer, V.E., Wagoner, J.K. and Lundin, F.E. (1973) Cancer mortality among uranium mill workers. **J. Occup. Med.** 15, 11-14.
- Ban, N., Kai, M. and Kusama, T. (1997) Chromosome aberrations in bone marrow cells of C3H/He mice at an early stage after whole-body irradiation. **J. Radiat. Res.** 38(4), 219-231.
- Bauchinger, M., Braselmann, H., Kulka, U., Huber, R. and Georgiadou-Schumacher, V. (1996) Quantification of FISH-painted chromosome aberrations after domestic radon exposure. **Int. J. Rad. Biol.** 70(6), 657-663.
- BEIR V. (1990) Health effects of exposure to low levels of ionising radiation. Committee on the Biological Effects of Ionising Radiations, National Research Council. Washington, DC: National Academy Press.
- Bender, M.A., Griggs, H.G. and Bedford, J.(1974) Mechanisms of chromosomal aberration production III. Chemicals and ionising radiation. **Mutat. Res.** 23, 197-212.
- Bennett, J.M., Catovsky, D., Daniel, M.T., Flandrin, G., Gralnick, H.R. and Sultan, C. (1985) Proposed Revised Classification of Acute Myeloid Leukaemia. **Am. Intern. Med.** 103, 626.

- Bowen, A and Yoshida, Y. (1998) Pathogenesis, etiology and epidemiology of myelodysplastic syndromes. **Haematologica** 83(1), 71-86.
- Bryant, P.E. (1997) DNA damage, repair and chromosomal damage. **Int. J. Rad. Biol.** 71(6), 675-680.
- Cardis, E., Gilbert, S., Carpenter, L., Howe, G., Kato, I., Armstrong, B.K., Beral, V., Cowper, G., Douglas, A., Fix, J., Fry, S.A., Kaldor, J., Lave, C., Salmon, L., Smith, P.G., Voelz, G.L. and Wiggs, L.D. (1995) Effects of low doses and low dose rates of external ionising radiation : cancer mortality among nuclear industry workers in three countries. **Rad. Res.** 142, 117 - 132.
- Conibear, S.A. (1983) Long term health effects of thorium compounds on exposed workers : The complete blood count. **Health Phys.** 44 (Suppl 1) : 231-237.
- Countenay, V.D. (1969) Radioresistant Mutants of L5178y cells. **Radiat. Res.** 38, 186.
- Countryman, P.I. and Heddle, J.A. (1976) The production of micronuclei from chromosome aberrations in irradiated cultures of human lymphocytes. **Mutat. Res.** 41, 321-332.
- Crompton, N and Ozsahin, M. (1997) A versatile and rapid assay of radiosensitivity of peripheral blood leukocytes based on DNA and surface-marker assessment of cytotoxicity. **Rad. Res.** 147, 55-60.
- Darzynkiewicz, Z., Bruno, S., Del Bino, G., Gorczyca, W., Hotz, M.A., Lassota, P. and Traganos, F. (1992) Features of apoptotic cells measured by flow cytometry. **Cytometry** 13, 795-808.
- Du Toit, R.S.J. (1964) Experience in the control of radiation at a small thorium mine in South Africa. **Radiological Health and Safety in the Mining and Milling of Nuclear Material 1**, IAEA Symposium.

- Ehrlich, R. (1996) Occupational medical surveillance. **CME** 14(9), 1301-1307.
- Evans, H.J. and O'Riordan, M.L., (1975) Human peripheral blood lymphocytes for the analysis of chromosome aberrations in mutagen tests. **Mutat. Res.** 31, 135-148.
- Fairbairn, D.L., Olive, P.L. and O'Neil, K.L. (1995) The Comet assay: a comprehensive review. **Mutat. Res.** 339,37-59.
- Falkvol, K.H. (1990) The occurrence of apoptosis, abnormal mitosis, cells dying in mitosis and MN in a human melanoma xenograft exposed to single dose irradiation. **Strahlentherapie und Onkologie** 166, 487-492.
- Farmer, P.B. and Sweetman, G.M.A. (1995) Mass spectrometric detection of carcinogenic adducts. **J. Mass Spectr.** 30, 1369-1379.
- Fenech, M. and Morley, AA. (1985) Measurement of micronuclei in lymphocytes. **Mutat. Res.** 147, 29-36.
- Fliedner, T.M., Andrews, G.A., Crookie, E.P. and Bond, V.P. (1964) Early and late cytological effects of whole body irradiation on human marrow. **Blood** 23, 471-476.
- Gaugler, M-H., Squiban, C., Claraz, M., Schweitzer, K., Weksler, B., Gourmelon, P. and Van der Meern, A. (1998) Characterisation of the response of human bone marrow endothelial cells to in vitro irradiation. **Br. J. Haem.** 103, 980-989.
- Groopman, J.D. and Kensler, T.W. (1999) The light at the end of the tunnel for chemical-specific biomarkers: daylight or headlight? **Carcinogenesis** 20, 1-11.
- Gutierrez, E., Carbonell, E., Galofre, P., Creus, R. and Marcos, R. (1998) The alkaline single-cell gel electrophoresis (SCGE) assay applied to the analysis of radiation-induced DNA damage in thyroid cancer patients treated with ¹³¹I. **Mutat. Res.** 413(1998) 733- 736.

- Hall, R.H., Straud, CA., Scott, JK. *et al.* (1951) Acute toxicity of inhaled thorium compounds. Atomic Energy Project, University of Rochester, Rochester, NY. Report No. UR-190.
- Harris, C.C. and Hollstein, M.(1993) Clinical implications of the p53 tumour suppressor gene. **N. Engl. J. Med.** 1318-1326.
- Hartley, B.M. and Hewson, G.S. (1993) Summary of radiation research into thorium (monazite) dosimetry. **Rad. Prot. Austr.** 11, 165-169.
- Hartmann, A., Herkommer, K., Glück, M. and Speit, G.(1995) DNA-damaging effect of cyclophosphamide on human blood cells in vivo and in vitro studies with the single-cell gel test (comet assay).**Environ. Mol. Mutagen.** 25(1995) 180-187.
- Hayashi, M., Sofumi, T. and Ishidate Jr. M.(1983) An application of acridine orange fluorescent staining to the micronucleus test. **Mutat. Res.** 120, 241-247.
- Hayashi, M., Morita, T., Kodama, Y., Sofuni, T. and Ishidate Jr, M. (1990) The micronucleus assay with mouse peripheral blood reticulocytes and acridine-orange coated slides. **Mutat. Res.** 245, 245-249.
- Hayashi, M. *et al* (1992) Micronucleus test with mouse peripheral blood erythrocytes by acridine orange supravital staining : The summary report of the 5th collaborative study by CSGMT/ JEMS- MMS. **Mutat. Res.** 278, 83-98.
- Hayashi, M. and Sofuni, T. (1994) The micronucleus assay with rodent peripheral blood and acridine orange supravital staining. **Chromosomal Alterations** Springer Verlag, Berlin, 203-213.
- Heddle, JA. (1973) A rapid in vivo test for chromosomal damage. **Mutat. Res.** 18, 187-190.
- Heddle, JA., Hite, M., Kirkhart, B., Mavournin, K., MacGregor, J.T., Newell, G.W.. and Salamone, M.F. (1983) The induction of micronuclei as a measure of genotoxicity. A report of the U.S. Environmental Protection Agency Gene-Tox Program. **Mutat. Res.**

- Hemminki, K., Dipple, A., Shuker, D.E.G., Kadlubar, F.F., Segerbäck, D. and Bartsch, H. (1994) DNA adducts, identification and biological significance, International Agency for Research on Cancer, Lyons. IARC Scientific Publications. 125, 478pp.
- Henshaw, D.L. (1995) In : **Radiation toxicology : bone marrow and leukemia**. Chapter 3 : Human Radiation Exposure (Ed: Henry and Lord).
- Hertveldt, K., Philippé, J., Thierrens, H., Cornelissen, M., Vral, A. and de Ridder, L. (1997) Flow cytometry as a quantitative approach and sensitive method to evaluate low dose radiation induced apoptosis *in vitro* in human peripheral blood lymphocytes. **Int. J. Rad. Biol.** 71(4), 429-433.
- Hodge, H.C., Maynard, E.A. and Leach, L.J. (1960) The chemical toxicity of thorium dioxide following inhalation by laboratory animals. University of Rochester - Atomic Energy Project. Report UR-562. University of Rochester, Rochester, NY, 1-33.
- Ibrahim, SA., Wrenn, M.E., Singh, N.P. *et al.* (1983) Thorium concentration in human tissues from two US populations. **Health Phys.** 21 : 173-207.
- Iggo, R., Gatter, K., Bartek, J., Lane, D. and Harris, A.L. (1990) Increased expression of mutant forms of p53 oncogene in primary lung cancer. **Lancet** 335, 675-679.
- Imumara, M. and Edgreen, M.R. (1994) Significance of the proportion of binucleated cells in the micronucleus assay : a methodological study. **Journal of Rad. Res.** 35, 11-15.
- Kassie, F., Parzefall, W. and Knasmüller, S. (2000) Single cell gel electrophoresis assay : a new technique for human biomonitoring studies. **Mutat. Res.** 463(2000), 13-31.
- Kemp, C.J., Wheldon, T. and Balmain, A. (1994) p53-deficient mice are extremely susceptible to radiation-induced tumorigenesis. **Nature Genet.** 8, 66-69.

- Čnehr, S., Zitzelsberger, H., Braselmann, H., Nahrstest, U and Bauchinger, M. (1996) Chromosome analysis by fluorescence *in situ* hybridisation : further indications for a non-DNA-proportional involvement of single chromosomes in radiation-induced structural aberrations. **Int. J. Radiat. Biol.** 70(4), 385-392.
- Kolanko, C.J, Pyle, M.D., Loats, H., Parton, J, Blakeky, W.F. and Nath. J. (1999) Fast *in situ* hybridisation and immunoenzymatic colour pigment detection of mouse bone marrow nucleus. **Biotechnic and Histochemistry** 74(3), 111-115.
- Laird, J.R., Carter, A.J., Kufs, W.M., Hoopes, T.G., Farb, A., Nott, S.H., Fischell, R.E., Virmani, R. and Fischell, T.A. (1996) Inhibition of neointimal proliferation with low-dose irradiation from a beta-particle-emitting stent. **Circulation** 193, 529-536.
- Lebailly, P., Vigreux, C., Godard, T., Sichel, F., Bar, E., Le Talaer, J.Y., Henry-Amar, M. and Gauduchon, P. (1997) Assessment of DNA damage induced *in vitro* by etoposide and two fungicides (carbendazim and chlorothalonil) in human lymphocytes with the comet assay. **Mutat. Res.** 375, 205-217.
- Levine, A.J., Momand, J., Finlay, C.A. (1991) The p53 tumour suppressor gene. **Nature** 351, 435 - 456.
- Likhachev, YuP., Lyarskii, P.P. and Elovskaya L.T. (1973) Pulmonary neoplasms in rats in chronic inhalation of thorium dioxide. **Med. Radiol.** 18, 35-41.
- Lindholm, C., Salomaa, S., Tekkel, M., Paile, W., Koivistoinen, A., Ilus, T and Veiderbaum, T (1996) Biodosimetry after accidental radiation exposure by conventional chromosome analysis and FISH. **Int. J. Rad. Biol.** 70(6) 647-656.
- Lord, B.I. and Henry, J.H. (1995) In : **Radiation Toxicology : Bone Marrow and Leukemia.** (Ed : Lord and Henry). Taylor and Francis, UK.

- Luckey, T.D. (1991) In : **Radiation Hormesis**. CRC Press, USA.
- Lumniczky, K., Antal, S., Unger, E., Wunderlich, L., Hidvegi, E.J. and Safrany, G. (1998) Carcinogenic alterations in murine liver, lung and uterine tumours induced by in utero exposure to ionising radiation. **Mol. Carcinog.** 21(2), 100-110.
- Macallum, D.E., Hupp, T.E, Carole, A.M. *et al* (1996) The response to ionising radiation in adult and developing murine tissues. **Oncogene** 13, 2757-2785.
- MacGregor, J.T., Wehr, C.M. and Gould, D.H. (1980) Clastogen-induced micronuclei in peripheral blood erythrocytes: the basis of an improved micronucleus test. **Environ. Mutagen.** 2, 509-514.
- Malkin, D. (1994) Germline p53 mutations and heritable cancer. **Ann. Rev. Genetics** 28, 443-465.
- Mavournin, K.H., Blakey, D.H., Cimino, M.C., Salamene, M.F. and Heddle, J.A. (1990) The in vivo micronucleus assay in mammalian bone marrow and peripheral blood. A report of the US Environmental Protection Agency Gene-Tox Program. **Mutat. Res.** 239, 29-80.
- McBride, O.W., Merry, D.E., Givol, D. (1986) The gene for human p53 cellular tumour gene is located on chromosome 17 short arm (17p13). **Proc. Nat. Acad. Sci.** 83, 130-134.
- McKelvey-Martin, V.J., Green, M.H.L., Schmezer, P., Pool-Zobel, B.L., De Meo, M.P. and Collins, A. (1993) The single cell gel electrophoresis assay (comet assay) : A European review. **Mutat. Res.** 288, 47-63.
- Meyn, R.E., Stephens, L.C., KianAng, K, Hunter, N.R., Brock, W.A., Milas, L. and Peters, L.J. (1993) Heterogeneity in the development of apoptosis in irradiated murine tumours of different histologies. **Int. J. Rad. Biol.** 64, 583-591.

- Miller, C., Mohandas, T., Wolf, D., Prokocimer, M., Rotter, V. and Koeffler, H.P. (1986) Human p53 gene localised to short arm of chromosome 17. **Nature** 319, 783-784.
- Miller, C., Siemann, D., Scott, P., Dawson, D., Muldrew, K., Trepanier, P. and McGann, L. (1986) A semiquantitative probe for radiation-induced normal tissue damage at the molecular level. **Radiat. Res.** 105(1), 76-83.
- Müller, R. and Rajewsky, M.F. (1981) Antibody specific for DNA components structurally modified by chemical carcinogens. **J. Cancer Res. Clin. Oncol.** 102, 99-113.
- Nehls, P., Adamskiewicz, J. and Rajewsky, M.F. (1984) Immuno-slot-blot : a highly sensitive immunoassay for the quantification of carcinogen-modified nucleosides in DNA. **J. Cancer Res. Clin. Oncol.** 108, 23-29.
- Nowack, R.M. (1994) In: **Walker's Bats of the World**. Johns Hopkins University Press, Baltimore.
- O'Neill, J.P., Mc Ginniss, M.J., Berman, J.K., Sullivan, L.M., Nicklas, J.A. and Albertini, R.J. (1987) Refinement of a T lymphocyte cloning assay to quantify the *in vivo* thioguanine-resistant mutant frequency in humans. **Mutagenesis** 2, 87-94.
- Olive, P.L., Banath, J.P. and Durand, R.E. (1990) Heterogeneity in radiation-induced DNA damage and repair in tumour and normal cells measured using the "comet" assay. **Radiat. Res.** 122, 86-94.
- Oscier, D. (1997) ABC of clinical haematology. The myelodysplastic syndromes. **BMJ.** 314, 883-886.
- Osterman-Golkar, S. and Bond, J.A. (1996) Biomonitoring of 1,3-butadiene and related compounds. **Environ. Health Perspect.** 104 (Suppl. 5), 907-915.

- Östling, O. and Johanson, K.J. (1984) Microelectrophoretic study of radiation-induced DNA damages in individual mammalian cells. **Biochem. Biophys. Res. Commun.** 123, 291-298.
- Paul, B.N. and Chakravarty, A.K. (1987) Phytohaemagglutinin mediated activation of bat (*Pteropus giganteus*) lymphocytes. **Indian Journal of Experimental Biology.** 25, 1-4.
- Peterson, L.M., Evans, M.L., Graham, M.M., Eary, J.F. and Dahlen, D.D. (1992) Vascular response to radiation injury in the rat lung. **Radiat. Res.** 129(2), 139-148.
- Pierre, R.V. (1978) Preleukaemic Syndrome. **Virchows Arch. (Cell Pathol)** 29, 29.
- Polednak, A.P., Stehney, A.F. And Lucas, H.F. (1983) Mortality among male workers at a thorium- processing plant. **Health Phys.** 44 (Suppl 1) : 239 - 251.
- Prahalad, A., K., Ross, J.A., Nelson, G.B., Roop, B.C., King, L.C., Nesnow, S. and Mass, M.J. (1997) Dibenzo[*a,l*]pyrene-induced DNA adduction, tumorigenicity, and Ki-ras oncogene mutations in strain A/J mouse lung. **Carcinogenesis** 18, 1955-1963.
- Qumsiyeh, M.B., Owen, R.D. and Chesser, R.K. (1988) Differential rates of genic and chromosomal evolution in bats of the family Rhinolophidae. **Genome** 30, 326-335.
- Roesch, W.C. (1987) Final Report : US Japan Joint Reassessment of A-bomb Radiation in Hiroshima and Nagasaki. **Rad. Effects Res. Foundation, Hiroshima.**
- Rotblat, J. (1988) A Tale of Two Cities. **New Scientist** Jan 7, 46-50.
- Ruutu, T. (1986) The Myelodysplastic Syndromes. **Scan. J. Haem.** Suppl 45 Vol 36.
- Sachs, R.K., Chen, A.M. and Brenners, D.J. (1996) Review : Proximity effects in the production of chromosome aberrations by ionising radiation. **Int. J. Radiat. Biol.** 71(1), 1-19.

- Sali, D. Cardis, E., Sztanyik, L., Auvinen, A., Bairakova, A., Dontas, N., Grosche, B., Kerekes, A., Kuzic, Z., Kusoglu, C., Lechpammer, S., Lyra, M., Michaelis, J, Petridou, E., Szibinski, Z A., Tominaga, S., Tulbure, R, Turnbull, A and Valerianova, Z (1996) Cancer consequences of the Chernobyl accident in Europe outside the former USSR : a review. **Int. J. Cancer** 67, 343-352.
- Sankaranarayan, K. (1993) Ionising Radiation, Genetic Risk Estimation and Molecular Biology: Impact and Inferences. **Trends in Genetics** 9 (3), 79-83.
- Schmidt, W. (1975) The micronucleus test. **Mutat. Res.** 31, 9-15.
- Seed, T.M., Kaspar, L.V., Tolle, D.V. and Fritz, T.E. (1987) Chronic Radiation Leukemogenesis: postnatal hematopathological effects resulting from in-utero irradiation. **Rad.Res.** 11 (2) 171-179.
- Seed, T.M. and Meyers, S.M. (1993) Chronic radiation-induced alteration in haematopoietic repair during preclinical phases of aplastic anaemia and myeloproliferative disease: assessing unscheduled DNA synthesis response. **Cancer Res.** 53(19), 4518-4527.
- Singh, N.P., McCoy, M.T., Tice, R.R. and Schneider, E.L.(1988) A simple technique for quantitation of low levels of DNA damage in individual cells. **Exp. Cell Res.** 175, 184-191.
- Singh, N.P., Wrenn, M.E., Ibrahim, S.A. (1982) Thorium concentrations in human tissues from two geographic locations of the United States. **Nat. Rad. Env.** 258-268.
- Smith, H. (Ed)(1993) Annals of the (ICRP). Publication # 60. **Recommendations of the International Commission on Radiological Protection.** ICRP, Didcot, Oxfordshire.

- Smith, M.T, Zhang, L., Wang, Y., Hayes, R.B., Li, G. and Wiemels, J. (1998) Increased translocations and aneusomy in chromosomes 8 and 21 among workers exposed to benzene. **Cancer Res.** 58, 2176-2181.
- Stephan, G and Pressl, S. (1996) Chromosome aberrations in hman lymphocytes analysed by fluorescence in situ hybridisation after in vitro irradiation, and in radiation workers, 11 years after accidental radiation exposure. **Int. J. Rad. Biol.** 71(3), 293-299.
- Stephens, L.C., KianAng, K., Schultheiss, T.E., Milas, L and Meyn, R.E. (1991) Apoptosis in irradiated murine tumours. **Rad. Res.** 127, 308-316.
- Stephens, L.C., Hunter, N.R., KianAng, K, Milas, L. and Meyn, R.E. (1993) Development of apoptosis in irradiated murine tumours as a function of time and dose. **Rad. Res.** 135, 75-80.
- Sullivan, M.F. (1980) Absorption of actinide elements from the gastrointestinal tracts of neonatal animals. **Health Phys.** 38, 173-185.
- Sullivan, M.F., Miller, B.M. and Ryan, J.L. (1983) Absorption of thorium and protactinium from the gastrointestinal tract in adult mice and rats and neonatal rats. **Health Phys.** 44, 425-428.
- Sumner, A. T. (1972). A simple technique for demonstrating centromeric heterochromatine. **Exp. Cell Res.** 75, 304 - 306.
- Sunta, C.M., Dang, H.S. and Jaiswal, D.D. (1987) Thorium in man and environment: Uptake and clearance. **J. Radional. Nucl. Chem.** 115, 149-158.
- Takahashi, T., Nau, M.M., Chiba, I, Birrer, M.J., Rosenberg, R.K., Vinocour, M., Levitt, M., Pass, H., Gazdar, A.F. and Minna, J.D. (1989) p53 : a frequent target for genetic abnormalities in lung cancer. **Science** 246, 491-494.

- Tannenbaum, S.R., Skipper, P.L., Wishnok, J.S., Stillwell, W.G., Day, B.W. and Taghizadeh, K. (1993) Characterisation of various classes of protein adducts. **Environ. Health Perspect.** 99, 51-56.
- Tanaka, K., Popp, S., Fischer, C., van Kaiks, G., Kamada, N., Cremer, T. and Cremer, C. (1996) Chromosome aberration analysis in atomic bomb survivors and Thorotrast patients using two- and three-colour chromosome painting of chromosomal subsets. **Int. J. Rad. Biol.** 70(1), 95-108.
- Tates, A.D., Grummt, T., Törnqvist, M., Farmer, P.B., van Dam, F.J., van Mossel, H., Shoemaker, H.M., Osterman-Golkar, S., Uebel, C., Tang, Y.S., Zwinderman, A.H., Natarajan, A.T. and Ehrenberg, L. (1991) Biological and chemical monitoring of occupational exposure to ethylene-oxide. **Mutat. Res.** 250, 483-497.
- Thierens, H., Vral, A. and de Ridder, L. (1991) Biological dosimetry using the micronucleus assay for lymphocytes: Interindividual differences in dose response. **Health Phys.** 61 (5), 623-630.
- Thomas, C.B., Nelson, D.O., Pleshanov, P., Vorobstova, I., Tureva, L., Jensen, R. and Jones, I.M. (1999) Elevated frequencies of HPRT mutants are detected in Russian liquidators 6-10 years after exposure to radiation from Chernobyl nuclear power plant accident. **Mutat. Res.** 439, 105-119.
- Törnqvist, M and Ehrenberg, L. (1994) On cancer risk estimation of urban air pollution. **Environ. Health Perspect.** 102 (Suppl.4), 173-181.
- Törnqvist, M., Mowrer, J., Jensen, S. and Ehrenberg, L. (1986). Monitoring of environmental cancer initiators through haemoglobin adducts by a modified Edman degradation method. **Anal. Biochem.** 154, 255-266.

- van Kleef, E.M., Zurcher, C., Oussoren, Y.G., Te Poel, J.A., van der Valk, M.A., Niemer-Tucker, M.M., van der Hage, M.H., Broerse, J.J., Robbins, M.E., Johnston, D.A. and Stewart, F.A. (2000) Long-term effects of total body irradiation on the kidneys of Rhesus monkeys. **Int. J. Rad. Biol.** 76 (5), 641-648.
- van der Kogel, A.J., Jarrett, K.A., Paciotti, M.A. and Raju, M.R. (1998) Radiation tolerance of the rat rectum to fractionated X-rays and pi-mesons. **Radiother. Oncol.** 12 (3), 225-232.
- Vander, J.B., Harris, C.A. and Ellis, S.R. (1963) Reticulocyte counts by means of fluorescence microscopy. **J. Lab. Clin. Med.** 62, 132-140.
- Vijayalaxmi, R., Tice, R. and Strauss, G.H.S. (1992) Assessment of radiation-induced DNA damage in human blood lymphocytes using the single cell gel electrophoresis technique. **Mutat. Res.** 271, 243-252.
- Vojtseek, B., Bartek, J., Midgley, C.A. and Lane, D.P. (1992) An immunochemical analysis of the human nuclear phosphoprotein p53. New monoclonal antibodies and epitope mapping using recombinant p53. **J. Immunol. Meth.** 151, 237-244.
- Waksman, R., Robinon, K.A., Crocker, I.R., Wang, C., Gravanis, M.B., Cipolla, G.D., Hillstead, R.A. and King, S.B. 3rd (1995) Intracoronary low-dose beta-irradiation inhibits neointima formation after coronary balloon injury in the swine restenosis model. **Circulation** 92(10), 3025-3031.
- White, N. (1996) An overview of occupational diseases seen in South Africa. **CME** 14(9), 1313-1318.
- Wrenn, M.E., Singh, N.P., Cohen, N. *et al.* (1981) Thorium in human tissues. **NTIS NUREG/CR-1227**, 1-97.

- Wu, L-J., Randers-Pehrson, A.X, Geard, C.R, Waldren, C.A., Yu, Z.L. and Hei, T.K., (1999) Targeted cytoplasmic irradiation with alpha particles induces mutations in mammalian cells. **Proc. Nat. Acad. Sci.** 96(6), 4959.
- Xhing-an, C., Hui-juan, X., Yong-e, C., Zhi-hua, D., Ying-Jie, Y., Lian, C., Jing-fang, H., Qui-chen, H., Guo-dong, F. and Yun-hui, D. (1993) A follow-up study (1982-1991) on the relationship between thorium lung burden and health effects in miners at the Baiyan Obo rare earth and iron mine. **Rad. Prot. Austr.**11, 157-161.
- Yau, T.M., Gregg, E.C. *et al.* (1979) Production of Radioresistant Mutants in Murine L5178y Lymphoma Cells. **Radiat. Res.** 80, 502.

APPENDIX

1. TISSUE STAINING

1.1 Haematoxylin and Eosin (Harris' Technique)

i) Harris' Haematoxylin

Haematoxylin	2.5g
Absolute alcohol	25ml
Potassium alum	50g
Distilled water	500ml
Mercuric Oxide	1.25g
Glacial acetic acid	20ml

ii) Eosin Y

0.1 % aqueous solution

iii) H & E staining method

Stain with Harris' Haematoxylin for 10 minutes

Wash briefly in tap water

“Blue” in Scott's tap water

Wash briefly in tap water

Stain with Eosin Y for 3 minutes

Wash in tap water

Dehydrate in alcohols, clear in xylene

Coverslip with Entellan

1.3 Alcian Blue PAS staining technique

i) Alcian blue solution

1% Alcian blue in 3% acetic acid

ii) Periodic Acid solution

periodic acid	1g
distilled water	200ml

iii) Schiff's reagent

acid fuchsin	1g
distilled water	200ml
potassium metabisulphite	2g
conc. HCl	2ml
activated charcoal	2g

Filter and store in the dark at 4°C

iv) Alcian Blue / PAS staining method

Stain with alcian blue for 5 minutes

Wash in tap water

Wash in distilled water

Treat with periodic acid for 5 minutes

Rinse in distilled water

Treat with Schiff's reagent for 15 minutes

Wash in tap water for 10 minutes

Stain with Harris' heamatoxylin for 2 minutes

Differentiate in 1 % acid alcohol, "blue" in Scott's solution and rinse in tap water

Dehydrate in alcohols, clear in xylol

Coverslip with Entellan

2. PERIPHERAL BLOOD ANALYSIS

2.1 Wright's Romanowsky Stain

Wrights haematological stain (Merk)

PBS (pH 6.8)

Wright's staining method

Flood glass slide with Wright's stain

Allow to stand for 2 minutes

Rinse in tap water

Flood the slide with buffer

Allow to stand for 10 minutes

Rinse in tap water and air dry

2.2 Non-specific esterase

i) Formalin vapour

Slides are fume fixed over a small layer of formaldehyde in a Coplin jar

ii) Sørensen's phosphate buffer pH 6.5

KH_2PO_4 (66mmol/l) 9.1g / l (A)

Na_2HPO_4 (66mmol/l) 9.5g / l (B)

$\text{Na}_2\text{HPO}_4 \cdot 2\text{H}_2\text{O}$ 11.9g

To obtain a solution of a pH of 6.5, add A and B in the proportion of 68:32.

iii) Pararosaniline

Pararosaniline 1g

HCl (2N) 25ml

iv) 4% Sodium nitrite

Sodium nitrite 0.4g

Dist. H_2O 10ml

v) 2% Methyl green

Methyl green 10g

Dist. H_2O 500ml

Purify from contamination with methyl violet by adding an equal volume of chloroform and

leave standing overnight in a burette. Tap off purified methyl green.

vi) Alpha naphthyl butyrate stock solution

Alpha naphthyl butyrate 0.2ml

N-N dimethyl formamide 10ml

vii) Alpha naphthyl butyrate working solution (freshly prepared)

Mix : 0.1 ml pararosaniline

0.4ml 4% Sodium nitrite

React for 3 minutes

Add 39ml Sørensen's phosphate buffer pH 6.15

Add 2.0ml alpha naphthyl butyrate stock solution

Adjust pH to 6.1 and filter into a Coplin jar

viii) Non-specific esterase staining method

Fix in formalin vapour for 4 minutes

Dry back and sides of slides

Incubate in alpha naphthyl butyrate working solution for 45 minutes

Rinse in distilled water

Counterstain in 2% methyl green for 2 minutes

Rinse briefly in distilled water

2.3 Myeloperoxidase

i) Formalin vapour

Slides are fume fixed over a small amount of formaldehyde in a Coplin jar

ii) DAB working solution (freshly prepared)

3,3 Diaminobenzidine tetrahydrochloride	0.005g
Tris HCl buffer - pH 7.6 (0.05M)	10ml
Hydrogen peroxide	0.1ml

iii) Tris HCl buffer pH 7.6

Tris (Hydroxymethyl aminomethane) 24.23g/ml	250ml
HCl (1N)	36ml

Make up to 1 litre with distilled water

iv) Myeloperoxidase stain

Fix slides in formalin vapour for 4 minutes

Dry back and sides of slides

Incubate in DAB working solution for 20 minutes

Rinse in several changes of Tris HCl buffer pH 7.6

Counterstain in Harris' haematoxylin for 2 minutes

"Blue" in Scott's tap water for 10 minutes

Air dry

3. TREPHINE BIOPSIES**3.1 Zenkers Acetic Fixative**

Mercuric chloride	5g
Potassium dichromate	2.5g
Sodium sulphate	1g
Distilled water up to 100ml	
Glacial acetic acid (add before use)	5ml

3.2 Formalin decalcifying solution

Neutral buffered formal saline(10%)	27.5ml
Formic acid (90%)	1.3ml
HCl (conc.)	1.3ml

4. MICRONUCLEI IN PERIPHERAL LYMPHOCYTES**4.1 RPMI 1640 Medium**

RPMI 1640	10.41 g
NaHCO ₃	2 g
Streptomycin Sulphate	20 mg (final - 20 µg/ml)
Penicillin	0.1 ml (final - 50 units/ml)

Make up to 1 litre, adjust pH to 7.1 with conc. HCl, filter and store at 4°C.

4.2 PHA (10 µg/ml)

PHA 13mg/ml

Make up to 10 ml i.e. 1.3 mg/ml.

Add 39 µl to 5 ml culture tube.

4.3 Ethidium Bromide (100 µg/ml)

Ethidium bromide 1mg

Dist. H₂O 10 ml

Dilute to required concentration and store at 4°C.

5. MICRONUCLEI IN PERIPHERAL RETICULOCYTES

5.1 Acridine orange (1 mg/ml)

Acridine orange 10 mg

Dist. H₂O 10 ml

Store at 4°C.

6. SINGLE CELL GEL ELECTROPHORESIS (COMET ASSAY)

6.1 Phosphate Buffered Saline (Ca ++, Mg++ free)

Dulbecco's PBS 1 packet

Make up to 1 litre, set pH to 7.4, filter and store at room temperature.

6.2 Lysing solution

NaCl (2.5M)	146.1g
EDTA (100mM)	37.2g
Tris (10mM)	1.2g
Dist. H ₂ O	890ml
Adjust pH to 10.0	

Final lysing solution

Add fresh 1% Triton X-100 and 10% DMSO

Refrigerate

6.3 Electrophoresis Buffer

i) Stock solution

NaOH (10N)	200g/500ml dist H ₂ O
EDTA (200mM)	14.89g/200ml dist H ₂ O

ii) 1 X Buffer (300mM NaOH / 1mM EDTA)

NaOH (10N)	30ml
EDTA(200mM)	5.0ml
Dist H ₂ O up to 1 litre	

6.4 Neutralisation Buffer (0.4M Tris)

Tris	48.5g
------	-------

Dist. H₂O up to 1 litre

pH to 7.5 with conc. HCl

Store at room temperature

6.5 Ethidium Bromide**i) 10 X stock solution (20µg/ml)**

Ethidium Bromide	10mg
------------------	------

Dist. H₂O up to 50ml

ii) 1 X stock solution (2µg/ml)

Ethidium Bromide(20µg/ml)	1ml
---------------------------	-----

Dist H ₂ O	9ml
-----------------------	-----

6.6 0.5 % Low Melting Point Agarose (LMPA)

LMPA	125mg
------	-------

PBS	25ml
-----	------

Heat to a boil until agarose dissolves.

6.7 1.0 % Normal Melting Point Agarose (NMPA)

NMPA 500mg

PBS 50ml

Heat to a boil until agarose dissolves.

7. CYTOGENETICS

7.1 Giemsa stain

i) Phosphate Buffer

0.01M $\text{NaH}_2\text{PO}_4 \cdot 2\text{H}_2\text{O}$ 1.38 g/l

0.01M $\text{Na}_2\text{HPO}_4 \cdot 7\text{H}_2\text{O}$ 2.68 g/l

ii) Giemsa solution

Gurr's improved R66

Add 1 part Giemsa to 9 parts phosphate buffer

iii) Giemsa staining method

Stain for 10 minutes

Rinse in running tap water and air dry